Proceedings of the Seventeenth Annual Pacific Climate Workshop

The Wrigley Institute for Environmental Studies
Two Harbors, Santa Catalina Island, California
May 22–25, 2000

Edited by
G. James West and Lauren D. Buffaloe

Technical Report 67
of the
Interagency Ecological Program for the
San Francisco Estuary

March 2001

PACLIM

Climate Variability
of the
Eastern North Pacific
and
Western North America

Single copies of this report may be obtained without charge from:

State of California
Department of Water Resources
P.O. Box 942836
Sacramento, CA 94236–0001

Proceedings of the Seventeenth Annual Pacific Climate Workshop

The Wrigley Institute for Environmental Studies
Two Harbors, Santa Catalina Island, California
May 22–25, 2000

Edited by
G. James West and Lauren D. Buffaloe

Technical Report 67
of the
Interagency Ecological Program for the
San Francisco Estuary

March 2001

PACLIM

Climate Variability
of the
Eastern North Pacific
and
Western North America

Contents

Authors. vi

Acknowledgments vii

Statement of Purpose ix

Introduction 1

Recent Accounts From the *Beachcombers' Alert* 3
Curtis Ebbesmeyer and W. James Ingraham Jr.

A Century-Length Tree-Ring $\delta^{13}C$ Chronology from Southeastern Arizona 11
Steven W. Leavitt, William E. Wright, Austin Long, and Harold C. Fritts

The Influence of Climate and Mechanistic Pathways that Drive Lower Food Web Production in Northern San Francisco Estuary 19
P.W. Lehman

The Effects of Galactic Cosmic Rays on Weather and Climate on Multiple Time Scales 35
Ed Mercurio

Water Year 2000—A February Save 57
Maurice Roos

Forecasting Ocean Ecosystem Responses to Various Climate Clocks 65
Gary D. Sharp, Leonid Klyashtorin, and James Goodridge

Pollen Analysis of Late Pleistocene-Holocene Sediments from Core CL-73-5, Clear Lake, Lake County, California: A Terrestrial Record of California's Cismountane Vegetation and Climate Change Inclusive of the Younger Dryas Event 91
G. James West

Abstracts 107

Appendix A: Agenda 129

Appendix B: Poster Presentations 135

Appendix C: Participants 137

Authors

Harold C. Fritts
Laboratory of Tree-Ring Research
The University of Arizona
Tucson, AZ 85721

James Goodridge
California State Climatologist, retired
Mendocino, CA
707-937-4709

Leonid Klyashtorin
VNIROV, Moscow
klyashtorin@mtu-net.ru

Steven W. Leavitt
Laboratory of Tree-Ring Research
The University of Arizona
Tucson, AZ 85721

P.W. Lehman
Environmental Services Office
California Department of Water Resources
3251 S Street
Sacramento, CA 95816

Austin Long
Departments of Geosciences
and Hydrology and Water Resources
The University of Arizona
Tucson, AZ 85721

Ed Mercurio
Hartnell College, Meteorology
156 Homestead Avenue
Salinas, CA 93901
831-755-6889
mercurio@jafar.hartnell.cc.ca.us

Gary D. Sharp
Center for Climate/Ocean Resources
Study
Monterey, CA
831-449-9212

G. James West
U.S. Bureau of Reclamation
and University of California, Davis
3429 Oyster Bay
Davis, CA 95616

William E. Wright
Laboratory of Tree-Ring Research
The University of Arizona
Tucson, AZ 85721

Acknowledgments

G. James West

PACLIM workshops are produced by volunteers who always manage to put together a topically interesting and timely gathering of a wide range of researchers. The 2000 workshop had fewer participants than previous years primarily because of conflicting meeting schedules. Nonetheless, the meeting continued the tradition started almost two decades ago by providing a forum for new ideas, information, and concepts.

For 2000, thanks go to the following people and institutions: USGS: Mike Dettinger, Program Chair; Long Beach City College: Janice Tomson, Meeting Organizer; Canie Brooks, Mindy Rigney, Katie Sison, Eric Tinseth Scripps Institution of Oceanography: Dan Cayan, Program Chair Emeritus; USC/WEIS: Special thanks to the Wrigley Institute for Environmental Studies and Anthony "Tony" Michaels for co-sponsoring and hosting the 2000 PACLIM on Santa Catalina; USC: Lowell Stott; AGU, Sandra Williams.

Sponsorship and funding for the workshops come from a wide variety of sources. This year's PACLIM Workshop was sponsored by: Wrigley Institute for Environmental Sciences, Anthony Michaels; U.S. Geological Survey Water Resources Division, Bill Kirby; U.S. Geological Survey Geological Research Division, Elliot Spiker; NOAA Office of Global Programs, Roger Pulwarty; American Geophysical Union, Sandra Williams; State of California Department of Water Resources, Randy Brown.

For the third year running Mike Dettinger chaired and organized the meeting and this year set up the web page. As she has done previously, Janice Tomson did a superb job of planning, organizing, and supervising the operation of the meeting- getting us there, getting us fed, watered, and roomed, and, with her Long Beach City College students, doing all the other numerous things that need to be done to make a successful meeting. The meeting moderators are also greatly acknowledged. Finally, we thank all our speakers and poster presenters (listed in agenda) for their contributions and enthusiasm.

For the production and printing of the proceedings, thanks go once again to the California Department of Water Resources Interagency Ecological Program for the Sacramento-San Joaquin Estuary. The editing and production of this volume was performed by my co-editor, Lauren Buffaloe, who I thank for her special expertise and knowledge. Katherine West assisted in editing several of the papers.

The precedents for the 2000 volume were established by the previous editors of the PACLIM Proceedings: Dave Peterson (1984-1988), with the able assistance of Lucenia Thomas; Julio Betancourt and Ana MacKay (1989-1990); Kelly Redmond and Vera Tharp (1991-1993); Caroline Isaacs and Vera Tharp (1994-1996); Ray Wilson and Vera Tharp (1997); Ray Wilson and Lauren Buffaloe (1998); and G. James West and Lauren Buffaloe (1999).

Statement of Purpose

In 1984, a workshop was held on "Climatic Variability of the Eastern North Pacific and Western North America." From it has emerged an annual series of workshops held at Asilomar and the Wrigley Institute for Environmental Studies at Two Harbors, Santa Catalina Island, California. These annual meetings, which involve 80–100 participants, have come to be known as the Pacific Climate (PACLIM) Workshops, reflecting broad interests in the climatologies associated with the Pacific Ocean and western Americas in both the northern and southern hemispheres. Participants have included atmospheric scientists, hydrologists, glaciologists, oceanographers, limnologists, and both marine and terrestrial biologists. A major goal of PACLIM is to provide a forum for exploring the insights and perspectives of each of these many disciplines and for understanding the critical linkages between them.

PACLIM arose from growing concern about climate variability and its societal and ecological impacts. Storm frequency, snowpack, droughts and floods, agricultural production, water supply, glacial advances, stream chemistry, sea surface temperature, salmon catch, lake ecosystems, and wildlife habitat are among the many aspects of climate and climatic impacts addressed by PACLIM Workshops. Workshops also address broad concerns about the impact of possible climate change over the next century. From observed changes in the historical records, the conclusion is evident that climate change would have large societal impacts through effects on global ecology, hydrology, geology, and oceanography.

Our ability to predict climate, climate variability, and climate change critically depends on an understanding of global processes. Human impacts are primarily terrestrial in nature, but the major forcing processes are atmospheric and oceanic in origin and transferred through geologic and biologic systems. Our understanding of the global climate system and its relationship to ecosystems in the Eastern Pacific area arises from regional study of its components in the Pacific Ocean and western Americas, where ocean-atmosphere coupling is strongly expressed. Empirical evidence suggests that large-scale climatic fluctuations force large-scale ecosystem response in the California current and, in a very different system, the North Pacific central gyre. With such diverse meteorologic phenomena as the El Niño–Southern Oscillation and shifts in the Aleutian Low and North Pacific High, the eastern Pacific has tremendous global influences and particularly strong effects on North America. In the western US, where rainfall is primarily a cool-season phenomenon, year-to-year changes in the activity and tracking of North Pacific winter storms have substantial influence on the hydrological balance. This region is rich in climatic records, both instrumental and proxy. Recent research efforts are beginning to focus on better paleoclimatic reconstructions that will put present-day climatic variability in context and allow better anticipation of future variations and changes.

The PACLIM Workshops address the problem of defining regional coupling of multifold elements as organized by global phenomena. Because climate expresses itself throughout the natural system, our activity has been, from the beginning, multidisciplinary in scope. The specialized knowledge from different disciplines has brought together climatic records and process measurements to synthesize and understand the complete system. Our interdsciplinary group uses diverse time series, measured both directly and through proxy indicators, to study past climatic conditions and current processes in this region. Characterizing and linking the geosphere, biosphere, and hydrosphere in this region provides a scientific analogue and, hence, a basis for understanding similar linkages in other regions and for anticipating the response to future climate variations. Our emphasis in PACLIM is to study the interrelationships among diverse data. To understand these interactive phenomena, we incorporate studies that consider a broad range of topics both physical and biological, time scales from months to millennia, and space scales from single sites to the entire globe.

Introduction

G. James West

The Seventeenth Annual PACLIM Workshop was held at the Wrigley Institute of Environmental Studies campus at Two Harbors, on Catalina Island, California. The island location of the workshop has served well for conferences on climate of the eastern Pacific. Attended by about 34 registered participants (see Appendix C), the workshop included 25 talks and 9 poster presentations. The talks consisted of a diverse range of issues ranging from climate change, decadal changes in the North Pacific, and paleoclimatic reconstruction in the Eastern Pacific and Western North America. In addition the future of the PACLIM Workshop was discussed. Throughout the remainder of the meeting shorter (20 minute) presentations were made. On the first evening, Kelly Redmond gave his synthesis on the Western Winter of 1999-2000, Maury Roos presented his annual California Water Year report, and Ed Mercurio presented a far ranging discussion on the causes of climatic change. Tuesday evening's speakers, Larry Riddle and Curt Ebbesmeyer, presented topics ranging from Neolithic pottery and climate to the tracing of currents by tracking a wide range of items, including sports shoes, hockey gloves and plastic ducks that had been lost from container ships. Wednesday evening was spent discussing the future of PACLIM. Poster presentations were displayed throughout the entire meeting and time was set aside for their presentation (see Appendix B).

All presenters were invited to expand their abstracts into a manuscript for inclusion in the Proceeding volume, and nearly all presentations are included in manuscript or abstract form. In this Proceedings volume, eight papers are presented. The abstracts submitted to the meeting are printed in a following section. The papers are not peer reviewed and editorial comments are generally limited to grammar, spelling, punctuation, and format. Editorial comments on the content on some submittals have been offered, but it is the responsibility of the author(s) for any errors of fact or logical inconsistencies.

PACLIM, a Personal View

A number of individuals have been integral in the PACLIM Workshops and their presence provides a continuity of knowledge and expertise. One these individuals is Maury Roos from the California Department of Water Resources. Maury has participated in PACLIM from its beginnings by providing his report on the California water year. His excellent summary presentation of the water year is something I always look forward to and find informative. While officially retired, I hope that Maury will continue to provide his extensive knowledge of California's hydrologic system to PACLIM.

Recent Accounts from the Beachcombers' Alert

Curtis C. Ebbesmeyer and W. James Ingraham, Jr.

Introduction

For the past five years, I've published the quarterly newsletter, the *Beachcombers' Alert*, to provide an outlet for the many fascinating materials beachcombers report to me. Topics include all things afloat. At present circulation is 500 subscribers.

In this paper, I recount some of my favorite reports from *Alerts* published in 1999 and 2000. For additional reports, please see the website www.beachcombers.org.

An *Alert* story usually develops as follows. A beachcomber reports an interesting find. If the account involves a long-distance drift in the North Pacific Ocean, Jim Ingraham often runs OSCURS to simulated the flotsam's trajectory. After additional research and correspondence, usually after a year, the account appears in the Alert.

There is no funding for the *Alert* other than the $12 annual subscription. The *Alert* persists because beachcombers continue reporting fascinating flotsam. The ocean I believe speaks to us rather directly with flotsam, telling of the materials we spill. She hints her displeasure with flotsam; it's up to us to interpret her language. You may e-mail reports of your finds to curtisebbesmeyer@msn.com or phone (206) 526-5622.

Coast-to-Coast Beachcomber Fairs

Only three beachcomber fairs occur annually in the United States, despite beachcombing's popularity and the massive population shift toward the sea. The first two take place in March on Washington's Pacific coast and the third in October on Florida's Atlantic coast. Timed to coincide with annual peaks of best beachcombing, the Washington fairs come at the end of winter after westerly winds beach fascinating drifting objects. The Florida Fair happens in October when easterly winds frequently drive flotsam ashore, including armadas of tropical seeds, the Fair's central focus (hence its name, Sea Bean Symposium).

To satisfy the coastal community's interest about ocean currents, we attended the Washington fairs in 2000 with a computer drift model of flotsam from the massive container spill in North Pacific Ocean (October 1998 from the containership *APL China* described later) and a display of the latest mystery beach finds.

The Washington fairs took place on weekends spaced a fortnight apart in Ocean Shores (March 4–5) and Grayland (March 18–19). Though located close to one another to the

north and south of the Grays Harbor entrance channel, differing atmospheres and approaches widely separate them.

The Ocean Shores Beachcombers' Fun Fair opened with a two-hour Kid's Science Fair during which hundreds of elementary school age children streamed by some dozen informational booths, including our *Beachcombers' Alert* booth. It took all six of us (Dave McCroskey, Connie Blakley, Jim Ingraham, Jan White, Jim White and myself) to answer kids' many eager questions about our display of flotsam such as Nike sneakers, bathtub toys and hockey gloves from lost cargo containers, as well as non-container gear such as Japanese glass floats, messages in bottles, derelict fishing gear, tropical seeds and nurdles (tiny industrial plastic spheres) (Figure 1).

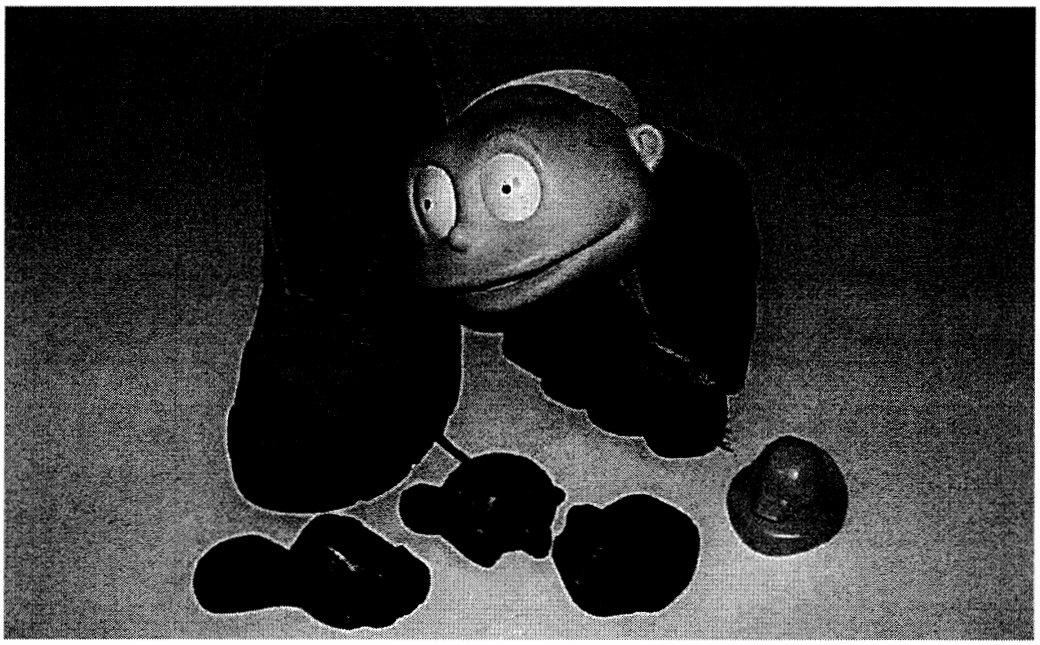

Figure 1 Photo of Nike sneakers, bathtub toys, hockey gloves, and Tommy Pickles heads.

Jim Ingraham included a touch of oceanographic science with video animations of ocean currents transporting shoes, toys, and hockey gloves. For a contest, each child tries to get each informational booth to stamp his or her program. Some of the other booths included Ocean Shores Surf Rescue Team, Ocean Shores Interpretive Center, Westport Maritime Museum, and the NOAA Marine Sanctuary.

On Saturday afternoon we explained to adults as well as children what's been washing up. In the process we learned much from beachcombers. At the *Alert* booth and in the lecture hall, we talked of the oceanographic and cultural significance of some twenty kinds of flotsam. With video animations projected to a movie-sized screen, Jim showed tracks of historical drifters around the North Pacific Ocean and off the nearby coast. Using daily sea level atmospheric pressures fed into his Ocean Surface Current Simulator (OSCURS), Jim computed daily currents across the Pacific. In turn, OSCURS moved the flotsam from its source to local beaches matching reported finds.

Since 1990 Jim has applied OSCURS to the drift of Nike sneakers (1990 container spill), bathtub toys (turtles, ducks, beavers, and frogs spilled in 1992) and hockey gloves (1994 container accident). His transpacific drift animations fascinated beachcombers. Once they realize the scientific significance of particular flotsam, beachcombers willingly make extra efforts to report them to us.

Why do professional oceanographers attend beachcombers' fairs? When we first began, OSCURS had only been compared with the daily or hourly locations of three-month long trajectories of satellite tracked drifters. Container spills, however, provided drifters not limited by marine fouling and battery power, but flotsam that kept drifting for years. Unfortunately, we knew only where and when they fell overboard (accident Point A) and recoveries by beachcombers (multiple Points B). Nevertheless, media attention to their large numbers (80,000 Nikes; 29,000 toys; 34,000 gloves) resulted in reports rivaling the results from numerous past oceanographic drift bottles studies.

OSCURS could simulate flotsam drifts lasting years. Knowing this, we kept showing passers-by the flotsam spilled years earlier. So long lived are these floaters, that we expect reports to trickle in during the coming decades and from other oceans (Arctic and North Atlantic).

Take the bathtub toys, for example, because they have been the most widely publicized. In January 1992 a container holding 29,000 bathtub toys fell overboard in the mid-Pacific at the International Date Line and 45 degrees North latitude. Sitting atop the water, winds assisted by currents quickly scooted the toys eastward to Sitka, Alaska, at 1.6 times the speed of surface water. Then, Alaska Coastal Currents sped them northward and westward halfway back around the Pacific to Shemya Air Force Base at the westward end of the Aleutian Island chain.

Three years after the spill, having passed Japan and migrated eastward back across the Pacific, beachcombers reported them along Washington and British Columbia coasts in agreement with OSCURS. In further accord, after another year and a half beachcomber Lucy Keith reported one from Kure Island, one of the Hawaiian Chain, in response to an article in *National Geographic*. Keep an eye out for them in the Atlantic Ocean as they should drift with the Arctic ice over the North Pole, then head south in the East Greenland Current and then on the Gulf Stream to Europe.

People often asked: "What's next to hit the beach?" In particular, where is the debris lost from the containership *APL China*? In October 1998, an intense storm, the regeneration of Typhoon Babs, overtook the containership in the mid-North Pacific at about 41°N latitude and the International Date Line. Unfortunately, the great ship lost power and broached in 60-foot waves. Nearly capsizing as she wallowed, some 406 containers crashed overboard resulting in lawsuits totaling $100 million, one of the costliest litigations in the container industry.

Manifests supplied by Michael S. McDaniel of Countryman & McDaniel Law Offices indicate that at least 14 containers of toys and shoes fell overboard. Experience from histor-

ical container mishaps further suggests that some 45,000 shoes (three containers) and 1.4 million toys (11 containers) may be adrift from these containers. We've initiated inquiries to obtain exact descriptions of these drifters.

Each month Jim updates OSCURS hoping to alert beachcombers as to the arrivals of the massive debris field. The map shows where *APL China* debris might be located now. By the time of the Washington fairs, he showed beachcombers that 17 months after the accident, the flotsam headed toward the Washington coast for several months but then was caught in the southward moving California Current and circled clockwise round the Eastern Pacific Subtropic Gyre roughly halfway between Hawaii and the fairs.

Figure 2 shows five OSCURS trajectories computed with different windage coefficients: 1.0 for surface water; 1.2 for shoes; 1.4 for hockey gloves; and 1.6 and above for toys with very high windage. Without detailed flotsam descriptions we can only guess at the proper windages. The majority of the flotsam will probably circle for a year the great Garbage Patch of the eastern Subtropical North Pacific Ocean with some spinning off to the northeast toward the West Coast next winter. There's only a remote chance that the latest mystery objects washing up on the West Coast may be part of this spill.

At the fairs we pick up hints of ongoing container spills. At Ocean Shores, we prominently displayed a Tommy Pickles head (a Rugrats cartoon character on the Nickelodeon TV channel), one of two found at Cannon Beach, Oregon, in January 2000. Just the heads, not the bodies were washing up (photo). Sure enough, within a mile of the fair, Kina Shriner's brother found a Pickles head which her teacher Bruce Hansen reported. It just so happened that Bruce's class had a booth next to ours and mentioned the find after seeing the head in our display.

By attending these fairs much happens by serendipity. The night before the Grayland Fair, Steve McLeod called excitedly from Cannon Beach saying he'd found another Rugrat doll head. Rodney Schatz had phoned Steve from the Queen Charlotte Island saying that he'd just found three more. This meant we had a real spill on our hands with heads now found in Oregon, Washington, and northern British Columbia. During the Grayland Fair we speculated endlessly on the possible drift patterns and how to find out from the container industry just where the toys had been spilled. "We were in a pickle," said Jim, always looking for a good pun.

Further OSCURS runs did indicate that low-windage objects could have reached the Oregon coast this winter if the angle of deflection to the right of the wind parameter in OSCURS was decreased by 10 degrees to 15 degrees. This seems excessive, but we have not yet examined the Pickles' head drift characteristics. Maybe, we wondered, one with a smile would drift differently from a head with a frown?

As hundreds streamed by our booth in Grayland's 1930 Grange Hall, we held up a Tommy Pickles toy, saying "Look for Tommy Pickles. Just the heads," against a background of video animations of drifting sneakers, toys and hockey gloves and 35 mm slides of the *APL China* debris drift.

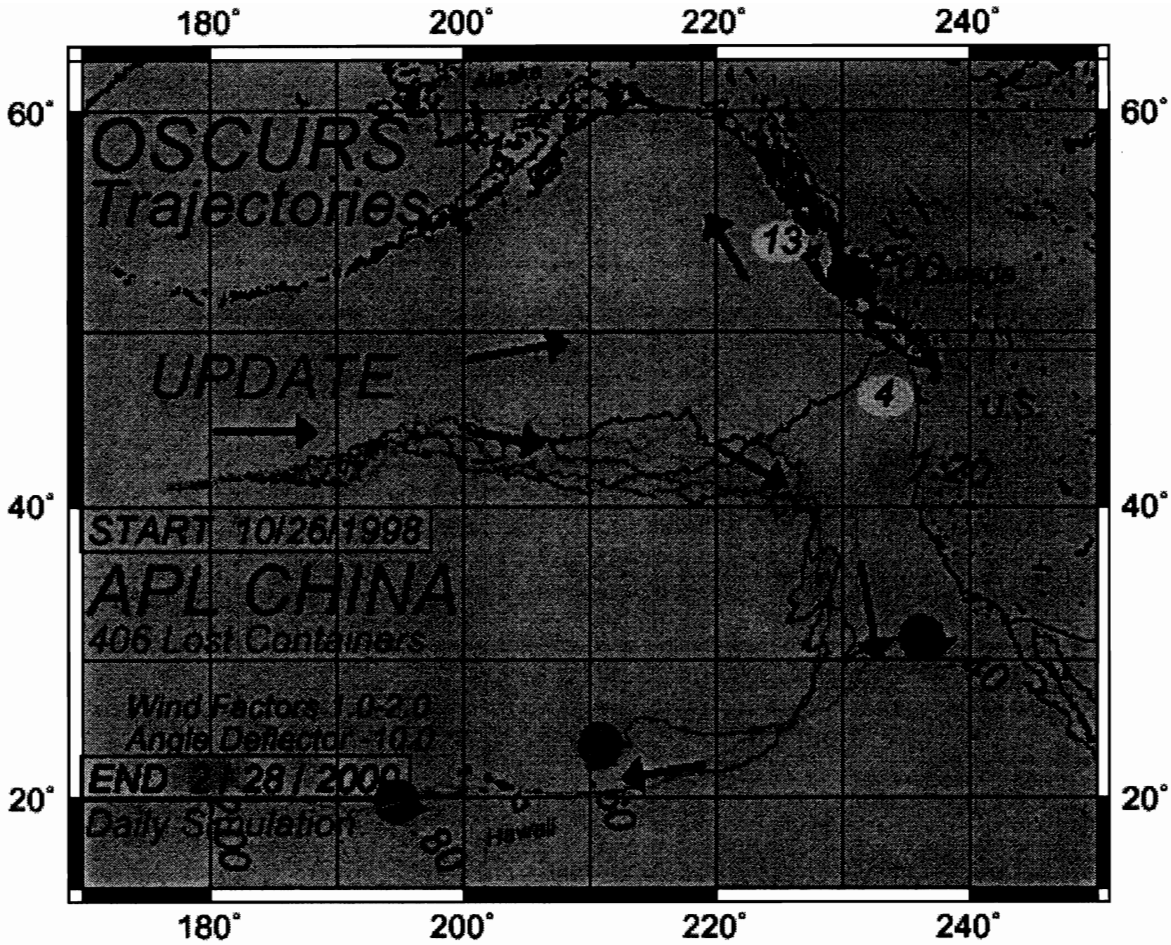

Figure 2 OSCURS trajectories for the *APL China* debris field with solid circles indicating location as of February 28, 2000. Each of the six simulated trajectories are for floating objects with different windages; model coefficients used were 1.0, 1.2, 1.4, 1.6, 1.8, and 2.0. Note that the flotsam moved east then south circling clockwise beneath the Subtropic High Pressure cell located halfway between Washington and Hawaii. The only items reported from this spill so far are the Tommy Pickles heads recovered as shown by the ellipses near the coast. In chronological order: two heads recovered in Cannon Beach during January; one in Warrenton and one in Ocean Shores during February; and three in the Queen Charlotte Islands during March.

How long could the *APL China* debris remain circling under the northeast Pacific High (area of persistent high atmospheric pressure)? Earlier OSCURS runs showed some container debris circling beneath the Subtropic High for as long as 15 years. For that reason, we suggested to Captain Charles Moore that he sail his 50-foot trimaran *Alguita* through the Subtropic High to obtain data with which to calibrate OSCURS. Unfortunately, last August, despite an arduous survey, Charles and crew, including veteran beachcomber Steve McLeod, found none of the *APL China* debris. But it's a Texas-sized area which Charles hopes to again search during summer 2000.

All this we try to explain to beachcombers. Meanwhile, they streamed by with fascinating new stories. Mary and Mike McGuire had just returned from beachcombing Molokai in the Hawaiian Islands. Amongst fantastic amounts of debris from years of accumulations, they found a channel marker stenciled with "Nova Scotia." If it did indeed drift from the Canadian province to the Hawaiian Islands, its trajectory would rank as perhaps the longest known to us. We will report research progress in future *Alerts*.

During a mid-afternoon lull at Grayland, we investigated a highly glazed emerald green jug displayed by Pat Wilson. In 1996, he'd found it washed up with big gooseneck barnacles growing around the corked opening. Back in Seattle (NOAA, Sand Point, WA), Jim's colleague Mei-Sun Yang translated what turned out to be Chinese characters inscribed on the 10-inch tall ceramic jar. Inside an embossed wreath tied at the bottom with a ribbon a large rectangular yellow label proclaimed the contents to be Shou Shing Jo, a special grade of high-class wine produced at a "Taiwanese government brewery." Mei-Sun commented, "Low grades of wine usually come in square bottles. This is a unique shape." Another yellow label circling the jar's base characters gave the brewery's address: Tobacco and Wine Monopoly Bureau, 4 Section 1, Nan Chung Road, Taipei, Taiwan, Republic of China.

Concurrent with the fairs, beachcombers discovered fascinating drifters. In 1998, for example, mammoth timbers known as "cants" from an 80-year-old wreck washed up (Table 1). In 1921 the vessel *Canadian Exporter* destined for Japan grounded not far south on Willapa Harbor's, Washington, treacherous entrance bar. Shifting sands quickly entombed the timber transport holding thousands of 2x2x20–40 foot timbers. Recent severe coastal erosion uncovered the timbers, many of which washed northward. So well had the sands preserved the old-growth cants that some beachcombers received $7,000 apiece!

Table 1 Cant reports. 28 giant beams measuring 2'x2'x20–40' have washed ashore along 60 miles of Washington coast.

Location where cant found	*Number of Cants*	*Date*	*Statute miles north/ south of Willapa Bay entrance*
Ocean Shores, WA	19	Feb. 24, 1999	20 North
Copalis Beach, WA	1	Feb. 24, 1999	25 North
Copalis River to Iron Springs Resort, WA	4	Unknown	25 North
Two to four miles south of Pacific Beach, WA	2	March 1–11, 1999	20 South
Point Grenville, WA	2	March 1–11, 1999	40 North
	Total reported = 28		Range = 60 miles

Table 2 Epic drifts round the North Pacific subtropical gyre. Drifters (1) – (4) began and ended near the same location. Bottles (5) – (8) orbited more than once, passing their points of origin. Estimates of the times for a single orbit (bold) were found by adding or subtracting average drifts for segments required to construct single orbits. The average for boomerang drifters (1) – (4) equals 6.2 years, close to the overall average of 6.0 years for drifters (1 – 8) combined.

Release (drifter, sender, date, location)	*Recovery (finder, date, location)*	*Years between release and recovery (bold = time to drift once around the Subtropical Gyre)*
1. Surfboard. Buzzy Trent, January – February 1972, Oahu, HI	Randy Rarick, summer 1977, Kauai, HI	5.5 years
2. Bottle. Michelle Stone, 1 March 1990, 28 miles west of Ilwaco, WA	Brian Regimbal, 14 December 1995, Willapa Bay	5.8 years
3. Bottle. Gordon Abbott, 16 January 1963, 24°N, 177°W	Scott Tachera, 23 November 1969, Kaneohe Bay, Oahu, HI	6.9 years
4. Bottle. Daniel Porter, August 1980, halfway to HI from Santa Cruz, CA	Anonymous young lady, summer 1997, Oregon	6.5
5. Bottle. Earth Science Club, August 1985, off Togane, Japan	Sandra Kitaoka, January 1995, Kaneohe Bay, Oahu, HI	9.4 years; subtract 4 years for time to Japan to HI, yields 5 years for one circuit.
6. Bottle. Kristine Warner, October 17,1968, off Hawaiian Islands	John Lee, 26 June 1981, Ozette, WA	12.7; add one year to complete circuit to HI, then divide by two for single circuit time of 6.9 years.
7. Bottle. HMCS Gatineau, May 1981, 39°N, 141°W	Steve McLeod, 11 April 1993, Cannon Beach, OR	11.9 years; divide by 2 for single circuit time of 6.0 years.
8. Bottle. James F. Mead, March 11, 1968, 400 miles off Japan	Grace Willers, January 10, 1976, Ocean Shores, WA	7.8 years; subtract 2.5 years for crossing from Japan to WA for single circuit time of 5.3 years.
Mean single circuit interval		6.0 (range = 5 – 6.9) years

Historical attendance at the Grayland Driftwood Fair hints to us of a multi-year shift in the climate corresponding to a dramatic change in beachcombing behavior. It's likely that the latest decadal shift (about 1976) from eastward to northeastward in the currents approaching Oregon or Washington may have decreased the supply of glass floats, thereby decreasing the finds and lessening the interest in more recent beachcomber fairs. During the 1960s, fairs proliferated along Oregon and Washington coasts, with attendance at the Grayland Fair peaking at 6,000 during a single weekend. During the 1990s attendance averaged some 500. We are long overdue for a shift back!

A Century-Length Tree-Ring $\delta^{13}C$ Chronology from Southeastern Arizona

Steven W. Leavitt, William E. Wright, Austin Long and Harold C. Fritts

Abstract

A 100-yr $\delta^{13}C$ chronology was developed from ponderosa pine tree rings collected at ca. 2,300 m in the Santa Catalina Mountains near Tucson, Arizona. Three subdivisions from each year were analyzed separately: 2 initial equal segments prior to (and including) the false-latewood band produced during arid June conditions ("pre-1" and "pre-2"), and the third segment after the false-latewood band when cambial growth is renewed by July-August southwestern monsoon precipitation ("post-F"). Trees were well represented and replicated by sampling four orthogonal radii from each of nine trees. Pooled tree rings from 2 subsets of the 9 trees contributed chronology segments in the first and second half of the century, with an overlap from 1940–1960 to identify and adjust for isotopic offset (ca. 1‰). Similar low-frequency patterns are exhibited by the separate pre-1, pre-2 and post-F chronologies, with high $\delta^{13}C$ at the beginning of the century, a secondary minimum around 1920–1930, a second maximum around 1950–1960, and a decline to lowest values after 1980. At least a portion of this pattern can be related to atmospheric changes in $\delta^{13}C$ of CO_2. In addition to significant correlation among the three chronologies, each time series exhibits significant correlation with climate parameters and ocean-atmosphere proxies (SOI), although the months (or seasons) of strongest correlation differ among the chronologies.

Introduction

Stable-carbon isotope studies have revealed inverse relationships of moisture and tree-ring $\delta^{13}C$ (Dupouey and others 1993; Leavitt and Long 1989, 1991; Saurer and others 1995; Livingston and Spittlehouse 1996). Under conditions of moisture stress, stomatal closure restricts entry of CO_2 into the leaves, and photosynthesis takes place with a limited reservoir of CO_2 resulting in a relatively high proportion of ^{13}C isotopes (to ^{12}C isotopes), i.e., higher $\delta^{13}C$ ([in ‰]= $[^{13}C/^{12}C_{sample} \div {}^{13}C/^{12}C_{PDB\ standard} - 1] \times 1000$) and closer to the $\delta^{13}C$ of atmospheric CO_2. We sampled trees from the Santa Catalina Mountains in S. Arizona, and analyzed $\delta^{13}C$ in three subdivisions of each ring since 1900. These trees contain a "false-latewood" band within each annual growth ring, resulting from interruption of ring development during the fore-summer drought conditions of May and June. The onset of precipitation from the Southwest Monsoon commonly results in re-initiation of growth and completion of the growth ring. This false-latewood band serves

as a time marker, the end of which approximates the onset of monsoon rainfall that occurs on average in the first week in July.

Methods

We cored four radii from each of nine trees near the Palisades Ranger Station (elevation 2300 m) to obtain a site-representative chronology (Leavitt and Long 1984). Tree rings were subdivided into pre-1, pre-2 and post-false latewood ("post-F") subdivisions. The pre-2 subdivision contained the false-latewood band. Because false rings are prominent only in trees younger than approximately 80 years, two different-age subsets of the nine trees were necessary to develop isotope chronologies in the first and second half of the century, with an overlap from 1940–1960 to identify and adjust for isotopic offset. Subdivisions contributed from four radii of trees in each of the two subsets were composited. Samples were ground, extracted first with toluene/ethanol and then ethanol alone, and delignified to holocellulose in an acidified Na-chlorite solution (Leavitt and Danzer 1993). Holocellulose was combusted to CO_2 in the presence of excess oxygen in a recirculating microcombustion system. Mass-spectrometric measurements on CO_2 are expressed as $\delta^{13}C$ with respect to the international PDB standard (Craig 1957; Coplen 1996). Repeated combustion and analysis of holocellulose lab standards reveals a reproducibility of within about 0.2‰ (one standard deviation).

Results

The two $\delta^{13}C$ time series representing subsets of the nine trees span most of the 20th century (Figure 1). Generally, the pre-2 subdivision containing the false-latewood band is isotopically heaviest (high $\delta^{13}C$). However, for a large proportion of years the pre-1 subdivision is heaviest and for a small minority of years the post-F subdivision is heaviest.

The 20-year overlap period (Figure 2) indicates an offset of 0.91‰ between the chronologies. When the offset is subtracted from the "B" chronology to normalize isotopic values, an "adjusted-B" chronology more closely approaches the "A" chronology. This standardization method generally brings the two chronologies to within a few tenths parts per thousand or less.

The single, merged chronology composed of the "A" and adjusted-"B" chronologies shows a generally downward trend of 1‰ to 1.5‰ over the whole century (Figure 3), consistent with global changes in atmospheric $\delta^{13}C$. However, a secondary maximum in this record centers around 1920 to 1930, followed by a maximum around 1950 to 1960. Arizona precipitation was very low at the turn of the century and from 1945 to 1965. The fairly wet period from 1910 to 1920 corresponds to low $\delta^{13}C$.

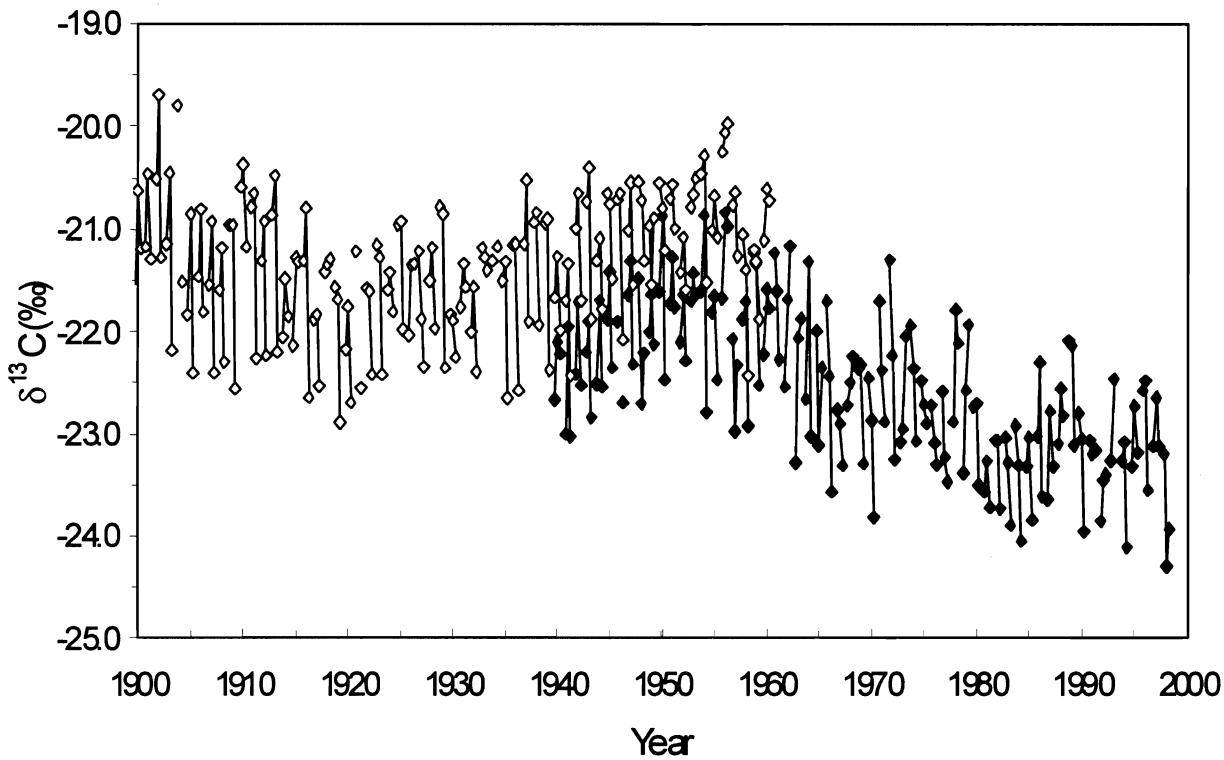

Figure 1 Santa Catalina Mountains $\delta^{13}C$ chronologies from two subsets (open and filled diamonds) of nine ponderosa pine trees. Each ring is subdivided into three parts: pre-1, pre-2 and post-F.

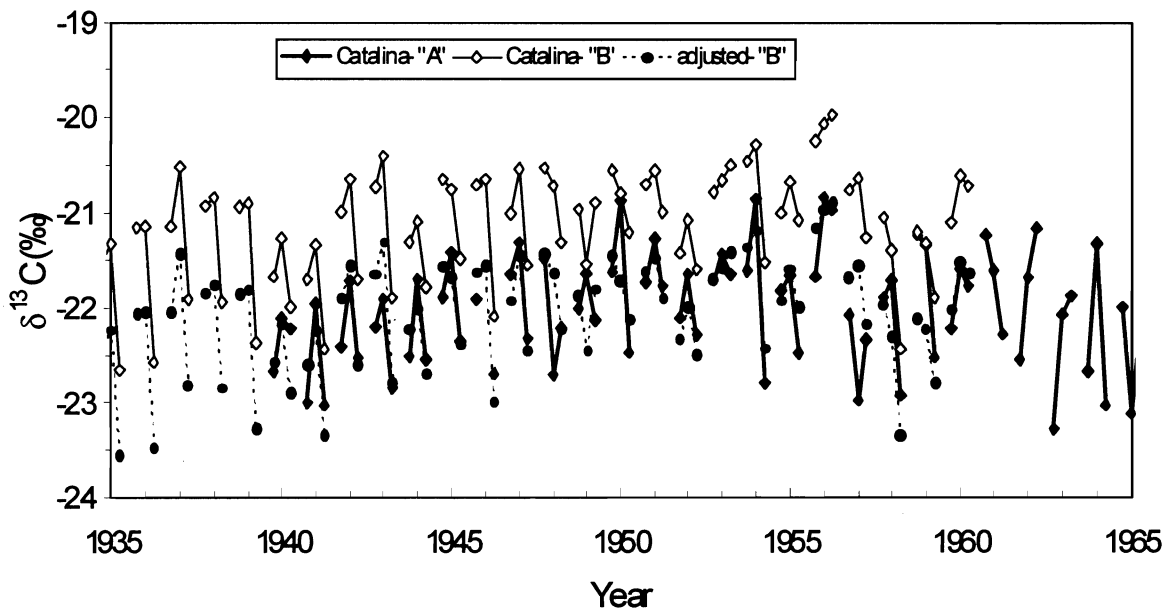

Figure 2 The 20-year period of overlap (1940-1960) for the Catalina "A" (filled diamond) and "B" (open diamond) $\delta^{13}C$ chronologies, and the resulting adjusted-"B" chronology (filled circles) derived by subtracting the average difference (0.91‰) between the "A" and "B" chronologies from the "B" chronology

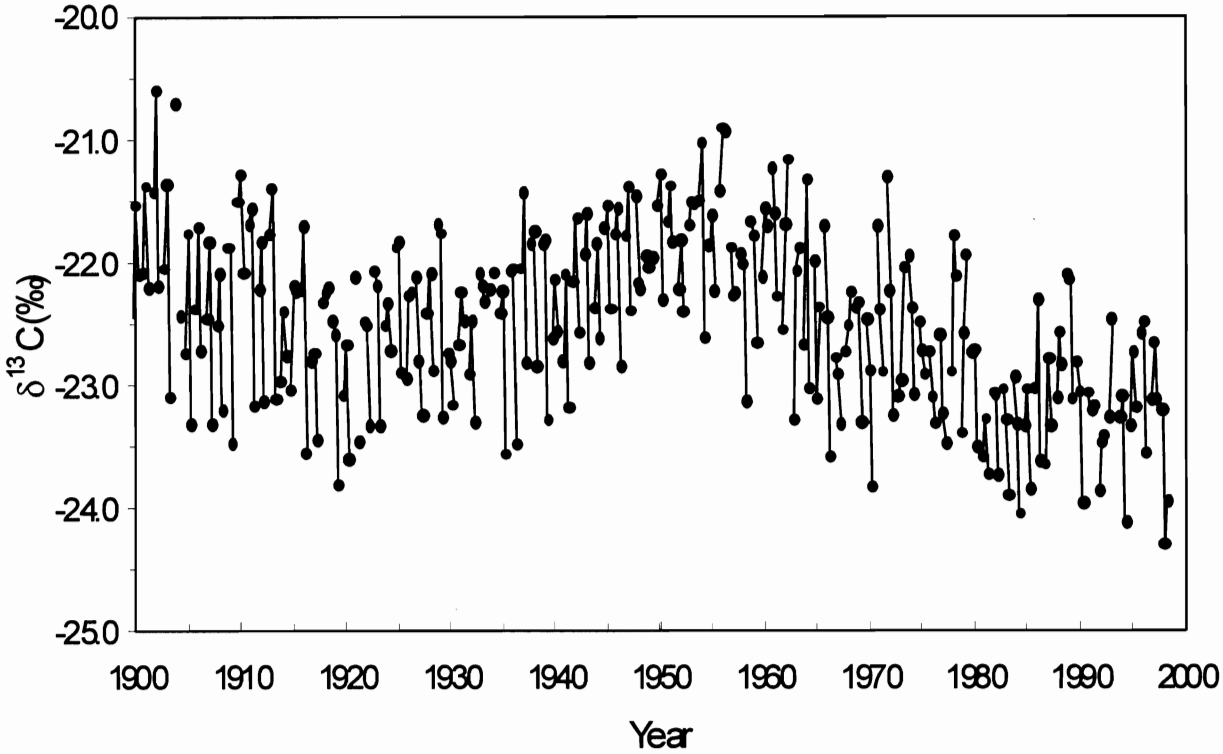

Figure 3 Composite $\delta^{13}C$ chronology derived from merging the Catalina "A" and adjusted-"B" chronologies. For the 1940-1960 period, the "A" and adjusted-"B" chronologies were averaged.

The separate pre-1, pre-2 and post-F time series correlated with monthly SOI, T_{max}, T_{min}, precipitation, dew point, and Palmer Drought Severity Index (PDSI) records, and the strongest significant relationships with precipitation, dew point (also seen by Saurer and Siegenthaler 1989). PDSI shows highest correlation coefficients, typically only between 0.3 and 0.6. Generally, the relationships with PDSI were uniformly the strongest, with some PDSI-pre-1 correlations exceeding 0.5.

An isotopic parameter known as discrimination, D, (Francey and others 1982) removes the influence of changing atmospheric $\delta^{13}C$ from the plant isotopic composition:

$$\Delta = (\delta^{13}C_{air} - \delta^{13}C_{plant})/(1 + \delta^{13}C_{plant}) \quad \delta^{13}C_{air} - \delta^{13}C_{plant}$$

Calculation of Δ (Figure 4) using available $\delta^{13}C_{air}$ from direct measurements and ice core analysis (Francey and others 1999; Neftel and others 1995; Trolier and others 1996) removes most of the post-1960 trend, but does not produce stronger correlations with environmental indices. We calculated other ecophysiological parameters such as C_i/C_a, C_i, and water-use efficiency [$WUE = A/g$] using the expressions:

$$\delta^{13}C_{plant} = \delta^{13}C_{air} - a - (b - a)C_i/C_a$$

$$A/g = (C_a - C_i)/1.6$$

wherein C_i/C_a is the ratio of intercellular CO_2 concentration (C_i) to atmospheric CO_2 concentration (C_a). The term a represents the fractionation during CO_2 diffusion through stomata (about 4.4‰) and b represents fractionation by ribulose bisphosphate (RuBP) carboxylase (about 27‰). *A* is rate of CO_2 assimilation and *g* is rate of stomatal conductance. Correlation of the ecophysiological parameters with environmental parameters did not significantly strengthen the correlation.

First differences of climate and isotope parameters ($\delta^{13}C$, *D*, C_i/C_a, C_i, and *WUE*) were likewise not correlated any more strongly with environmental indices. One particularly notable outcome is that *WUE* appears to have been increasing in these trees over the century (Figure 5), consistent with the possible effects of rising atmospheric CO_2 concentrations.

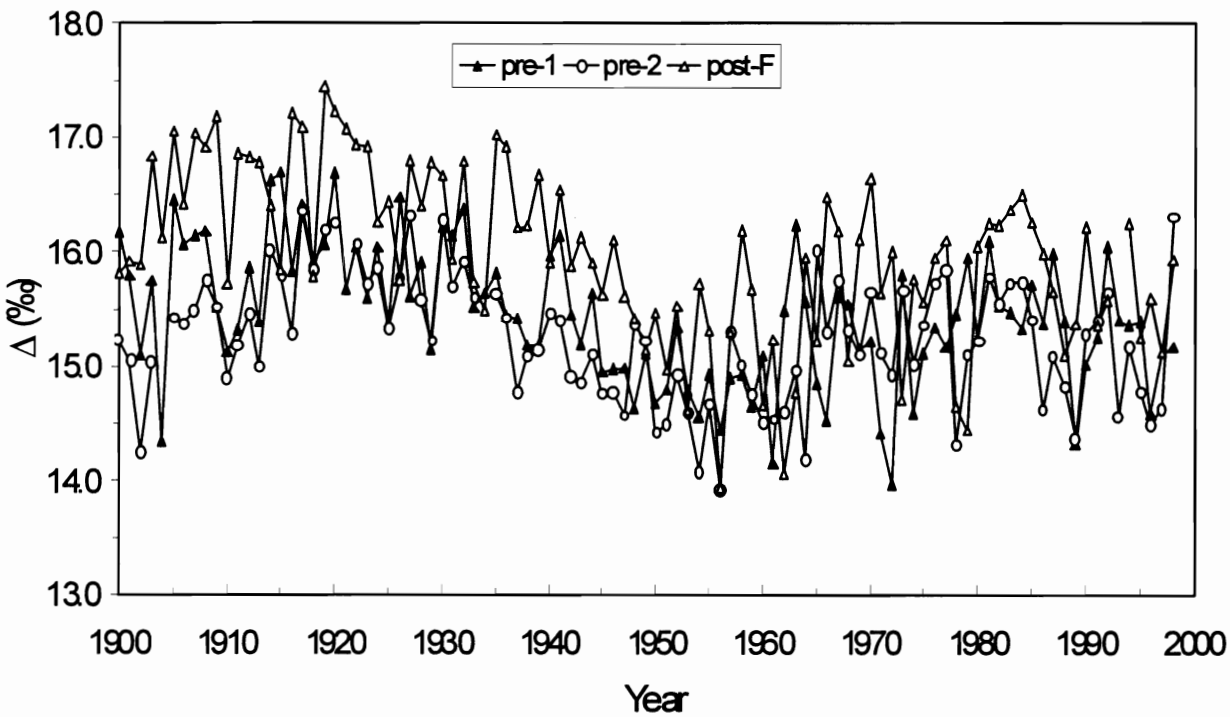

Figure 4 Discrimination (D) chronologies for pre-1, pre-2 and post-F segments derived by removing the effect of atmospheric $\delta^{13}C$ from the tree-ring isotopic values

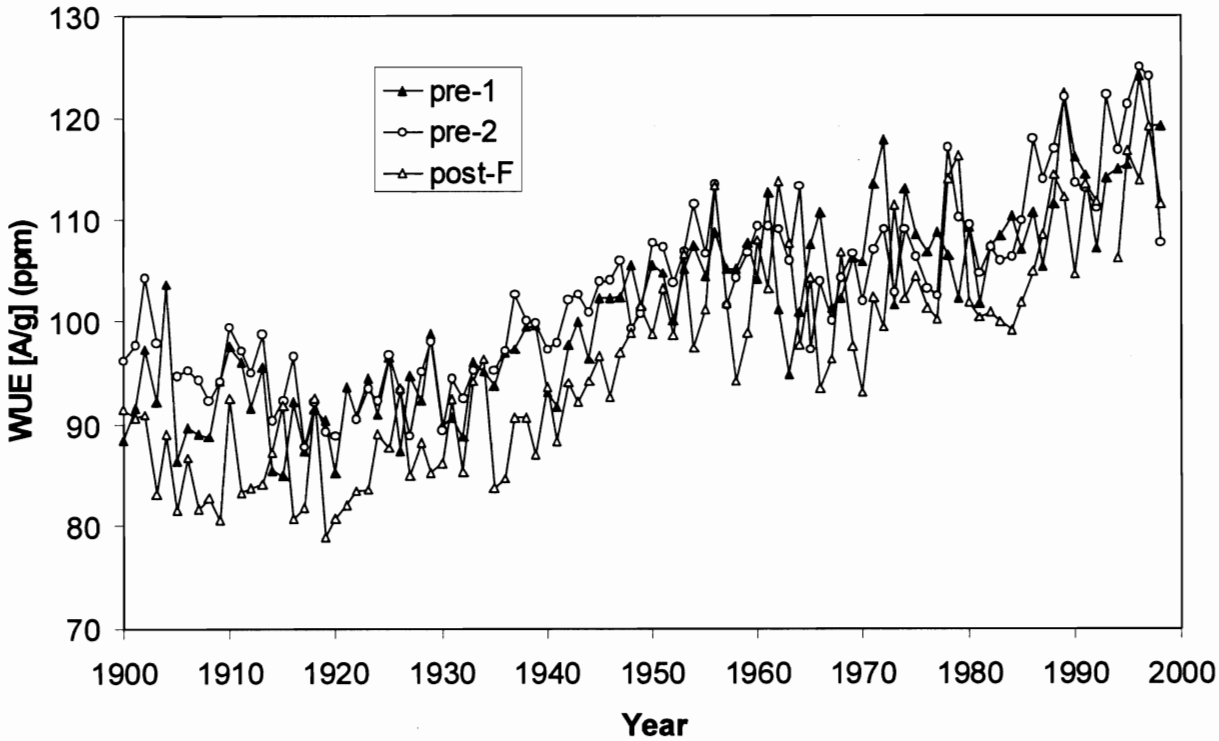

Figure 5 Intrinsic water-use efficiency (*A/g*) for pre-1, pre-2 and post-F derived from tree-ring $\delta^{13}C$ and estimates of atmospheric $\delta^{13}C$ and CO_2 derived from ice core gas samples and atmospheric measurements

Conclusions

Because the false-latewood bands are commonly found in ponderosa pine trees less than about 80 years old, trees of different ages are necessary to develop long chronologies. Using two subsets of trees with an overlap of 20 years, we successfully developed a near century-long chronology by using the overlap period to match the absolute values of the chronologies and adjust them to fit seamlessly.

Over the length of the chronology, the pre-2 segment containing the false-latewood band was most frequently the least negative (^{13}C-enriched), consistent with the elevated water stress associated with the foresummer drought. The pattern of $\delta^{13}C$ change shows some association with climate events such as the elevated values during 1900–1904 and the 1950s consistent with extended drought conditions, and the minimum at about 1920 consistent with a wet period from 1910–1920. There is an overall $\delta^{13}C$ decline that may be an expression of the decrease in $\delta^{13}C_{air}$.

Ecophysiological parameters ($\delta^{13}C$, D, C_i/C_a, C_i, and WUE) correlate significantly with environmental parameters (SOI, T_{max}, T_{min}, precipitation, dew point, and PDSI), but they

generally explain only 20-30% of the variability. Further analysis to remove trends and perhaps account for autocorrelation is needed to assess better the potential for long-term reconstruction of some of these parameters. Because no long-term climate data exist from this site, we will necessarily be limited to interpolation from distant stations, often at different elevations, which is particularly problematic for precipitation. Finally, these ponderosa pine trees may be showing the influence of rising atmospheric CO_2 in the isotopically-derived trend in water-use efficiency.

Acknowledgments

We gratefully acknowledge field, laboratory, and data analysis assistance from D. Hemming, K. Porter, N. Ricketts, L. Cheng, J. Burns, L. Ababneh, T. Farrington and D. Meko. This research was supported by NSF Grants #ATM-9421041 and ATM-9810474.

References

Coplen TB. 1996. New guidelines for reporting stable hydrogen, carbon and oxygen isotope-ratio data. Geochimica et Cosmochimica Acta 602:3359–60.

Craig H. 1957. Isotopic standards for carbon and oxygen and correction factors for mass spectrometric analysis of carbon dioxide. Geochimica et Cosmochimica Acta 12:133–49.

Dupouey JL, Leavitt S, Choisnel E, Jourdain S. 1993. Modeling carbon isotope fractionation in tree rings based on effective evapotranspiration and soil water status. Plant, Cell and Environment 16:939–47.

Francey RJ, Allison CE, Etheridge DM, Trudinger CM, Enting IG, Leuenberger M, Langenfelds RL, Michel E, Steele LP. 1999. A 1000-year high precision record of d13C in atmospheric CO2. Tellus 51B:170–93.

Leavitt SW, Danzer SR. 1993. Method for batch processing small wood samples to holocellulose for stable-carbon isotope analysis. Anal Chem 65:87–9.

Leavitt SW, Long A. 1984. Sampling strategy for stable carbon isotope analysis of tree rings in pine. Nature 311:145–7.

Leavitt SW, Long A. 1986. Stable-carbon isotope variability in tree foliage and wood. Ecology 67:1002–10.

Leavitt SW, Long A. 1989. Drought indicated in carbon-13/carbon-12 ratios of southwestern tree rings. Water Resources Bull 25:341–7.

Leavitt SW, Long A. 1991. Seasonal stable-carbon isotope variability in tree rings: possible paleoenvironmental signals. Chem Geol (Isot Geos Sec) 87:59–70.

Leavitt SW. 1993. Seasonal 13C/12C changes in tree rings: species and site coherence, and a possible drought influence. Can J For Res 23:210–8.

Livingston NJ, Spittlehouse DL. 1996. Carbon isotope fractionation in tree ring early and late wood in relation to intra-growing season water balance. Plant, Cell and Environment 19:768–74.

Neftel A, Moore E, Oeschger H, Stauffer B. 1995. Evidence from polar ice cores for the increase in atmospheric CO2 in the past two centuries. Nature 315:45–7.

Saurer M, Siegenthaler U. 1989. 13C/12C ratios in trees are sensitive to relative humidity. Dendrochronologia 7:9–13.

Saurer M, Siegenthaler U, Schweingruber F. 1995. The climate-carbon isotope relationship in the tree rings and the significance of site conditions. Tellus 47B:320–30.

Trolier M, White JWC, Tans PP, Masarie KA, Gemery PA. 1996. Monitoring the isotopic composition of atmospheric CO2: measurements from the NOAA Global air sampling network. Journal of Geophysical Research 101:25897–916.

The Influence of Climate and Mechanistic Pathways that Drive Lower Food Web Production in Northern San Francisco Estuary

P.W. Lehman

Introduction

Climate probably contributed to the decline in food web production in northern San Francisco Estuary (NSFE) since the late 1970s. The late 1970s were characterized by a climate regime shift in the eastern Pacific (Quinn and Neal 1985) that increased the frequency of wet and critically dry water year types in NSFE (Trenberth and Hurrell 1994). A link between the climate regime shift and aquatic production in NSFE was suggested by a coincident decrease in total phytoplankton biomass (Lehman 1992, 1996), a shift in phytoplankton species composition and a loss of diatom biomass (Lehman and Smith 1991; Lehman 2000a) and the 1977 climate shift. The potential for additional effects on multiple levels of the aquatic food web is high in NSFE because climate affects many mechanisms that control production (Carpenter and others 1992).

The influence of precipitation on streamflow is probably one of the most important mechanisms that link climate and phytoplankton production in NSFE because streamflow is a direct function of winter atmospheric circulation in the eastern Pacific (Cayan and Peterson 1989). Streamflow affects mechanisms that influence the distribution and magnitude of phytoplankton biomass in NFSE, including transport processes, residence time, nutrient concentration, and water transparency (Peterson and others 1989; Lehman 1992; Jassby and others 1996) and the abundance of pelagic benthic grazers (Nichols 1985) over a broad range of time scales (Cloern and Nichols 1985). Streamflow was also correlated with long-term changes in chlorophyll a concentration (Lehman 1992, 1996; Jassby and others 1996), species composition (Lehman and Smith 1991) and the distribution of biomass within the phytoplankton community (Lehman 2000a).

The potential for climate to affect secondary production through food web processes was suggested by correlation between phytoplankton biomass estimated by chlorophyll *a* concentration and both copepod and cladocera biomass in the Sacramento and San Joaquin rivers between 1970 and 1987 (Lehman 1992). Chlorophyll *a* concentration has frequently been correlated with long-term zooplankton density in NSFE (Orsi and Mecum 1986). This association is supported by recent research that suggests phytoplankton provide the primary source of nutrition for *Daphnia* in NSFE (Mueller-Solger, personnel communication).

An influence of climate on production at multiple trophic level is expected in NSFE because production and population density at multiple trophic levels coincided with the 1977 climate shift in both the eastern Pacific (Ebbesmeyer and others 1991; McGowen and others 1998) and North Sea (Aebischer and others 1990). However, even though previous research demonstrated the coincident change in population density or production patterns and the 1977 climate shift in NSFE, a detailed description of the physical, chemical, and biological mechanistic pathways that link the climate shift to production at multiple trophic levels is missing.

The purpose of this research is to identify the climate-related trends in physical, chemical, and biological production variables and to describe the mechanistic pathways by which climate influenced estuarine food web production in NSFE between 1975 and 1993. This information is important to gaining an understanding of how natural processes influence estuarine production and is needed to effectively incorporate the dynamics of climate change into the management of estuarine resources.

Methods

Phytoplankton and water quality samples were collected by Van Dorn sampler or submersible pump at 1-m depth on monthly or semi-monthly cruises by the California Department of Water Resources and U.S. Bureau of Reclamation at 15 stations between 1975 and 1993 (Figure 1). Water samples for nitrate, ammonia, soluble reactive phosphorus, silicate, and dissolved organic nitrogen were immediately filtered through 0.45-μm pore size membrane filter, placed in polypropylene bottles and frozen until analysis (EPA 1983; USGS 1985). Water samples for total and volatile suspended solids, specific conductance, total phosphorus and total organic nitrogen were refrigerated (–4 °C) until analysis (EPA 1983).

Water samples for phytoplankton identification and enumeration were placed in 50-ml glass bottles with 1 ml of Lugol's solution as a dye and preservative. Phytoplankton species identification, cell density (cells L^{-1}) and cell dimensions (um) were determined using the inverted microscope technique, 720X. Phytoplankton volume (μm^3 L^{-1}) was calculated from cell dimensions and included a correction for the large vacuole in diatoms (Strathmann 1967). This correction allowed the volume data to be used as a surrogate for carbon.

Zooplankton were collected between March and November by the California Department of Fish and Game using diagonal vertical tows through the water column. Zooplankton collected in the cod end of the net were preserved in 10% formalin and species identification, age class and enumeration were done by dissecting scope. Zooplankton carbon (mg C L^{-1}) was estimated from animal density and the average carbon per animal of rotifers, cladocerans and copepods (Lehman 2000b).

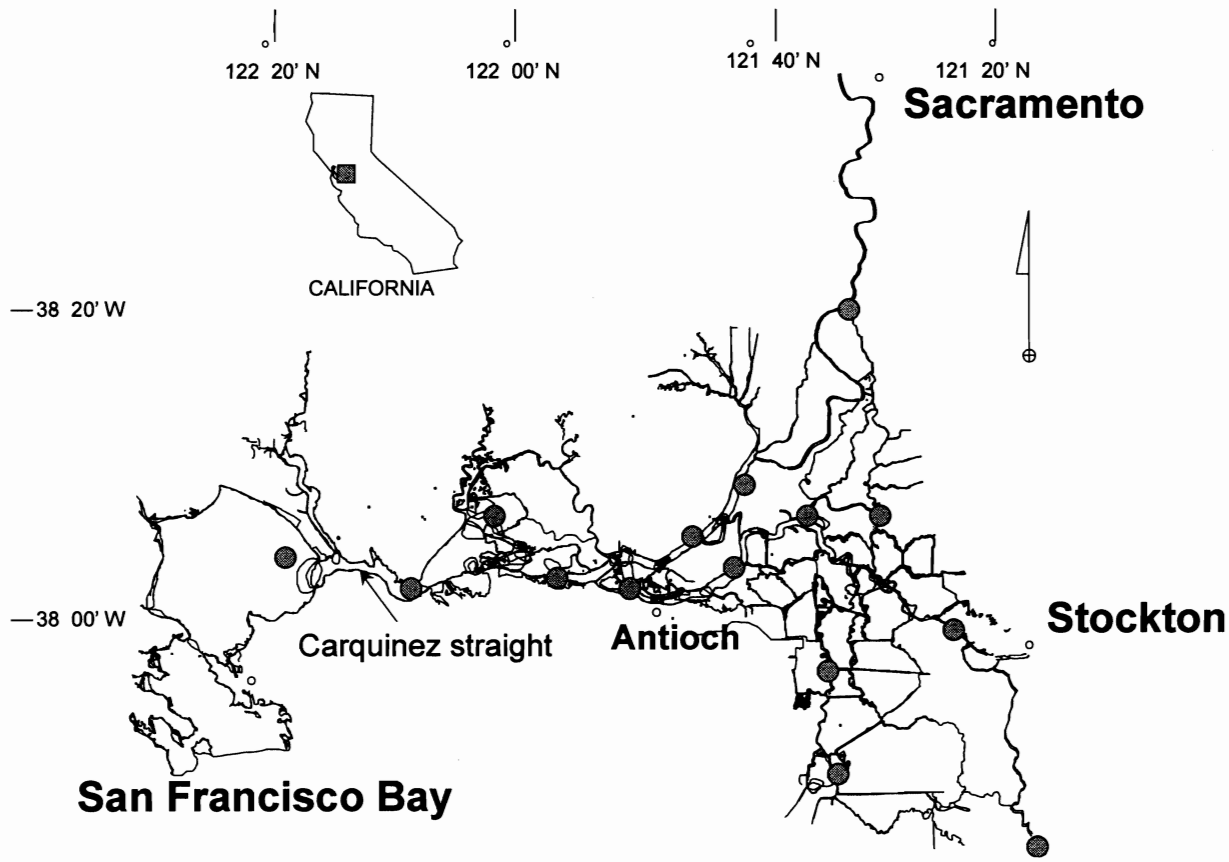

Figure 1 Map of northern San Francisco Bay Estuary with sampling stations

Analysis

Regional climate was described using sea level pressure at 40°N and 120°W. This index distinguishes wet versus dry precipitation patterns in the San Francisco Bay region (Peterson and others 1989).

Monthly continuous time series data were normalized by conversion to seasonally corrected standard deviation units. Standard deviation units were calculated as the difference between the average value for each month and the long-term average for that month divided by the standard deviation of the long-term average for that month. Time series for each variable were averaged into nine regions isolated by hierarchical cluster analysis of monthly water quality variables collected between 1970 and 1993: north Delta (ND), western Delta (WD), lower Sacramento River (LSR), lower San Joaquin River (LSJR), southern Delta (SD), eastern Delta (ED), central Delta (CD), Suisun Bay (SB) and San Pablo Bay (SPB) (Lehman 1996). Zooplankton data were only available for the ND, WD, LSJR, LSR, SD and SB regions. In addition, stations east and west of the confluence of the Sacramento and San Joaquin rivers were also grouped for discussion into upstream and downstream regions respectively.

Average time series for each region were pre-whitened to remove autocorrelation and cross correlation between time series was calculated using Box Jenkins time series analysis. Only significant correlation ($P < 0.05$) within 6 months (lag 6) was presented in this study. The maximum of a 6-month lag period was chosen in order to focus on direct and short term effects.

Results

Physical, Chemical and Biological Trend

A downward shift in sea level pressure at 40°N and 120°W characterized regional climate during the spring and summer between 1975 and 1993 (Figure 2). This spring-summer shift was accompanied by higher-than average rainfall in the spring and lower-than-average rainfall in the summer throughout the NSFE in the early 1980s (Figure 3). The shift in precipitation coincided with an increase in Secchi disk depth, water temperature, and wind velocity throughout most of the NSFE that varied somewhat spatially and temporally (Figure 4). The increase in Secchi disk depth was the most consistent change and occurred in all seasons throughout the NSFE. Wind velocity increased in all seasons downstream, but only in the spring and summer upstream. Increased water temperature occurred in the spring and fall both upstream and downstream.

The shift in regional climate and precipitation between 1975 and 1993 was poorly reflected in streamflow and water quality. The streamflow pattern was dominated by the record precipitation in 1982–1983 (Figure 5) and probably reflects the importance of snowmelt runoff on streamflow. The spring and early summer streamflow is dependent on both rainfall and snowmelt in NSFE where water accumulates in the Sierra Nevada mountains as snow during the winter and contributes to streamflow in the spring as snowmelt runoff. Specific conductance and nutrient concentrations are usually conservative variables in this eutrophic estuary and were tightly coupled with streamflow. Total nitrogen and orthophosphate concentration and specific conductance were low in the early 1980s when streamflow was high; the reverse occurred during the drought in the late 1980s.

A downward shift in total organic carbon estimated as volatile suspended solids accompanied the shift in physical conditions in the estuary during the 1980s (Figure 6). The shift to lower-than-average total organic carbon production began in the late 1970s or early 1980s for most seasons throughout NSFE and was accompanied by a decrease in diatom volume upstream and downstream (Figure 7). Diatom volume and total organic carbon were closely correlated ($P < 0.05$) among regions throughout NSFE.

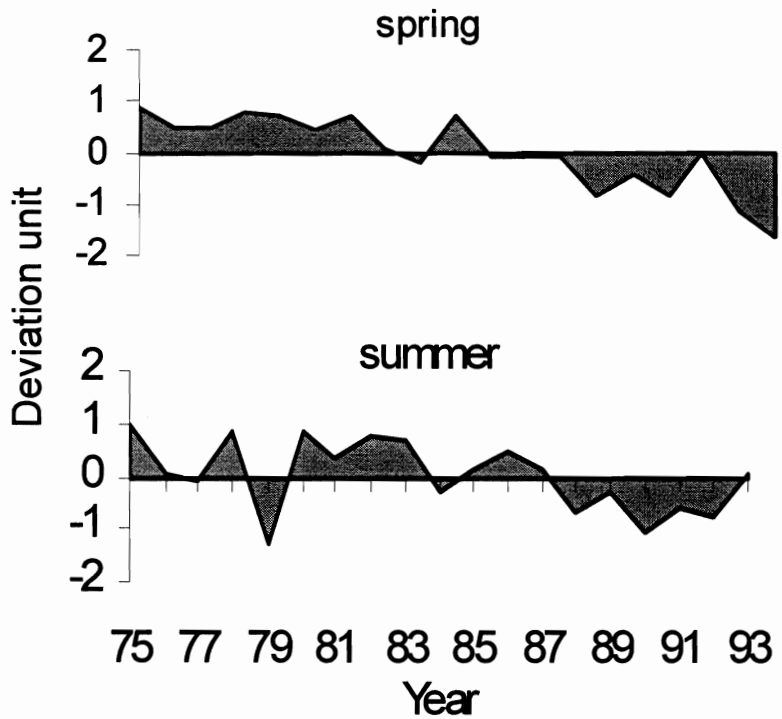

Figure 2 Climate index derived from sea level pressure at 40°N 120°W

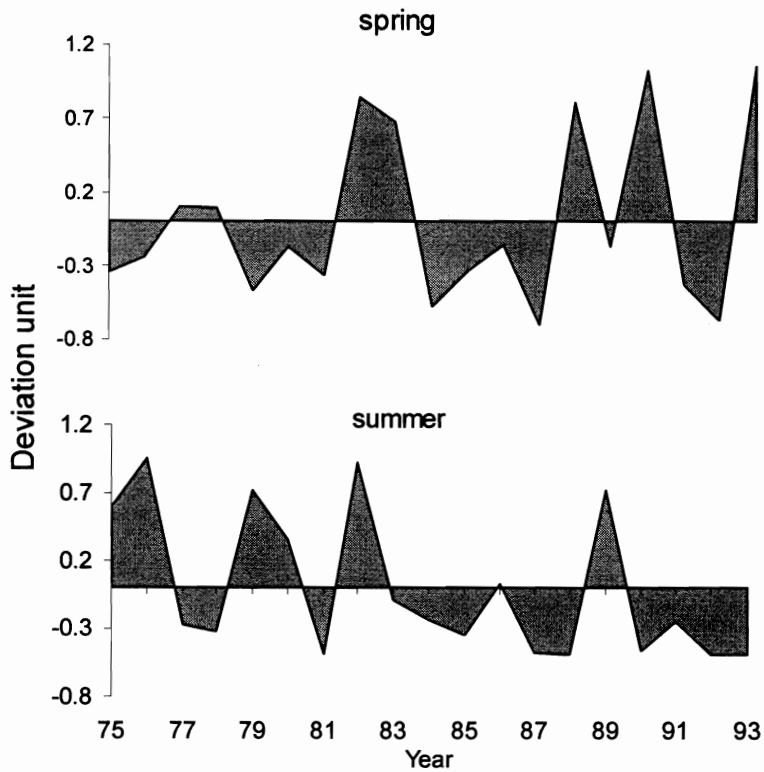

Figure 3 Deviation of spring and summer precipitation from the average

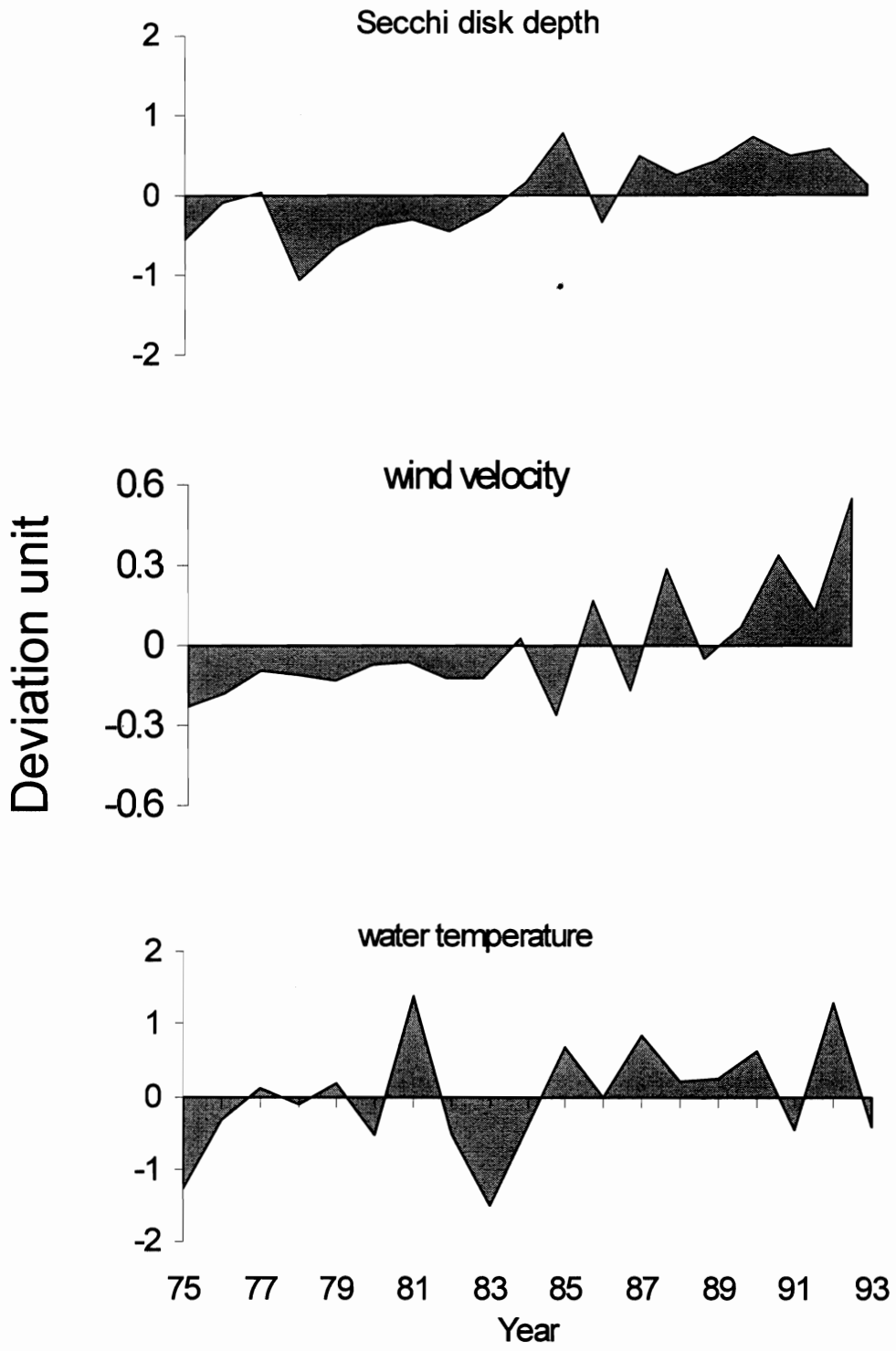

Figure 4 Deviation of Secchi disk depth, wind velocity and water temperature from the average

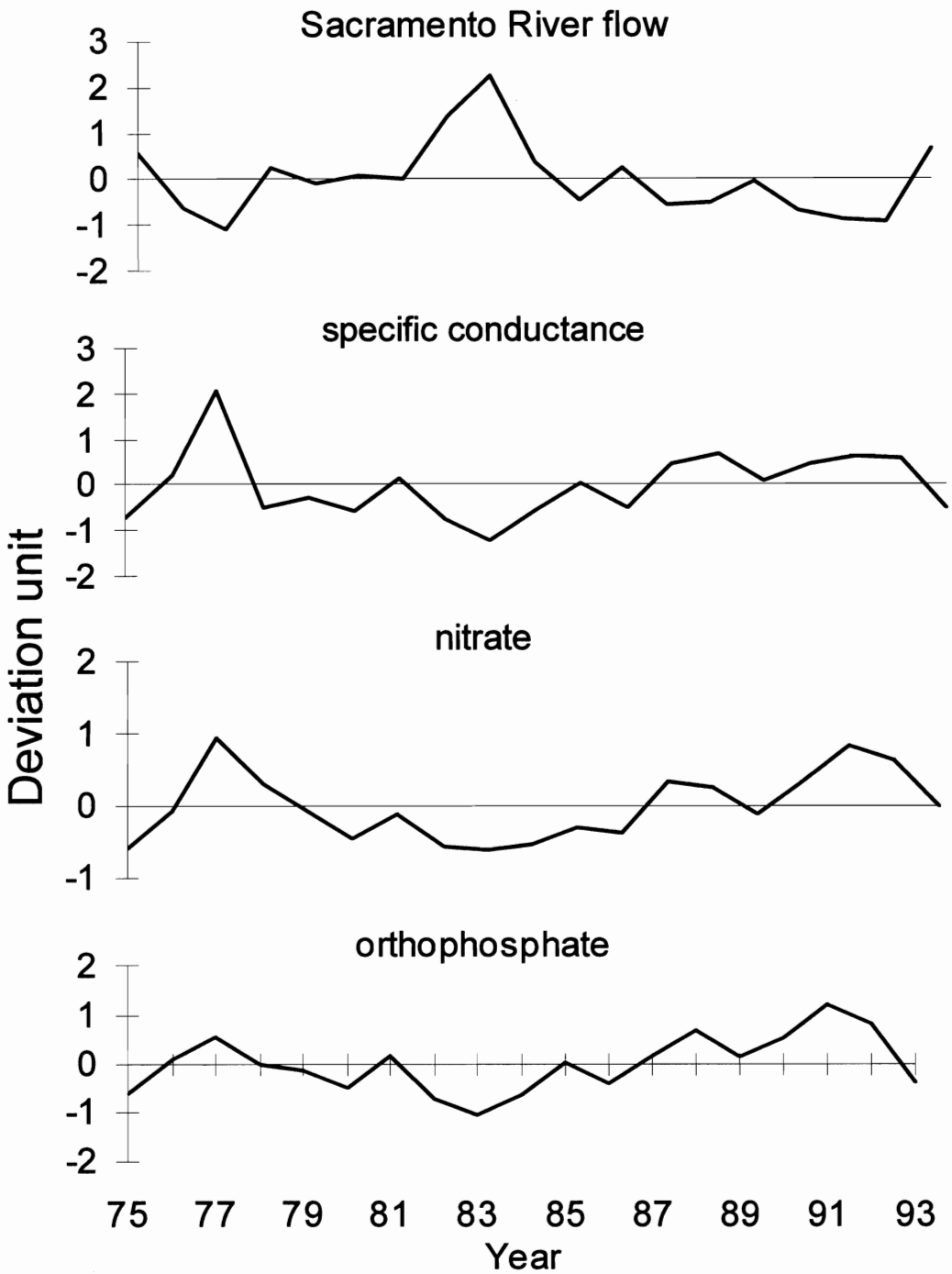

Figure 5 Deviation of Sacramento River flow and water quality variables from the average

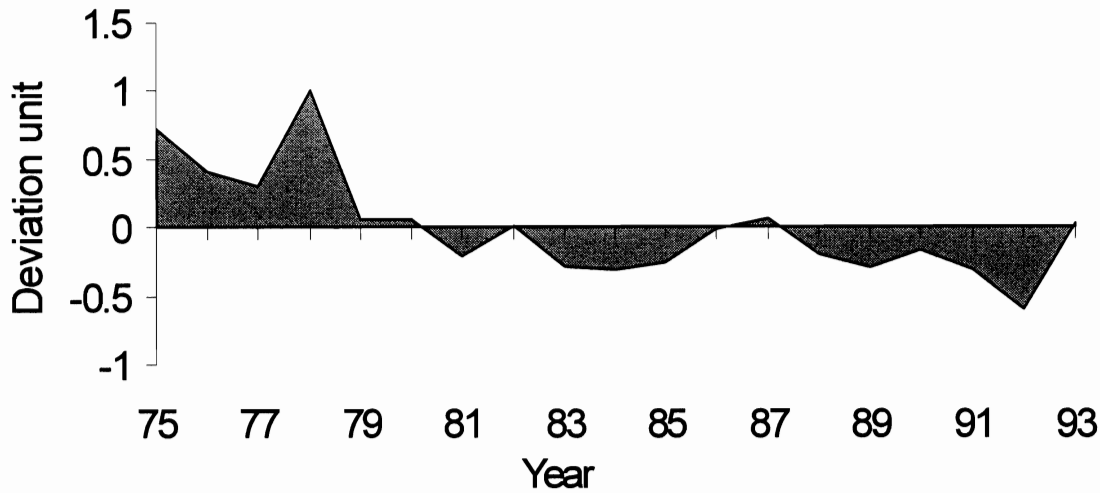

Figure 6 Deviation of organic carbon from the average. Carbon was estimated by volatile suspended solids.

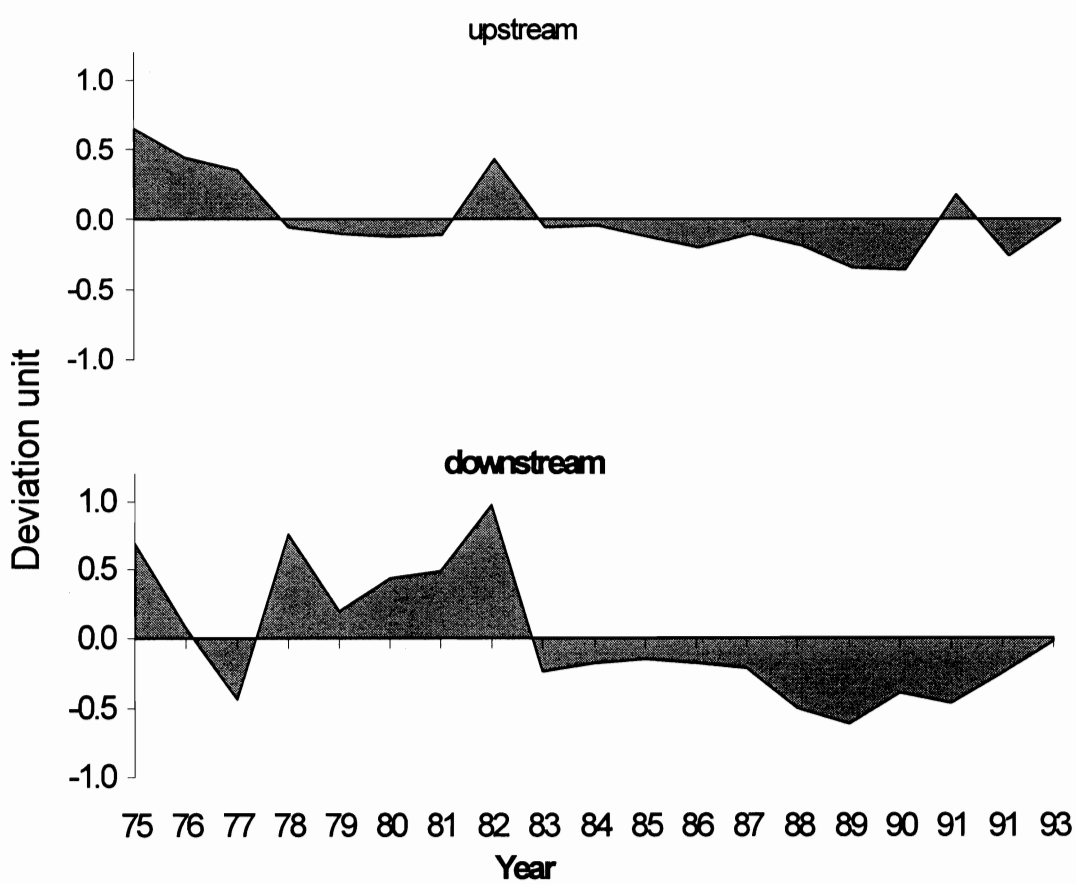

Figure 7 Deviation of diatom biovolume from the average for upstream and downstream regions

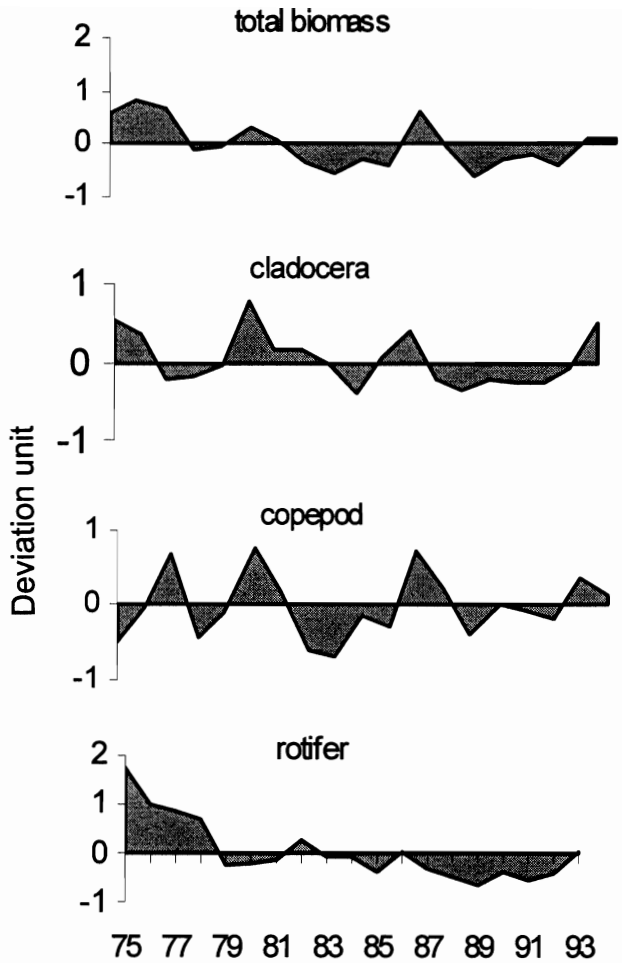

Figure 8 Deviation of total, cladocera, copepod and rotifer zooplankton biomass from the average

A downward shift in total zooplankton biomass also occurred in the NSFE during the 1980s (Figure 8). This shift occurred in both upstream and downstream regions and was a function of a combined shift in copepod, cladocera, and rotifer biomass. A strong downward shift characterized rotifer biomass in all seasons and regions in the late 1970s. Copepod and cladocera biomass was often lower than average in the 1980s, but the downward shift in total zooplankton biomass in the 1980s was largely a function of the high copepod biomass.

Cross Correlation Model

Significant high frequency correlation among physical, chemical, and biological variables was used to construct a cross correlation model describing the mechanistic links between regional climate variation and lower food web production in the NSFE (Figure 9). Regional climate change caused a downward shift in sea level pressure that caused an increase in precipitation as rainfall during the same month (lag 0) and Sacramento and San Joaquin river streamflow one month later (lag 1). Streamflow directly (lag 0)

influenced physical conditions and water quality variables throughout NSFE (Figure 10). Streamflow was inversely correlated with water temperature for all regions and Secchi disk depth for most regions. A strong negative correlation between Secchi disk depth and both total suspended solids and streamflow and a strong positive correlation between total suspended solids and streamflow suggested Secchi disk depth was influenced by suspended solids transported by streamflow. Secchi disk depth was inversely correlated ($P < 0.01$) with total organic carbon concentration in all regions, but was probably not commonly influenced by organic carbon transported by streamflow, because streamflow and organic carbon concentration were only significantly correlated ($P < 0.05$) in the ND, ED and CD.

The correlation between streamflow and other water quality variables varied somewhat between upstream and downstream regions. Orthophosphate concentration was inversely correlated ($P < 0.01$) with streamflow for both upstream and downstream regions. In contrast, silicate concentration was negatively correlated with streamflow upstream where silica concentration was high ($P < 0.01$), but positively correlated ($P < 0.01$) with streamflow downstream in SB and SPB where silica concentration is low and is a direct result of upstream load.

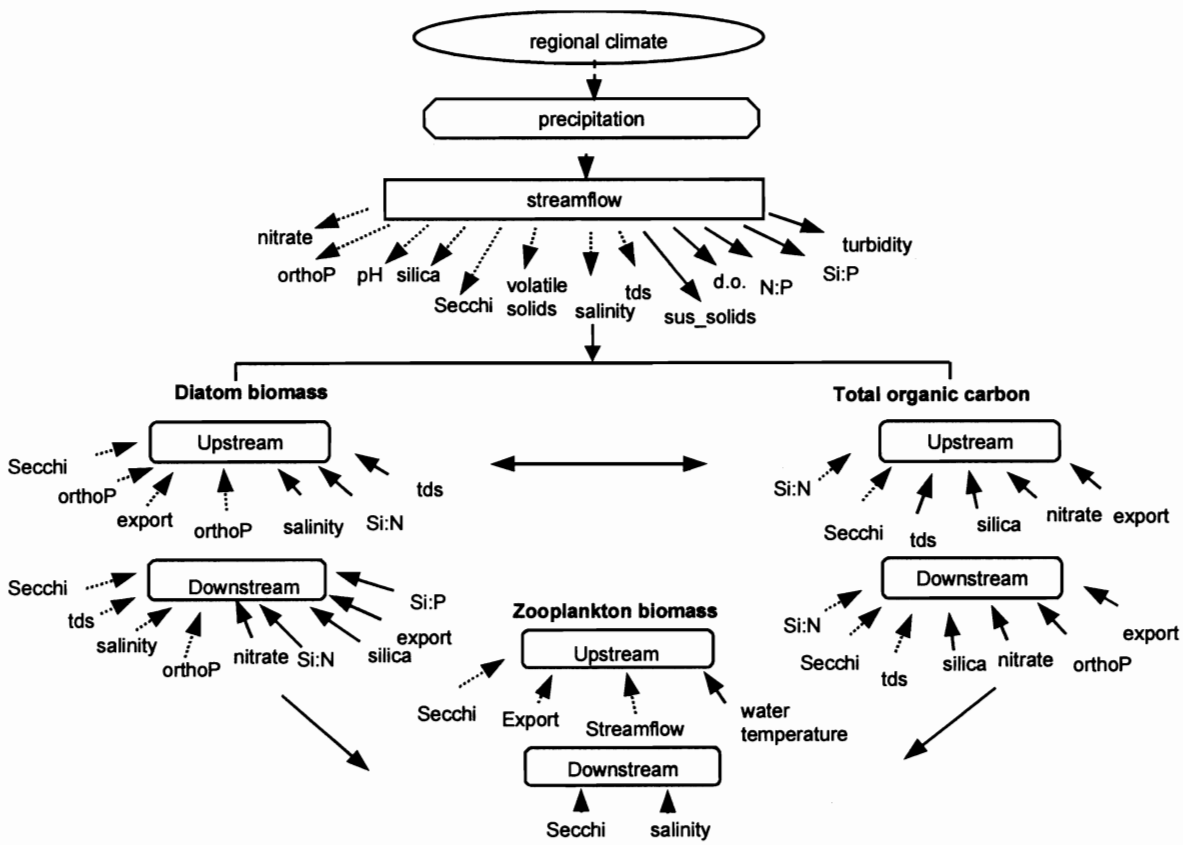

Figure 9 Summary diagram of cross correlation among time series of variables measured in nine regions of the estuary. Solid lines are positive correlation and dashed lines are negative correlation at the $P < 0.05$ significance level.

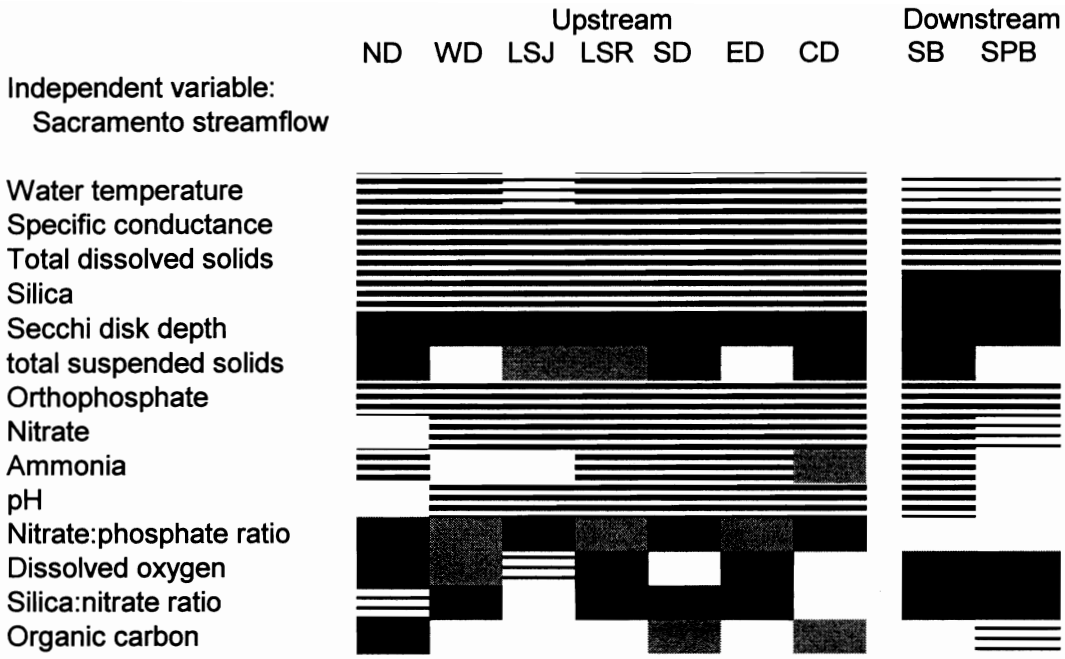

Figure 10 Cross correlation between streamflow and water quality time series for nine regions of the estuary. Solid squares are positive correlation and striped squares are negative correlation. Darker colors indicate significance at the $P < 0.01$ level and lighter colors indicate significance at the $P < 0.05$ level.

Diatom Biomass

Correlation between diatom biomass and physical and chemical variables controlled by streamflow suggested regional climate contributed to lower-than-average diatom volume in the 1980s. However, the influence of environmental variables on diatom biomass differed among regions (Figure 11). Diatom biomass was often negatively correlated with Secchi disk depth and water temperature among regions. In contrast, diatom biomass was positively correlated with specific conductance in the ND, where high specific conductance during drought is associated with high residence time and accumulation of diatom biomass upstream, but negatively correlated with specific conductance in the WD and downstream bays, where the import of biomass from upstream is reduced during drought.

Direct correlation between diatom biomass and streamflow suggested the importance of climate to regional differences in diatom biomass through transport processes. Diatom biomass and Sacramento River streamflow were positively correlated ($P < 0.05$) in the LSR, WD, and SB regions that receive biomass from upstream and negatively correlated in the SD and ED upstream where increased residence time allows accumulation of diatom biomass. The influence of streamflow on diatom production was probably strongly influenced by water management. Increased residence time downstream is associated with water diversion from the SD and may account for the positive correlation between diatom biomass and water diversion downstream of the SD. In contrast, removal of dia-

tom biomass by water diversion probably accounted for the negative correlation between diatom biomass and water diversion in the LSR, SD, ED and ND that are close to water diversion facilities.

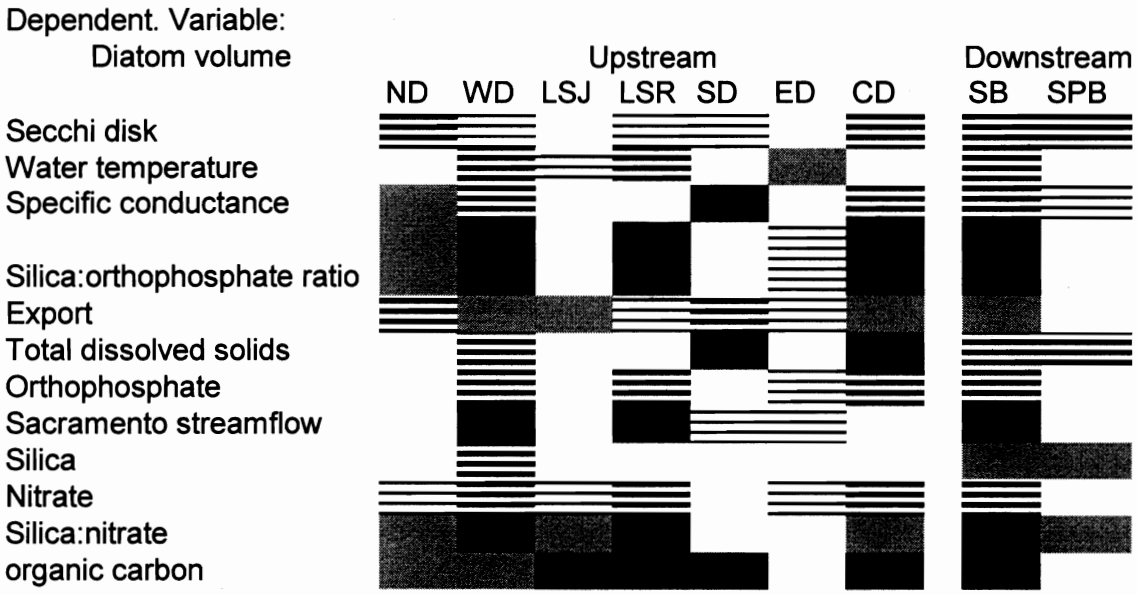

Figure 11 Cross correlation between diatom biomass and water quality time series for nine regions of the estuary. Solid squares are positive correlation and striped squares are negative correlation. Darker colors indicate significance at the $P < 0.01$ level and lighter colors indicate significance at the $P < 0.05$ level.

Nutrients probably had a small influence on diatom biomass because of long-term high and non-limiting nitrate (25 mm L^{-1}), soluble reactive phosphorus (3 mm L^{-1}) and silica (476 mm L^{-1}) concentration in NSFE. This was supported by the negative or non-significant correlation between nitrogen and soluble reactive phosphorus concentration and diatom biomass for all regions. Diatom biomass and silica concentration were positively correlated in SB and SPB, where silica is a function of load from upstream.

Zooplankton Biomass

Correlation between total zooplankton biomass and physical and chemical variables suggested regional climate directly influenced zooplankton biomass, but this correlation varied widely among regions (Figure 12). Streamflow was negatively correlated with zooplankton biomass near the confluence and in the southern Delta: WD, LSJR, LSR, and SD regions and may indicate the loss of biomass from downstream transport of zooplankton at high streamflow. This effect was supported by the positive correlation between high specific conductance and zooplankton biomass in WD, LSR, and SD, because specific conductance is high when streamflow is low. However, it may also indicate a direct influence of salinity on zooplankton species composition. Seasonal changes

in salinity may be important in SB, where total zooplankton biomass and specific conductance were negatively correlated at lag 6. Large regional variation was also suggested by different cross correlation between total zooplankton biomass and both Secchi disk depth and water temperature among regions.

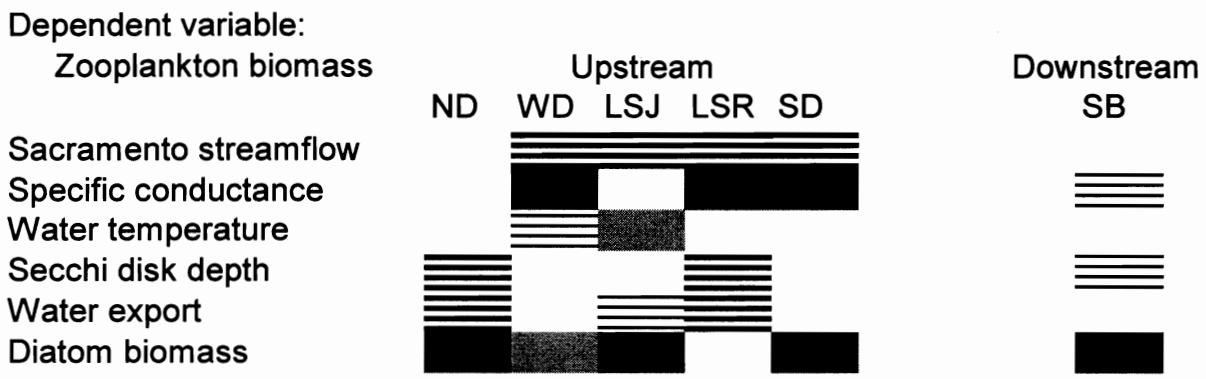

Figure 12 Cross correlation between zooplankton biomass and water quality time series for six regions of the estuary. Solid squares are positive correlation and striped squares are negative correlation. Darker colors indicate significance at the $P < 0.01$ level and lighter colors indicate significance at the $P < 0.05$ level.

Strong correlation between total zooplankton biomass and diatom biomass for most regions suggests climate may have influenced zooplankton production by affecting energy transfer through the food web. Total zooplankton biomass was directly (lag 0) correlated ($P < 0.05$) with diatom biomass for all regions, except LSR. In contrast, zooplankton biomass was correlated with total organic carbon only in the WD and SB.

Discussion

Regional climate directly affected long-term biological production in NSFE through effects on physical or chemical variables such as water temperature, salinity or water transparency that control estuarine production processes. This supports previous research in NSFE where a suite of climatically-related physical and chemical variables described by principal component analysis were correlated with 19 years of phytoplankton biomass among species groups (Lehman 2000a). Direct control of aquatic production by climate through physical variables occurs in European lakes where climate regulates zooplankton biomass (George and Harris 1985; Straile 2000) and the seasonal succession of phytoplankton and zooplankton biomass (Weyhenmeyer and others 1999; Gerten and Adrian 2000) through effects of water temperature on growth rate.

Indirect effects of climate on long-term biological production also occurred in NSFE through cascading effects on trophic level production. Diatom biomass was directly correlated with both total and copepod zooplankton biomass in many regions of the estuary. This supported previous research in which long-term copepod and cladocera biomass

was correlated with chlorophyll *a* concentration in the Sacramento and San Joaquin rivers in NSFE (Lehman 1992). The potential for climate to influence long-term aquatic production through a multiple level trophic cascade was previously suggested by correlation among population densities of organisms at four trophic levels and climate in the North Sea (Aebischer and others 1990). In the eastern Pacific, the potential influence of climate on aquatic production through trophic cascade was suggested by coincident changes in density and production of organisms at many trophic levels with the 1976 climate shift (Ebbesmeyer and others 1991; Francis and Hare 1994; McGowan and others 1998) and the 1958–1960 and 1983–1984 El Niño (McGowan and others 1998).

References

Aebischer NJ, Coulson JC, Colebrook JM. 1990. Parallel long-term trends across four marine trophic levels and weather. Nature 347:753–55.

Carpenter SR, Fisher SG, Grimm NB, Kitchell J. 1992. Global change and freshwater ecosystems. Annual Review Ecology and Systematics 23:119–39.

Cayan DR, Peterson DH. 1989. The influence of north Pacific atmospheric circulation on streamflow in the west. In: Peterson DH, editor. Aspects of climate variability in the Pacific and the Western Americas. Washington, DC: American Geophysical Union. p 375–97.

Cloern JE, Nichols FH. 1985. Time scales and mechanisms of estuarine variability, a synthesis from studies of San Francisco Bay. Hydrobiologia 129:229–37.

Ebbesmeyer CC, Cayan DR, McLain DR, Nichols FH, Peterson DH, Redmond KT. 1991. 1976 step in the Pacific Climate: forty environmental changes between 1968-1975 and 1977-1984. In: Betancourt JL, Tharp VL, editors. Proceedings of the Seventh Annual Pacific Climate (PACLIM) Workshop, April 1990. Interagency Ecological Studies Program Technical Report 26. Sacramento (CA): California Department of Water Resources.

Francis RC, Hare SR. 1994. Decadal-scale regime shifts in the large marine ecosystems of the Northeast Pacific: a case for historical science. Fish Oceanogr. 3:4:279–91.

George G, Harris GP. 1985. The effect of climate on long-term changes in the crustacean zooplankton biomass of Lake Windermere, UK. Nature 316:536–9.

Gerten D, Adrian R. 2000. Climate-driven changes in spring plankton and the sensitivity of shallow polymicitic lakes to the North Atlantic Oscillation. Limnology and Oceanography 45:1058–66.

Jassby AD, Koseff JR, Monismith SG. 1996. Processes underlying phytoplankton variability in San Francisco Bay. In: Hollibaugh JT, editor. San Francisco Bay: the ecosystem. Pacific Division of the American Association for Advancement of Science. p 325–50.

Lehman PW. 1992. Environmental factors associated with long-term changes in chlorophyll concentration in the Sacramento-San Joaquin Delta and Suisun Bay, California. Estuaries 15:335–48.

Lehman PW. 1996. Changes in chlorophyll *a* concentration and phytoplankton community composition with water-year type in the upper San Francisco Bay Estuary. In: Hollibaugh JT, editor. San Francisco Bay: the ecosystem. Pacific Division of the American Association for Advancement of Science. p. 351–74.

Lehman PW. 2000a. The influence of climate on phytoplankton community biomass in San Francisco Bay Estuary. Limnology and Oceanography 45:580–90.

Lehman PW. 2000b. Phytoplankton biomass, cell diameter and species composition in the low salinity zone of northern San Francisco Bay Estuary. Estuaries 23:216–30.

Lehman PW, Smith RW. 1991. Environmental factors associated with phytoplankton succession for the Sacramento-San Joaquin Delta and Suisun Bay Estuary, California. Estuarine Coastal and Shelf Science 32:105–28.

McGowan JA, Cayan DR, Dorman LM. 1998. Climate-ocean variability and ecosystem response in the Northeast Pacific. Science 281:210–7.

Nichols FH. 1985. Increased benthic grazing: an alternative explanation for low phytoplankton biomass in northern San Francisco Bay during the 1976-1977 drought. Estuarine Coastal Shelf Science 21:379–88.

Orsi JJ, Mecum WL. 1986. Zooplankton distribution and abundance in the Sacramento-San Joaquin Delta in relation to certain environmental factors. Estuaries 9:326–39.

Peterson DH, Cayan DR, Festa JF, Nichols FH, Walters RA, Slack JV, Hager SE, Schemel LE. 1989. Climate variability in an estuary: effects of riverflow on San Francisco Bay. In: Peterson DH, editor. Aspects of climate variability in the Pacific and the Western Americas. Washington, DC: American Geophysical Union. p 419–42.

Quinn WH, Neal VT. 1985. Long-term variations in southern oscillation, El Niño and Indonesian drought. Fish Bulletin 76:663–78.

Strathmann RR. 1967. Estimating the organic carbon content of phytoplankton from cell volume or plasma volume. Limnology and Oceanography 12:411–8.

Straile D. 2000. Meteorological forcing of plankton dynamics in a large and deep continental European lake. Oecologia 122:44–50.

Trenberth KE, Hurrell JW. 1994. Decadal atmosphere-ocean variations in the Pacific. Climate Dynamics 9:303–19.

Weyhenmeyer GA, Blenckner T, Pettersson K. 1999. Changes in plankton spring outburst related to the North Atlantic Oscillation. Limnology and Oceanography 44:1788–92.

The Effects of Galactic Cosmic Rays on Weather and Climate on Multiple Time Scales

Ed Mercurio

In this paper, I show that galactic cosmic rays (GCRs) may be a primary climatic forcing agent on many time scales. Levels of GCRs are inversely related to the small changes in solar radiation that have long been considered the primary agent in climatic forcing and help explain the effects of solar related climatic periodicities already established. When solar radiation is low, GCR levels are high, and both of these result in increased cooling. The magnitude of the effects of GCRs on cooling through increasing cloud cover and cloud albedo, however, is much greater and increases in levels of GCRs could be the primary cause of global cooling (Svensmark 1998; Landscheidt 1998).

GCRs are the only particles hitting the earth with enough energy to penetrate the stratosphere and troposphere. They are modulated by the sun's and earth's magnetic fields. GCRs are a major determinant of levels of ionization in the troposphere. The ionization of the lower atmosphere by GCRs is the meteorological variable subject to the largest solar cycle modulation (Svensmark 1998). Levels of ionization are a major determinant of relative humidities, levels of condensation, levels of cloudiness and cloud albedo which, in turn, are major determinants of temperatures, levels of surface moisture and levels of equability. GCRs may also increase levels of precipitation (Tinsley 1996) and storm intensities (vorticity area index) (Herman and Goldberg 1978).

Levels of global cloudiness were observed to increase between 3 and 4 percent from solar maximum to solar minimum over an ~11 year cycle period studied (Svensmark 1998). This is because the solar magnetic field is lower at solar minimum, allowing more GCRs to reach the earth.

In my investigation of the possible role of GCRs in the determination of weather and climate, I made the following observations and conclusions:

1. Approximately 11-year solar cycles alternate between parallel (–) and antiparallel (+), and consistently greater levels of GCRs reach the earth over most of the antiparallel cycles (Figure 1). This results in ~22 year meteorological cycles including such effects as major droughts on the western Great Plains and variations in precipitation from cyclonic storms in the westerlies in Southern California. A curve of Los Angeles yearly precipitation totals shows an approximately 22 year cycle with generally progressively increasing totals during antiparallel cycles and generally progressively decreasing totals during parallel cycles (Figure 2). This results in a pattern in which wettest years often occur around antiparallel to parallel solar maxima and the driest years often occur around parallel to antiparallel solar maxima.

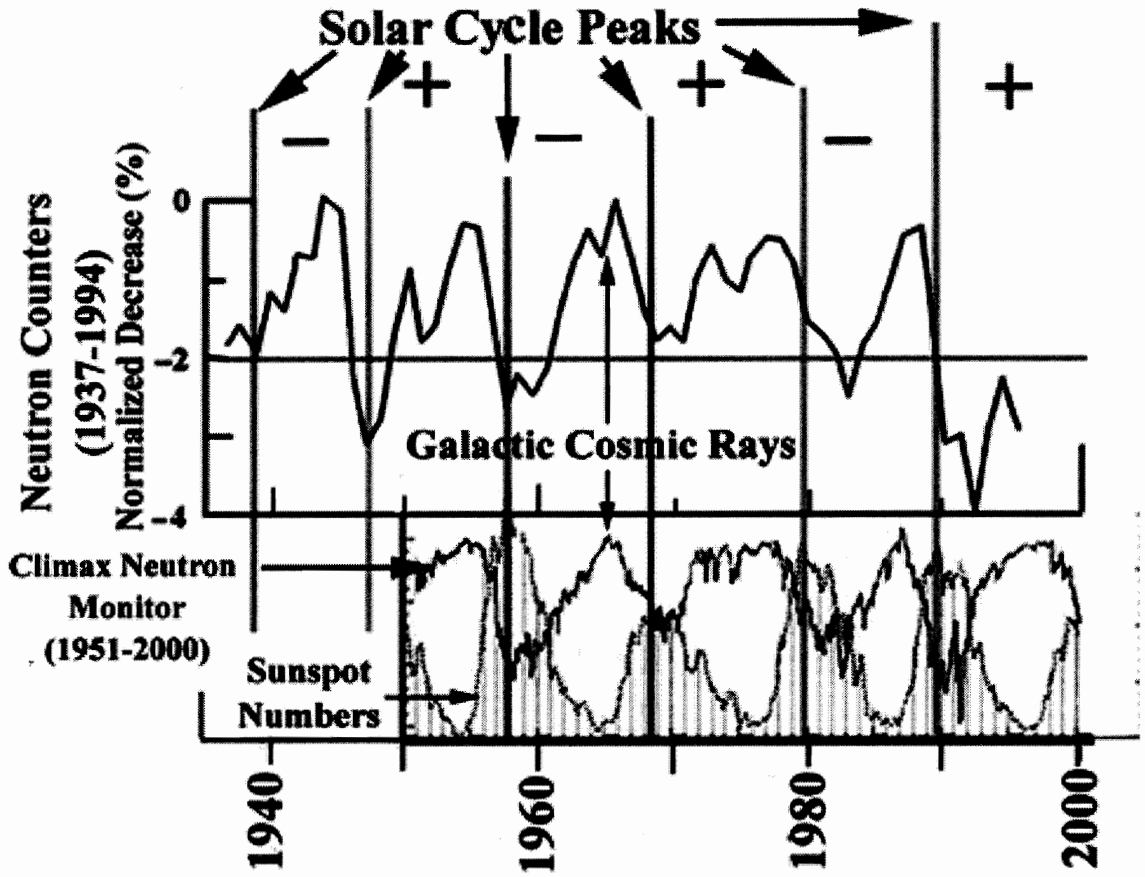

Figure 1 The top curve is the annual mean variation in cosmic ray flux as measured by ionization chambers from 1937 to 1994 (adapted from Svensmark 1998). The bottom curves are neutron flux, which is a proxy for galactic cosmic ray flux, from the neutron monitor in Climax, Colorado from 1951 to 2000 and sunspot number (adapted from University of Chicago/LASR GIF image). Note the differences in the shapes of the curves of GCRs in antiparallel (+) and parallel (-) solar cycles and the differences in GCR levels at solar maxima.

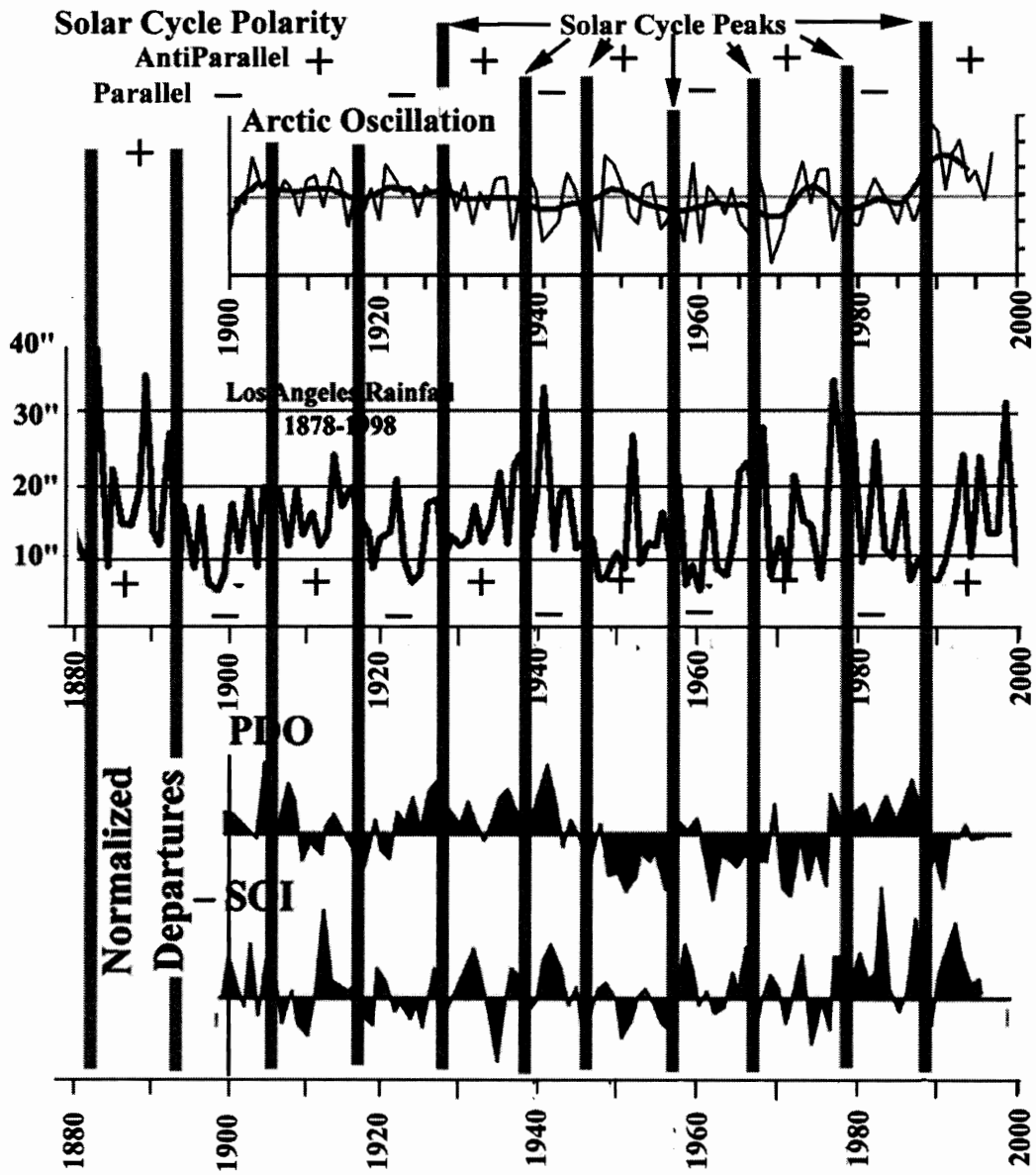

Figure 2 The top curve is the Arctic Oscillation Index with average values (adapted from Kerr 1999). More positive conditions indicative of a stronger, colder polar vortex are up in direction. The upper middle curve is July to June yearly U. S. Weather Bureau precipitation totals for Los Angeles civic center. The bottom curves are the Pacific Decadal Oscillation (PDO) and Southern Oscillation Index (SOI) (adapted from Mantua et. al 1997). In the SOI curve, values indicative of ENSO-Warm Event conditions are above the line and values indicative of ENSO-Cold Event conditions are below the line and in the PDO curve, warmer sea surface temperatures are above the line and colder sea surface temperatures below the line. Note the general relationship between antiparallel (+) solar cycles and a more positive average Arctic Oscillation, progressively increasing Los Angeles precipitation totals, more positive (ENSO-Cold Event) SOI conditions and to a certain degree, more negative (colder) PDO conditions and the opposite for parallel (-) solar cycles. Also note the general relationship between ENSO-Warm Event conditions and higher Los Angeles precipitation totals.

2. A curve of annual GCR intensities over the last four solar cycles shows higher GCR levels at sunspot maxima of longer ~11 year cycles (Figure 1). Solar maximum could be the time when the greatest variations in GCR levels occur and this could be an important factor in periods of cooling, especially on century and millennial time scales.

3. Levels of GCRs appear to have a relationship to the state of the polar vortex and the state of the polar vortex is related to the state of the El Nino Southern Oscillation (ENSO). Higher levels of GCRs appear to be associated with a stronger, colder polar vortex. Some indications of a ~22 year periodicity in winter stratospheric temperatures can be seen in Figure 3. A stronger, colder polar vortex is generally associated with ENSO-Cold Event conditions and a warmer, weaker polar vortex with ENSO-Warm Event conditions. Some indications of this also can be seen in Figure 3. An exception to this is ENSO-Warm Events associated with large, sulfurous volcanic eruptions. Over multidecadal and longer time periods, higher levels of GCRs are associated with a colder, more oscillating (frequent El Niños) tropical Pacific and lower levels with a warmer, more stable tropical Pacific. These effects, however, are also observable in the ~22 year solar cycle, and many correlations of climate to ~22 year cycles, including droughts on the western Great Plains, are related to an increase in ENSO-Cold Event conditions that develop over the duration of antiparallel solar cycles. Effects on ENSO appear to occur through effects on the strength of the Trade Winds which are directly related to the strength of the polar vortex (Stricherz 1999; Chanin 1993). The Arctic Oscillation index is a measure of the variations in the strength of the polar vortex and some evidence for ~11 and ~22 year cycles can be seen in long term records (Figure 2).

4. There appears to be a relationship between solar coronal hole area and the strength of the Arctic Oscillation. Areal extents of solar coronal holes change over solar cycles and are directly related to levels of GCRs and therefore directly related to levels of global cloudiness and inversely related to global temperatures (Soon and others 2000). There is a better correlation between solar coronal hole area specifically between solar latitudes 500 north to 500 south and the state of the Arctic Oscillation with greater coronal hole area correlated to a more positive state of the Arctic Oscillation (colder, stronger polar vortex) (Figure 4).

5. One effect of anthropogenic gasses that could contribute to global warming is to cool the stratosphere and in this way contribute to a more positive Arctic Oscillation. This may be a cause of recent highly positive levels (Figure 2, Figure 4).

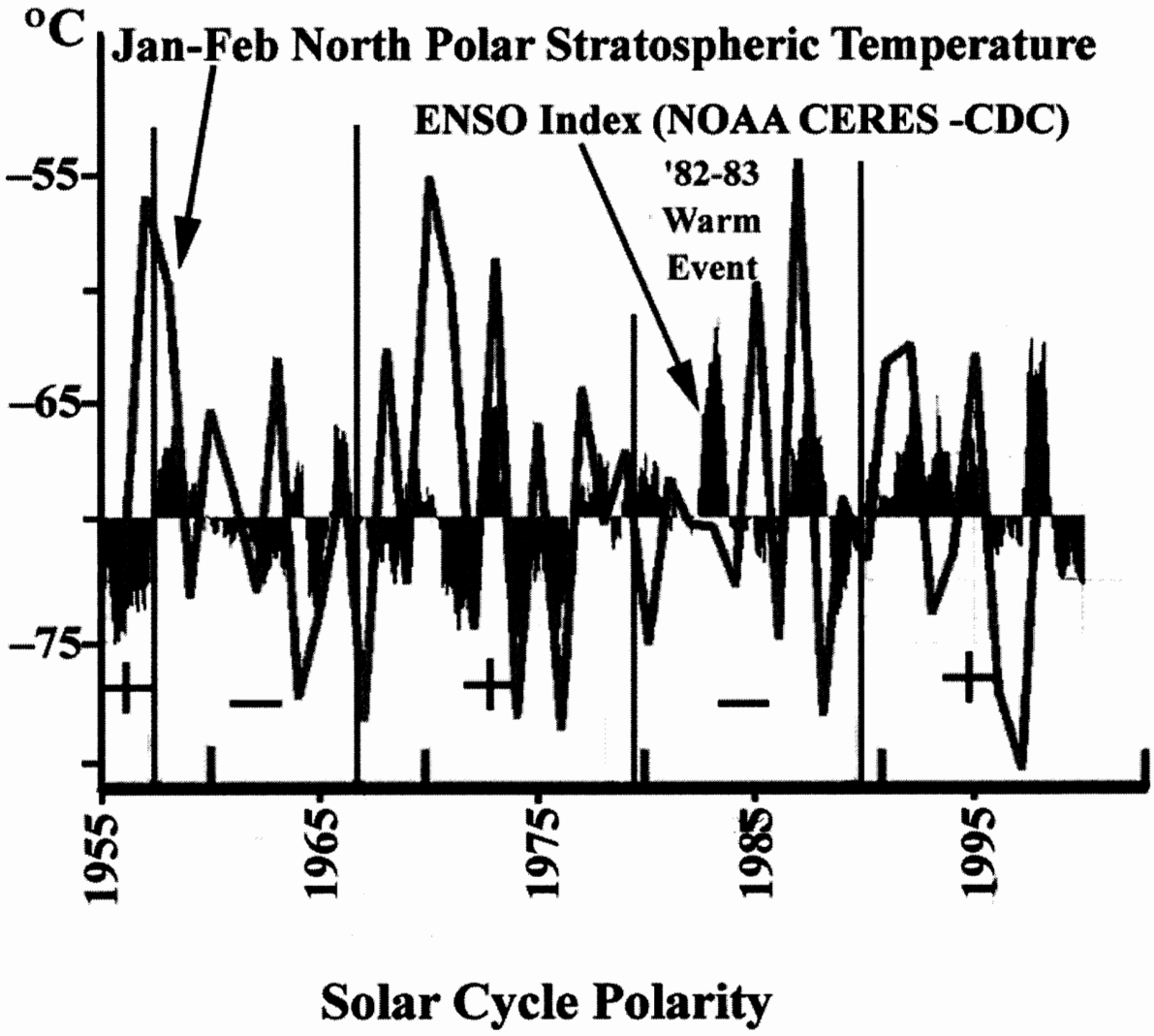

Figure 3 Comparison of January-February north polar stratospheric temperatures (adapted from Labizke and Van Loon 1999) and multivariate ENSO index (adapted from a NOAA-CIRES-Climate Diagnostic Center graphic). Note the relationship between higher temperatures and ENSO-Warm Event conditions and lower temperatures and ENSO-Cold Event conditions and ENSO-Warm Event anomalies that occur following large sulfurous volcanic eruptions such as El Chichon in 1982, Mount Pinatubo in 1991 and Mount Agung in 1963. (Unsmoothed data appears to show a closer relationship but is harder to visualize in a graphic, and up to date sources were unavailable).

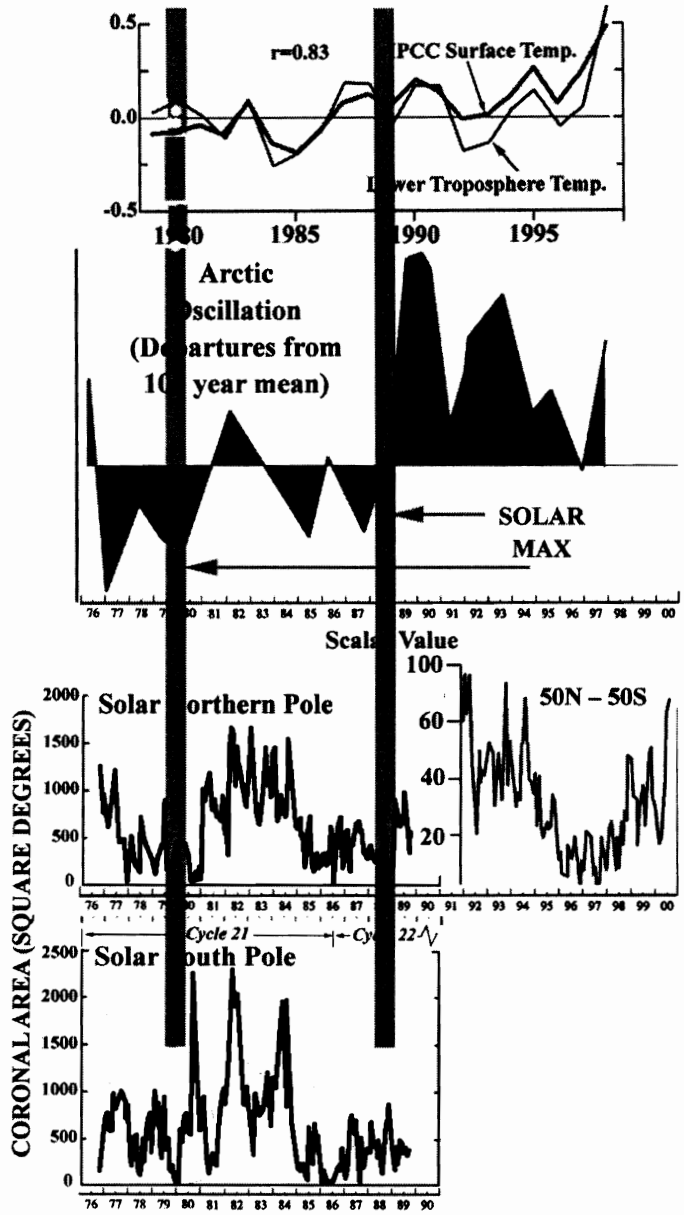

Figure 4 The upper curves are anomaly time series for observed surface and lower tropospheric temperature annual temperature data (adapted from Santer and others 2000). The upper middle curve is the Arctic Oscillation Index (adapted from Kerr 1999). The left side of the lower middle curve is solar coronal hole area in heliographic degrees between north solar hemisphere latitudes 100 to 500 (adapted from McIntosh and others 1992). The right side of the lower middle curve is solar coronal hole area in latitude correlated degrees between 500 north to 500 south solar latitudes (from K. Harvey, personal communication, 1999, derived from NSO helium 10830 data). The lowest curve is solar coronal hole area in heliographic degrees between south solar hemisphere latitudes 100 to 500 (adapted from McIntosh and others 1992). Note the relationship between total coronal hole area and Arctic Oscillation values. Note how the temperatures show an inverse relationship to the Arctic Oscillation Index with a two to three year lag time and how lower tropospheric temperatures are increasingly cooler than surface temperatures the greater the Arctic Oscillation Index and increasingly warmer than surface temperatures the smaller the Arctic Oscillation Index.

6. There could be a relationship between GCRs and the Quasibiennial Oscillation (QBO), an oscillation of equatorial stratospheric winds. There is a quasibiennial oscillation in solar coronal hole area between solar latitudes 500 north to 500 south and the corresponding quasibiennial fluctuations in GCRs could somehow be involved in the origin of the QBO. The relationship of the temperature of the polar vortex to phase of the QBO changes over the ~11 year solar cycle. The reason for this could be because the quasibiennial oscillation in solar coronal hole area between solar latitudes 500 north to 500 south is slightly shorter than the QBO. If the variation in GCR levels corresponding to coronal hole area affects the temperature of the polar vortex, the interplay of the two cycles could result in the changing temperature relationship over the solar cycle.

7. The shortest cyclic effects on climate of GCRs are on approximately weekly and monthly time scales and these may be the cause of reports of periodicities in weather phenomena on these time scales as reported in Glanz (1999). These effects arise because of variations in solar magnetism produced during the rotation of the sun. The sun has a 27 day rotation period and four magnetic sectors with boundaries equidistant from each other. Solar magnetic sector boundaries (heliospheric current sheet crossings) rotate past the earth approximately every 7 days and the increase in solar magnetic strength at these boundaries diminishes the levels of GCRs hitting the earth at the times of passage (Tinsley and others 1989). These decreases in levels of GCRs are called Forbush decreases and have been correlated with decreases in cloudiness (Veretenenko and Pudovkin 1995) and decreases in the vorticity area index (Herman and Goldberg 1978). There are variations in solar sector structure. One sector boundary will often differ from the others in strength leading to a monthly periodicity. This could be a factor in the origin of the intraseasonal oscillations with periods ranging from 10 to 90 days that strongly modulate global weather.

8. Carbon 14 and Beryllium 10 records indicate that GCR levels may be the major determinant of climate variation in longer solar cycles. The most observable of these cycles are those of around 70 to 90 years in length (Gleissberg cycles) and those of around 2400 years in length. These cycles appear to vary in length depending on the varying lengths of the ~11 year solar cycles within them. The following meteorological factors influenced by GCRs are seen to vary with these cycles: global temperatures, total ozone levels, ENSO frequencies and amplitudes, the size of the circumpolar vortex, the zonal index and the earth's rotational velocity (length of day). Slower rotational velocities (longer day lengths) occur at times of lower solar irradiance (Klyashtorin 1998; Courtillot and others 1982) which are times of higher levels of GCRs. This is probably due to greater meridionality at these times since the speed of rotation is directly related to the degree of zonality of the circumpolar vortex and overall strength of the westerlies. It appears that higher levels of volcanic and earthquake activity are associated with slower rotation speeds on most timescales.

9. In the longest climatic cycles that appear to be modulated by GCRs, the GCRs are modulated by geomagnetism instead of solar magnetism. These are the glacial-interglacial cycles and a ~13,000 year cycle. A direct relationship was found between the inclination of the earth with relation to external gravitational attraction and geomagnetic strength and this allowed the calculation of curves of the earth's geomagnetic history. The dynamo theory predicts that greater inclination will result in higher geomagnetism (Vanyo and Paltridge 1981). Four inclination data series are needed to calculate curves of past geomagnetism that would be induced (Figure 5, Figure 6). They are:

    a. The inclination of the earth's orbital plane with relation to the invariable plane of the solar system. I used a data series that had already been calculated for the last three million years by Dr. Richard A. Muller for his work on the astronomical forcing of glacial cycles. It has a ~100,000 year periodicity and a range over the last 3 million years of from ~0.1100 to ~2.940. It is currently ~1.670.

    b. The earth's B angle. This is the inclination of the earth's orbital plane with relation to the solar equatorial plane. I could find no existing data series for this. It was calculated by Dr. E. Myles Standish Jr. for the last three million years for this investigation. It has a ~70,000 year periodicity and a range over the last 3 million years of from ~3.250 to ~8.50. It is currently ~7.250.

    c. The earth's orbital obliquity. Data sets for this have been in existence for a long time since this was one of the three data sets used by Milankovitch in his hypothesis. I used a recent calculation of this by A. Berger available on the internet. It has a ~41,000 year periodicity and a range of from ~22.50 to ~24.50. It is currently 23.50.

    d. The times of the year of the earth's maximum B angle value. These times change because of the precessional motions of the earth. I could find no existing data set for this. This was also calculated by Dr. E. Myles Standish Jr. for the last three million years for this investigation. The time of the year of B angle values changes with the ~25,800 year cycle of precession of the earth's axis, but since the earth encounters the same angular relationship twice a year in its revolution around the sun, the cycle of angular change is actually ~13,000 years. It has a ~13,000 year cycle of times of the two times a year when maximum and minimum values occur. The maximal values currently occur in March and September.

Curves and models were produced from this numerical data by Dr. Douglas McLain for this investigation.

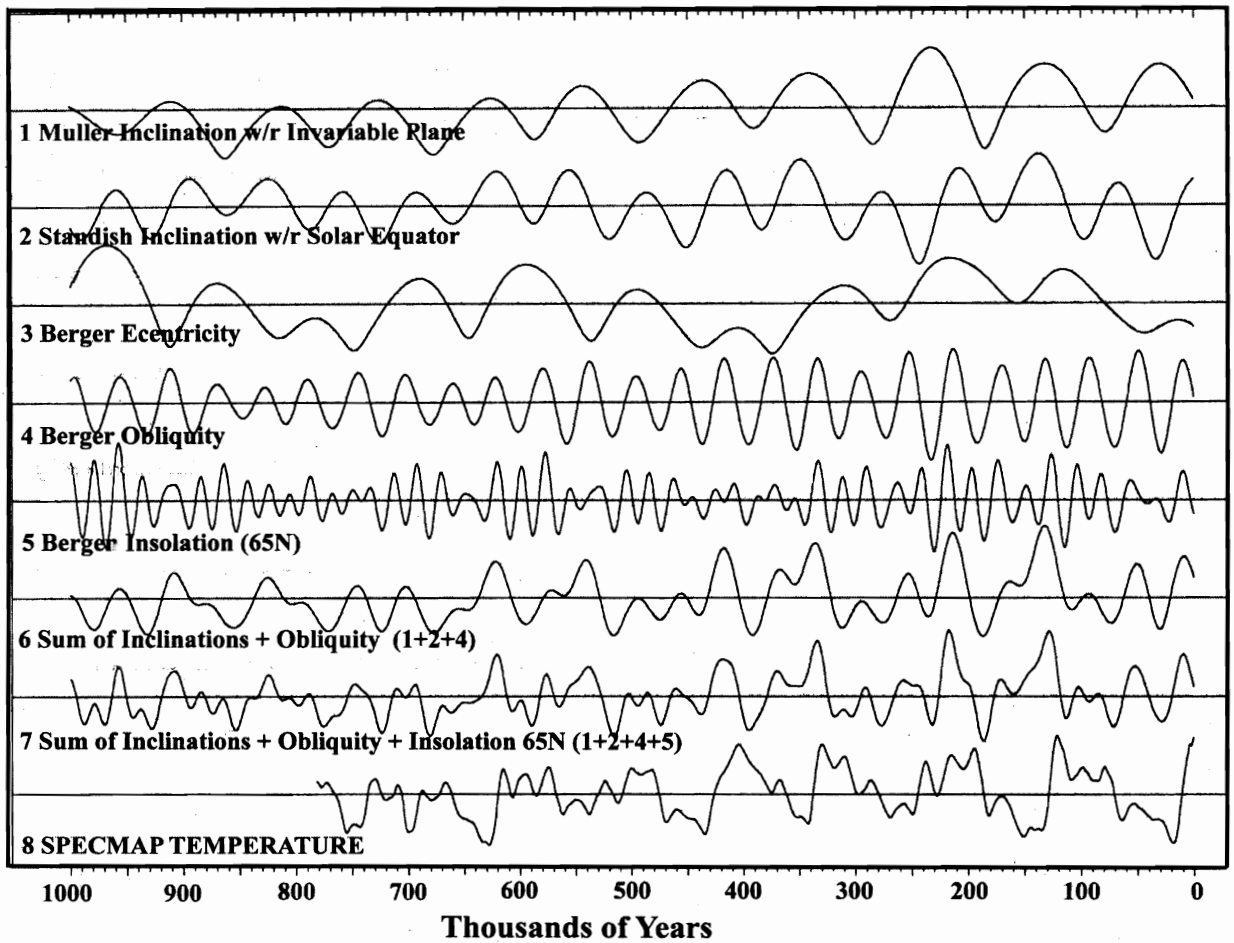

Figure 5 1. Inclination of the earth's orbital plane with relation to the invariable plane of the solar system (by Muller, personal communication). 2. Inclination of the earth's orbital plane with relation to the equatorial plane of the sun (by Standish, for this project). 3. Orbital eccentricity of the earth (by Berger, World Data Center-A for Paleoclimatology). 4. Orbital obliquity of the earth (by Berger, World Data Center-A for Paleoclimatology). 5. June insolation at 650 north latitude (by Berger, World Data Center-A for Paleoclimatology). 6. Curve calculated from the sum of the inclination of the earth's orbital plane with relation to the invariable plane of the solar system + the inclination of the earth's orbital plane with relation to the equatorial plane of the sun + the earth's orbital obliquity. The height of this curve is hypothesized to be directly related to geomagnetic strength. 7. Curve calculated from the sum of the inclination of the earth's orbital plane with relation to the invariable plane of the solar system + the inclination of the earth's orbital plane with relation to the equatorial plane of the sun + the earth's orbital obliquity + June insolation at 650 north latitude. The height of this curve is hypothesized to be directly related to geomagnetic strength and summer northern high latitude insolation and to have the best direct relationship to paleotemperatures relating to glacial-interglacial chronology. Note the relationship of this curve to the SPECMAP curve. The highest points on this curve correlate to the starts of interglacial periods and the lowest points correlate to the starts of glacial periods and glacial periods get progressively colder until ended by one of the highest points which correlates to the start of the next interglacial. 8. SPECMAP paleotemperatures inferred from Atlantic Ocean sediment cores (by Duffy and Imbrie, World Data Center-A for Paleoclimatology).

5. The 13,000 year B angle timing cycle is the shortest of the inclination cycles and appears to have significant effects on climate. Maximal inclination, minimal GCRs and maximum warmth occur in this cycle when maximum B angles are in June and December due to the additive effect of the inclination to the obliquity of the earth's axis at these times. Minimal inclination, maximal GCRs and maximum cold over this cycle occur when maximum B angles are in March and September when they do not add to the tilt of the earth's axis.

The effects of this ~13,000 year cycle are most easily observed during glacial periods where they often correspond to what are termed Bond Cycles. In Figure 7, the curve of B angle times shown in Figure 8 is compared to temperature changes over much of the last glacial period. Note how the June-December B angle maxima are often associated with the major warmings following colder periods and iceberg discharges into the North Atlantic termed Heinrich Events at the end of Bond Cycles.

The March-September B angle maxima are often associated with colder periods not followed by rapid warmings. Since both of these are associated with colder periods, this often gives the appearance of ~6000 year cycles in the paleorecord.

The ~13,000 year cycle can also be related to events from deglaciation through the Holocene. They are: the start of deglaciation (June-December, 19-20,000 years ago), the Younger Dryas period (March-September, 12-14,000 years ago), the Altithermal period (June-December, 6-7000 years ago) and the Little Ice Age, the coldest period since deglaciation (March-September, 1000 years ago to present).

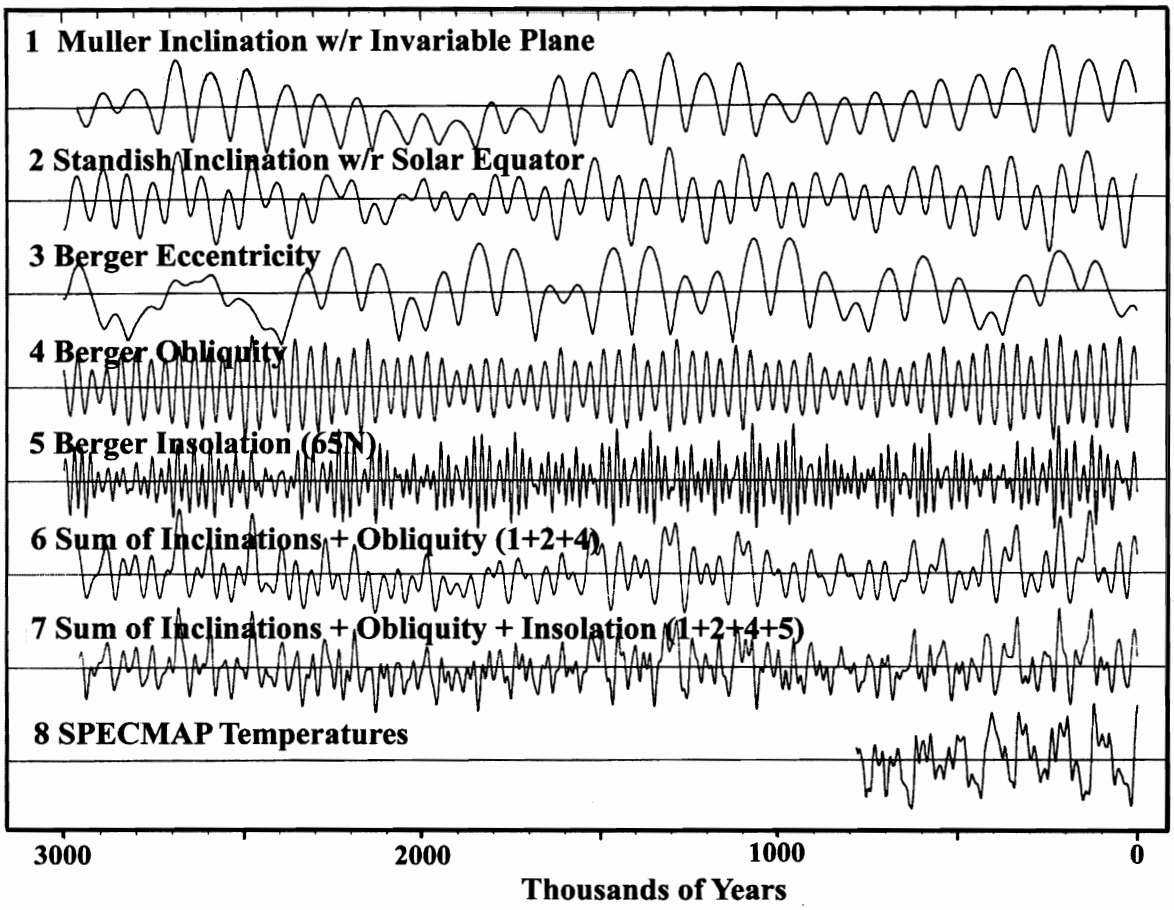

Figure 6 See caption for Figure 5.

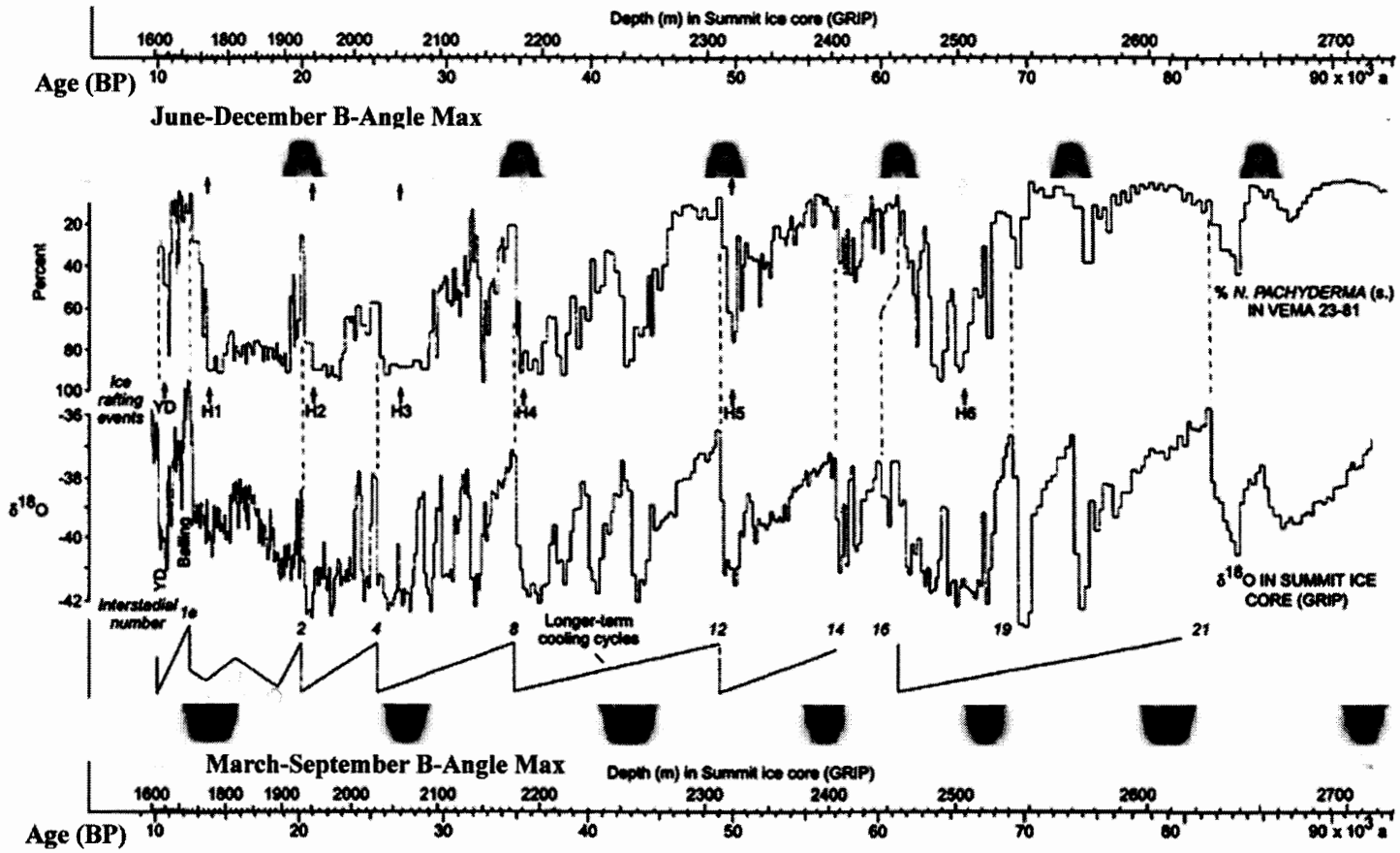

Figure 7 Comparison of times of the year of maximum B angle taken from peaks of curve 1 in Figure 13 (calculated by Dr.E. Myles Standish Jr. for this project) with the GRIP Greenland ice core temperature record as indicated by O18 and a deep sea core temperature record from the North Atlantic as indicated by foraminifera percentages (adapted from Bradley 1999). The bottom curve, also from Bradley 1999, shows general trends in temperatures. Note the general relationship of June-December B angle maxima to periods of rapid warming including some Heinrich events and the general relationship of March-September B angle maxima to cooing events between periods of rapid warming.

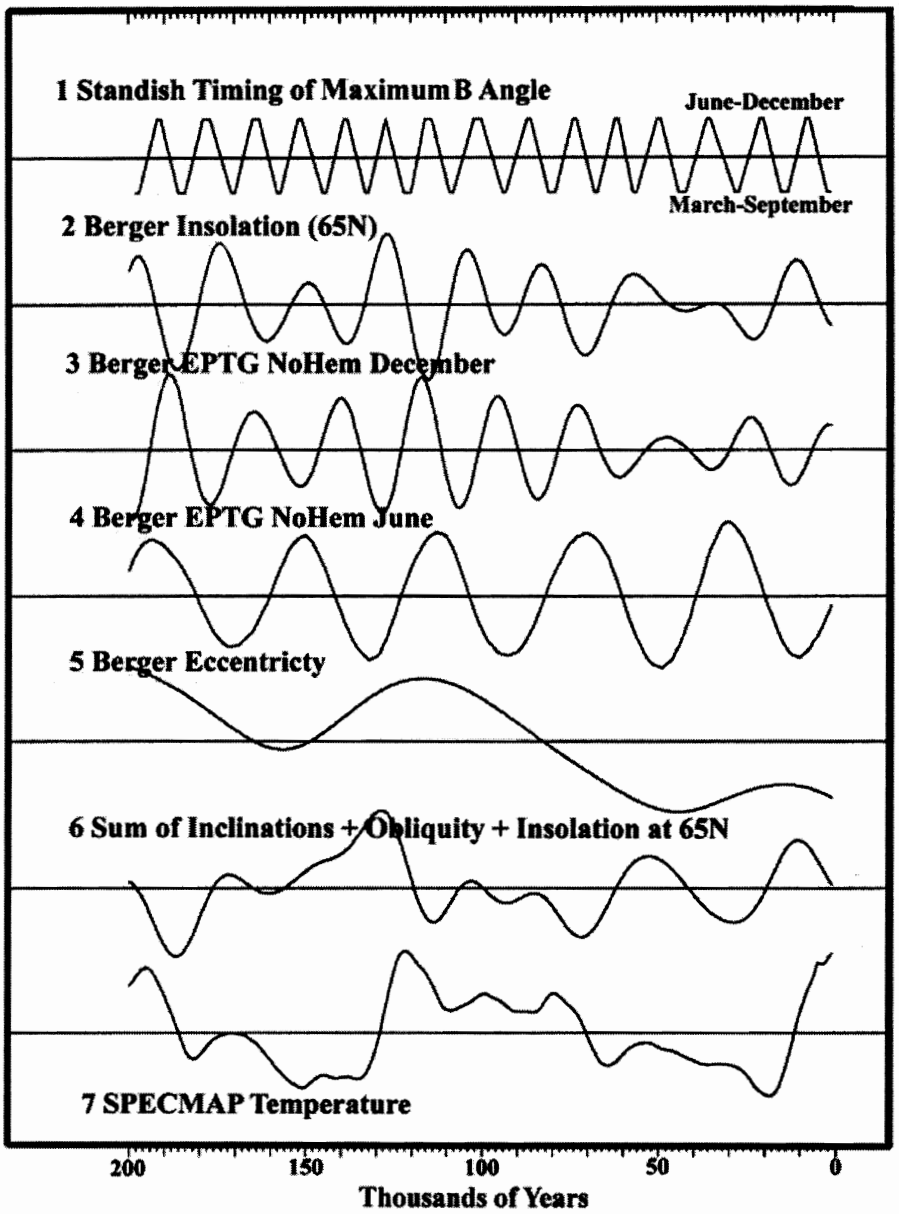

Figure 8 1. Curve of the time of the year of the maximum B angle with June-December as top points and March-September as bottom points (by E. Myles Standish Jr. for this project). 2. June insolation at 650 north latitude (by Berger, World Data Center-A for Paleoclimatology). 3. Equator to pole temperature gradient for Northern Hemisphere in December (from data from Berger, World Data Center-A for Paleoclimatology). 4. Equator to pole temperature gradient for Northern Hemisphere in June (from data from Berger, World Data Center-A for Paleoclimatology). 5. Orbital eccentricity of the earth (by Berger, World Data Center-A for Paleoclimatology). 6. Curve calculated from the sum of the inclination of the earth's orbital plane with relation to the invariable plane of the solar system + the inclination of the earth's orbital plane with relation to the equatorial plane of the sun + the earth's orbital obliquity (see Figures 5 and 6). The height of this curve is hypothesized to be directly related to geomagnetic strength. 7. SPECMAP paleotemperatures inferred from Atlantic Ocean sediment cores (by Duffy and Imbrie, World Data Center-A for Paleoclimatology).

6. The largest variations in the inclination related motions of the earth cause the largest variations in geomagnetism which cause the largest variations in GCR levels resulting in glacial-interglacial periodicities. In my curves, inclination with relation to the invariable plane plus inclination with relation to the solar equator establishes the basic beat frequency seen in paleotemperatures of alternating ~80,000 and ~120,000 year periods (see Figures 5 and 6). This is especially observable in comparisons of times of peak interglacial warmth. This is the first explanation for the origin of this beat frequency that I know of. Adding obliquity to the above mentioned curve gives a curve that includes the ~41,000 year periodicity that is present in glacial-interglacial cycles even when the ~100,000 year periodicities are not. The ~41,000 year cycle was dominant prior to ~800,000 years ago and one possible reason for the switch to~100,000 year cycles was the climatic effects of increasing mountain heights. Another can be seen in the curves. The values for inclination with relation to the solar equator and inclination with relation to the invariable plane were less immediately prior to this time and at other times possibly allowing obliquity to play a more dominant role (Figure 9). Adding summer insolation at 650N further increases the similarity to the SPECMAP curve by adding the precession related periodicities. Summer high latitude insolation values are matched in time and magnitude by corresponding winter equator to pole temperature gradient values that result in similar effects on climate (see Figure 8). Insolation fits in best at a 1/4 to 1/6 weighting. In the Milankovitch hypothesis, this is usually used as the primary determinant of the timing of glacial-interglacial periodicities. Compare the curve of summer insolation at 650N and my curve to SPECMAP. The origin of glacial-interglacial periodicities by changing levels of GCRs does not have the numerous inadequacies seen in the Milankovitch hypothesis as described by Karner and Muller (2000) and others.

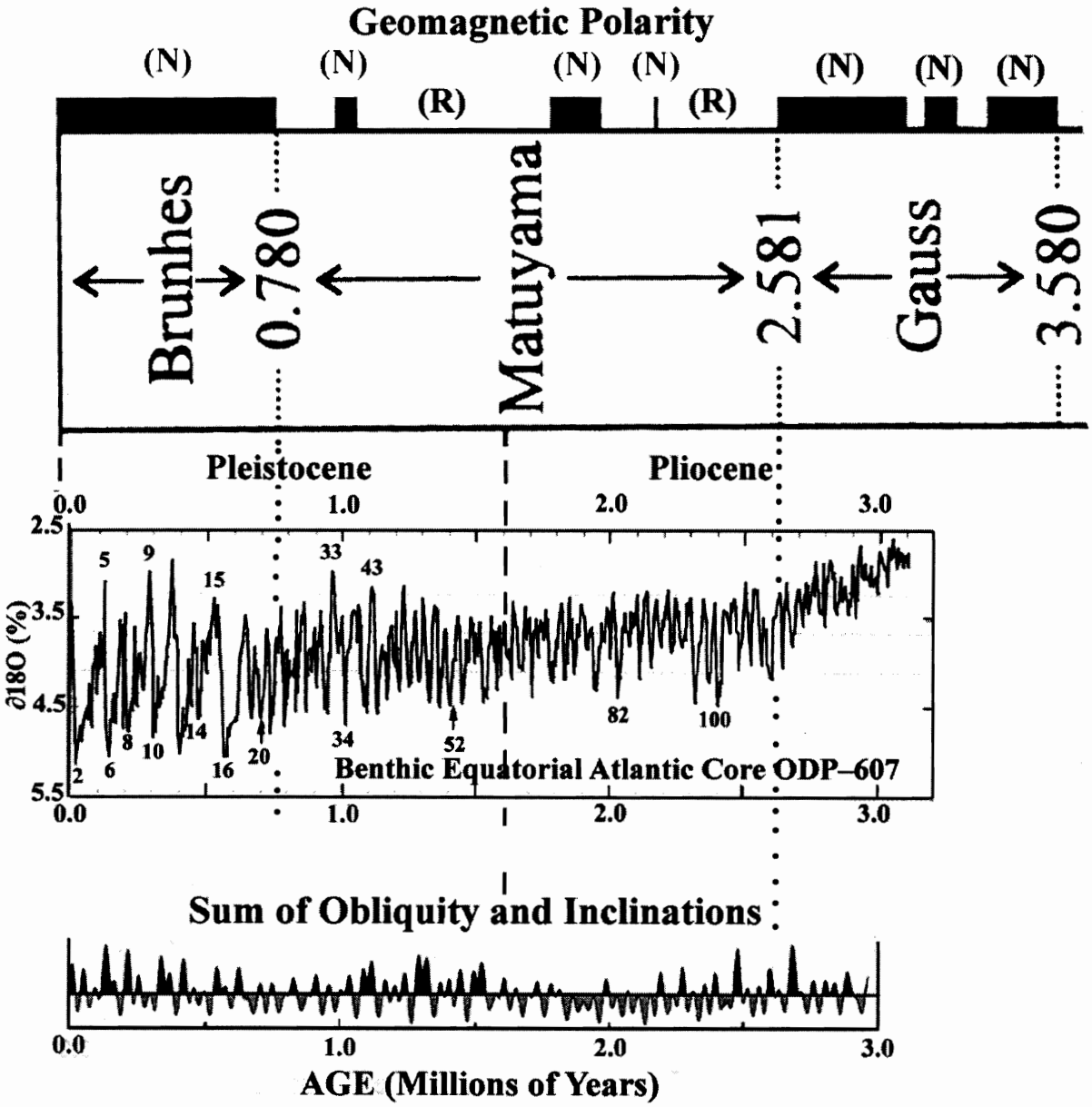

Figure 9 Comparison over 3 million years of sum of inclinations + obliquity curve, temperature records indicated by O18 from equatorial Atlantic deep sea core ODP-607 (adapted from Bradley 1999) and geomagnetic polarity (adapted from Merrill and others 1996). Note general relationship of greater amplitudes and more ~100,000 year glacial cycles in temperature variations curve with greater amplitudes in sum of inclinations + obliquity curve, especially in the last 1,200,000 years, and lower frequency of geomagnetic reversals in times of higher amplitudes in sum of inclinations + obliquity curve.

7. A ~ 412,000 year cycle is present. It is caused by changes in geomagnetism induced by the earth's orbital eccentricity. The effects of this cycle are not indicated in the inclination related curves presented here. The modulation of geomagnetism by the ~ 412,000 year cycle can be seen in Figures 10 and 11. The Stage 11 interglacial at around 400,000 years ago and the Holocene interglacial are considerably warmer than their inclination based curves on my figures indicate due to the highest geomagnetism induced by the lowest eccentricities of this cycle. The sea level was 15 to 20 meters higher in Stage 11 than it is today (Chappell 1998). That interglacial also lasted more than 40,000 years longer than the Holocene has so far (60,000 years in all) (Howard 1997). The glacials preceding these previously mentioned large interglacials are longer and colder than their curves indicate since geomagnetism appears to progressively decrease over most of the ~412,000 years, reaching its lowest point before rapidly rising to maximum levels (Yamazaki and others 1995) (Figures 10 and 11). The Stage 12 glacial that preceded the Stage 11 interglacial was the coldest on record with an ice volume estimated to be 15 to 20% greater than at the peak of the last glacial period and a sea level depression of 140 meters (Chappell 1998). This is 20 meters greater than that of the last glacial.

8. Records of paleomagnetism support the forcing of glacial-interglacial cycles by geomagnetically modulated GCR levels. Figure 11 includes an 800,000 year curve of geomagnetism, which is an integration of 33 records of relative paleointensity. The ~412,000 year cycle of geomagnetism is prominent in this curve of geomagnetism with peaks around 800,000 and 400,000 years ago and now and the beat frequency of alternating ~80,000 and ~120,000 year cycles can be observed within the last ~450,000 years. Within the last ~200,000 years, periods of glacial initiation appear to correspond to well known geomagnetic excursions. This indicates that at least one cause of geomagnetic excursions is the lowest of inclination values.

Figure 12 includes a curve of geomagnetism over the last 130,000 years. It is one of the most accurate and detailed available. Note how closely it matches the curve derived from the sum of inclinations plus obliquity values alone and the similarity of both of these curves to the Vostok Antarctic surface temperatures and Beryllium 10 record. Also note the thin spikes at ~120,000 and ~15,000 to ~10,000 years ago that may indicate the presence of short duration high values that exceeded the threshold for interglacial climates. The similarities between the curves in this figure provide strong evidence for the origin of glacial-interglacial periodicity through variations in GCR intensity modulated by geomagnetism.

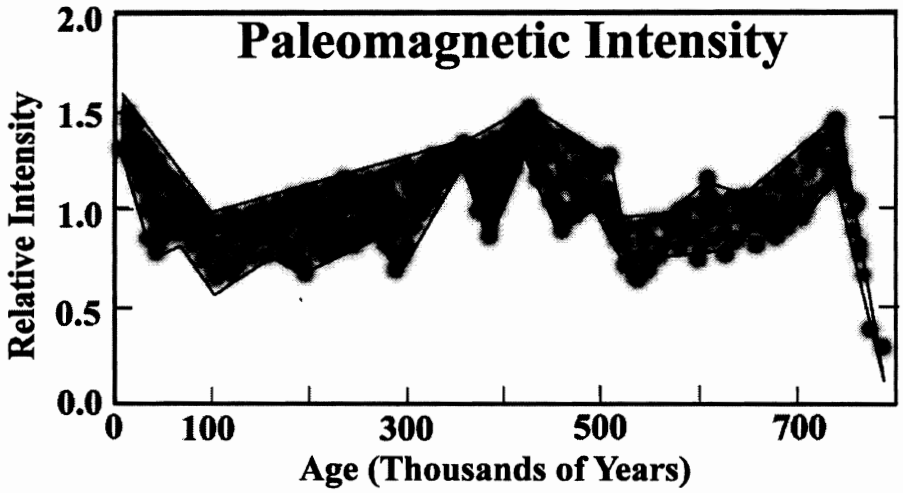

Figure 10 This is a curve of paleomagnetic intensity over the last 800,000 years that shows the effects of the ~412,000 year eccentricity cycle (adapted from Yamazaki and others 1995). Note the high points now, around 400,000 years ago and what may be around 800,000 years ago interrupted by a geomagnetic reversal. Also note the long term, progressively decreasing geomagnetism leading to the lowest values just before the fast increases around the times of maxima.

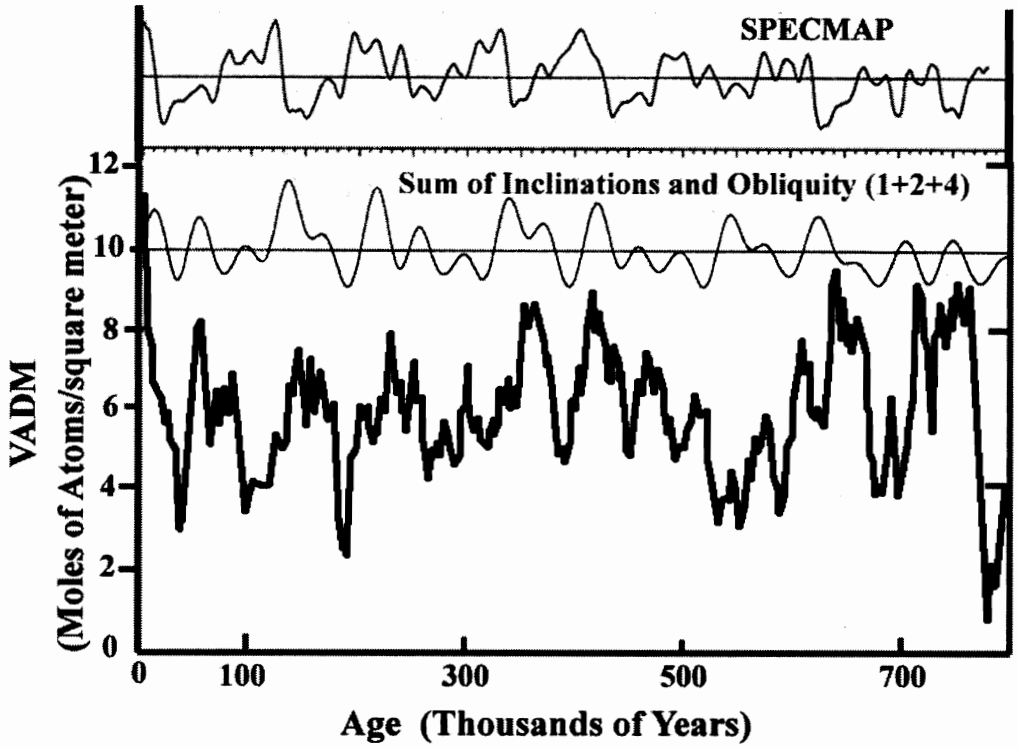

Figure 11 Comparison of 800,000 year synthetic curve of geomagnetism derived from 33 records of paleointensity (adapted from Guyodo and Valet 1999) with sum of inclinations + obliquity curve and SPECMAP curve of deep ocean core temperatures. Note general relationship of higher values on the sum of inclinations + obliquity curve with higher geomagnetism. Note how turns towards glacial or interglacial conditions generally occur in SPECMAP at minimal or maximal geomagnetic values respectively.

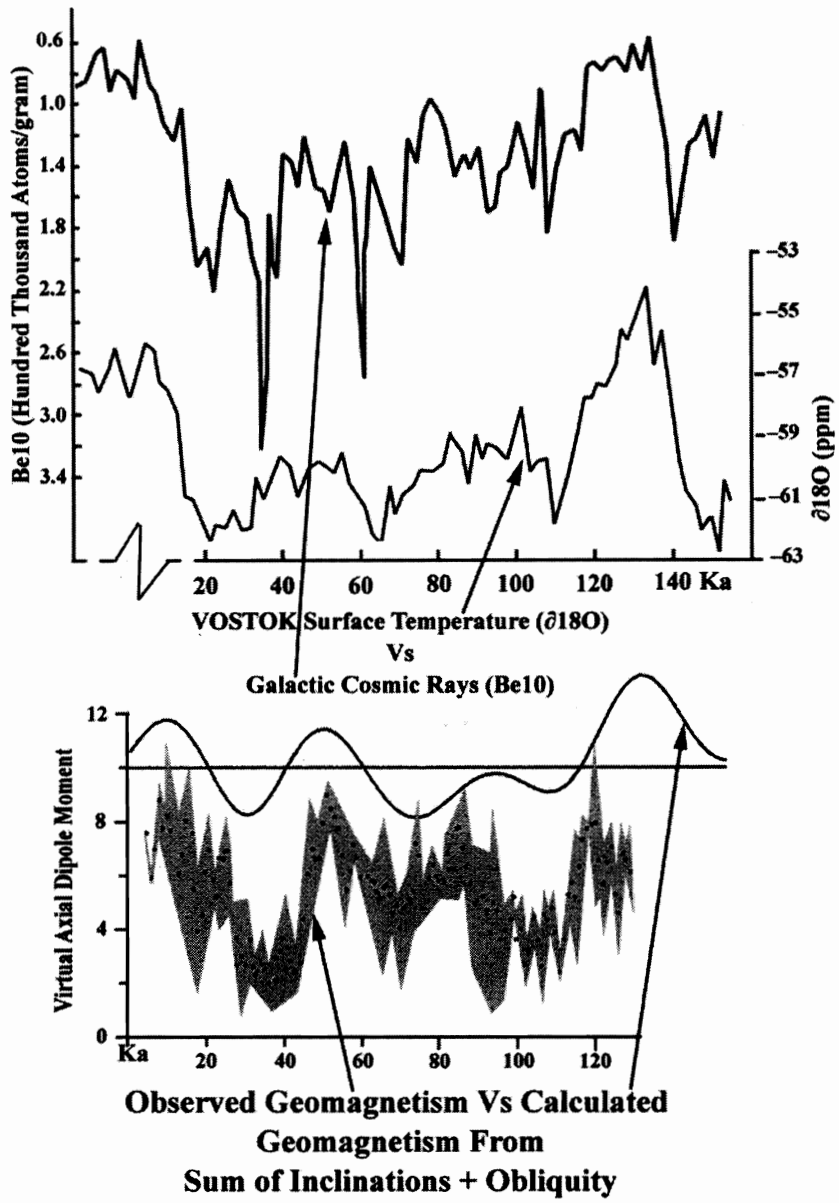

Figure 12 Comparison of observed geomagnetism obtained from four deep sea sediment cores from the Sulu Sea (Philippines) (adapted from Merrill and others 1996) with geomagnetism as indicated from the calculated sum of inclinations + obliquity curve. The geomagnetism curves are compared to temperatures as inferred from O18 levels from the Vostok Antarctic ice core and the Be10 concentration from the Vostok ice core which provides a record of galactic cosmic ray intensity (adapted from Raisbeck and others 1987). Note the inverted scale for the Be10 curve indicating greater galactic cosmic ray intensity in a downward direction. The sediment cores from the Sulu Sea show strong, stable magnetizations at high sedimentation rate and provide a geomagnetic history regarded as one of the most accurate available. Note the similarity between the curves providing evidence that inclinations + obliquity modulate geomagnetism, geomagnetism modulates galactic cosmic ray intensity, and galactic cosmic ray intensity modulates climate, in this case glacial-interglacial periodicity.

9. Calculations of the increases in ionization levels at glacial maximum are consistent with modulation of glacial-interglacial periodicities by GCRs. Data from Lingenfelter and Ramaty (1970) indicate that the GCR levels at the geomagnetism of the last glacial maximum (dipole moment of 1) at sunspot minimum would be approximately 200% of today's values as measured by C14 at 730 latitude. Data from Volland (1995) indicate that the atmospheric ionization at tropopause levels produced by 200% of today's GCR levels would be approximately 306% of current ionization levels.

At today's levels of geomagnetism, (dipole moment 8) there is approximately a 12% difference in GCR levels between sunspot maximum and minimum. Theoretically, there is currently about a 20% difference in ionization at tropopause levels between sunspot maximum and minimum, but a 50% difference has been reported (Tinsley and others 1989). At a dipole moment of 1, the differences between sunspot maximum and minimum would be much greater. Data from Lingenfelter and Ramaty (1970) indicate that the range in GCR levels would be approximately 243% of today's and data from Volland (1995) indicate that the theoretical range in ionization at tropopause levels at 730 latitude would be approximately 340% of today's. This is interesting because a 60 year tree ring record from Rancho La Brea in the Los Angeles area near the end of the last glacial period shows both substantially higher precipitation totals at times and substantially greater precipitation variability than today (Templeton 1977). The ~22 year cycle is evident in this record with the wettest periods (presumably antiparallel to parallel transitions) reaching a maximum of 75 inches per year and the driest periods (presumably parallel to antiparallel transitions) reaching a minimum of 10 inches per year.

10. Evidence for strong glacial ENSO-Cold Event conditions with frequent, short term oscillations to ENSO-Warm Event conditions can be found by looking at the paleoenvironmental evidence for glacial climatic conditions and glacial sea surface temperatures, especially in the tropical Pacific.

11. Consistently high relative humidities, condensation and equabilities produced by the high levels of GCRs present in glacial periods helps in the understanding of what are often said to be "paradoxical glacial environments with no modern analogs." These environments have been termed "heterogeneous mosaic savannas" (Guthrie 1984). This type of environment often appears to be associated with considerable dryness but with abundant superficial moisture available from condensation during periods of low precipitation. There is often evidence of less precipitation than today, but there is unusually high productivity and unusually high numbers and diversities of species, often including species together that are characteristic of very different environments today. Even environments at the margins of continental ice sheets were mostly free of snow cover year round and had much milder winter temperatures than the same areas do today. One need only to look at the present distribution of Pleistocene relict species, and the numbers and diversities of species per area to see the connection to consistently high relative humidity, condensation and equability.

12. The extinctions of Pleistocene megafauna that occurred around the start of the Holocene can be best understood by looking at environmental changes produced by changes in levels of GCRs. As mentioned previously, due to the ~412,000 year geomagnetic cycle, the Holocene is unique in having the consistently highest levels of geomagnetism since those of Interglacial Stage 11 around 400,000 years ago. These consistently high levels of geomagnetism have created a Holocene environment that is unique in its climatic stability and environmental segregation and zonation. The Holocene environment is very different from those of interglacials occurring at other times in the ~412,000 cycle which were characterized by climate fluctuations as great as those seen in glacial periods (Kerr 1993). It is only during the extreme climates of interglacials occurring during these highest periods of geomagnetism of the ~412,000 year cycle that the "heterogeneous mosaic savannas" of worldwide distribution that supported the Pleistocene megafauna largely disappeared.

The last major extinctions and migrations to occur before those of the last glacial-Holocene transition were the Irvingtonian which occurred between Glacial Stage 12 and Interglacial Stage 11. This was the last time geomagnetic conditions, and hence environmental conditions, were similar to those of the late glacial-Holocene transition.

The fact that the Holocene is unique among the three most recent interglacials negates one of the main arguments in favor of Pleistocene overkill and other hypotheses for the late Quaternary extinctions not involving major changes in environmental factors. That argument is: "the megafauna survived other interglacials, so the transition from the last glacial to Holocene interglacial environmental conditions could not have been a major factor in these extinctions."

The start of civilization coincides with the decline of the "hererogeneous mosaic savanna" and the extinction of the megafauna. This "fall from Eden" was probably a major factor in the start of agriculture. Other factors were the simplification and zonation of ecosystems and the anomalous stability of Holocene climate, both of which also made a sedentary existence in optimum areas and agriculture to augment environmental deficiencies desirable.

References

Anderson RY. 1992. Solar variability captured in climatic and high-resolution paleoclimatic records: a geological perspective. In: Sonnet CP, Giampapa MS, Matthews MS, editors. The Sun in time. Tucson (AZ): University of Arizona Press. p 543–61.

Bradley RS. 1999. Paleoclimatology, reconstructing climates of the quaternary. International Geophysics Series. Volume 64. Harcourt-Academic Press.

Chanin M-L. 1993. The role of the stratosphere in global change. NATO ASI Series. Volume 8. Springer-Verlag.

Chappell J. 1998. Jive talking. Nature 394:130–1.

Courtillot V, Le Mouel JL, Ducruix J. 1982. Geomagnetic secular variation as a precursor of climatic change. Nature 297:386–7.

Glanz J. 1999. Landscape changes make regional climate run hot and cold. Science 283:317–20.

Guthrie RD. 1984. Mosaics, allelochemics and nutrients: an ecological theory of Late Pleistocene megafaunal extinctions. In: Martin PS, Klein RG, editors. Quaternary extinctions, a prehistoric revolution. Tucson (AZ): University of Arizona Press. p 259–98.

Guyodo Y, Valet J. 1999. Global changes in intensity of the Earth's magnetic field during the past 800 kyr. Nature 399:249–52.

Herman JR, Goldberg RA. 1978. Sun, weather and climate. National Aeronautics and Space Administration.

Howard W. 1997. A warm future in the past. Nature 388:418–9.

Karner DB, Muller RA. 2000. A causality problem for Milankovitch. Science 288:2143–4.

Kerr R. 1993. Even warm climates get the shivers. Science 261: 292.

Kerr RA. 1999. A new force in high-latitude climate. Science 284: 241–2.

Klyashtorin LB. 1998. Long term climate change and main commercial fish production in the Atlantic and Pacific. Fisheries Research 37:115–25.

Landscheidt T. 1998. Solar activity: a dominant factor in climate dynamics. Available via the Internet: http://www.microtech.com.au/daly.solar.htm. Accessed on Dec. 18, 1998.

Lingenfelter RE, Ramaty R. 1970. Astrophysical and geophysical variations in C14 production. In: Olsson IU, editor. Nobel Symposium 12; Radiocarbon variations and absolute chronology. J Wiley & Sons, Inc. p 513–35.

Mantua NJ, Hare SR, Zhang Y, Wallace JM, Francis RC. 1997. A Pacific interdecadal climate oscillation with impacts on salmon production. Bulletin of the American Meteorological Society 78:1069–79.

McIntosh PS, Thompson RJ, Willock EC. 1992. A 600-day periodicity in solar coronal holes. Nature 360:322–4.

Merrill RT, McElhinny MW, McFadden PL. 1996. The magnetic field of the Earth: paleomagnetism, the core, and the deep mantle. Academic Press.

Muller RA. 1997. Glacial cycles and astronomical forcing. Science 277:215–8.

Raisbeck GM, Yiou F, Bourles D, Lorius C, Jouzel J, Barkov NI. 1987. Evidence for two intervals of enhanced 10Be deposition in Antarctic ice during the last glacial period. Nature 32:273–7.

Santer BD, Wigley TML, Gaffen DJ, Bengtsson L, Doutriaux C, Boyle JS, Esch M, Hnilo JJ, Jones PD, Miihl GA, Roeckner E, Taylor KE, Wehner MF. 2000. Interpreting differential temperature trends at the surface and in the lower troposphere. Science 287:1227–32.

Soon W, Baliunas S, Posmentier ES, Okeke P. 2000. Variations of solar coronal hole area and terrestrial lower tropospheric air temperature from 1979 to mid-1998: astronomical forcings of change in earth's climate? New Astronomy 4(8):563–79.

Stricherz V. 1999. UW scientists say Arctic oscillation might carry evidence of global warming. News and Events. University of Washington 1-3.

Svensmark H. 1998. Influence of cosmic rays on Earth's climate. Available via the Internet: http://www.millengroup.com/repository/global/CREC.html. Accessed on Feb. 15, 2000.

Templeton B. 1977. Comparative precipitation values in Los Angeles, 1877-1966 and approximately 15,000 years B.P. In: Stout ML. 1977. California Geology 30(5):99–105.

Tinsley B, Brown GM, Sherrer PH. 1989. Solar variability influences on weather and climate: possible connections through cosmic ray fluxes and storm intensification. Journal of Geophysical Research 94:(14)783–92.

Vanyo JP, Paltridge GW. 1981. A model for energy dissipation at the mantle-core boundary. Geophysical J. Royal. Astronomical Society 66:677–90.

Veretenenko SV, Pudovkin MI. 1995. The galactic cosmic ray Forbush decrease effects on total cloudiness variations. Geomagnetism and Aeronomy 34(4):463–8.

Volland H, editor. 1995. Handbook of atmospheric electrodynamics. Volume 1. CRC Press.

Yamazaki T, Ioka N, Eguchi N. 1995. Relative paleointensity of the giomagnetic field during the Brunhes Chron. Earth and Planetary Science Letters 136:525–40.

Water Year 2000—A February Save

Maurice Roos

Water year 1999–2000 was the second La Niña year in a row. Looking at total seasonal amounts, it was about as close to average as one could expect in California. Most of the State was in the normal range of precipitation this year. This in itself was unusual. The statewide snowpack water content on April 1 was average too, about 10% under last year's 110% peak. But the southern Sierra pack was about 30% more than in 1999, which will provide better supplies in the Fresno to Bakersfield area.

The total seasonal amounts mask some strong monthly departures. Most of the rainy season was dry, especially in the south where drought prevailed until January. December, especially, was extremely dry. We were saved from a bleak water supply outlook by a wet February, double the monthly average. In fact most of the rain and snow of the season fell during a 60-day window from about mid-January to mid-March.

For the four rivers of the Sacramento River system the estimated runoff is slightly under 19 million acre-feet, about 105% of average. Although forecasted on May 1 to be barely over the threshold of "wet," actual observed runoff slipped into the "above normal" category (Figure 1). If it had remained wet, this would be 6 years in a row, unprecedented in the instrumental record. The reconstructed record from tree rings indicates a 6-year run of wet years in 1801–1806 and also 1601–1606.

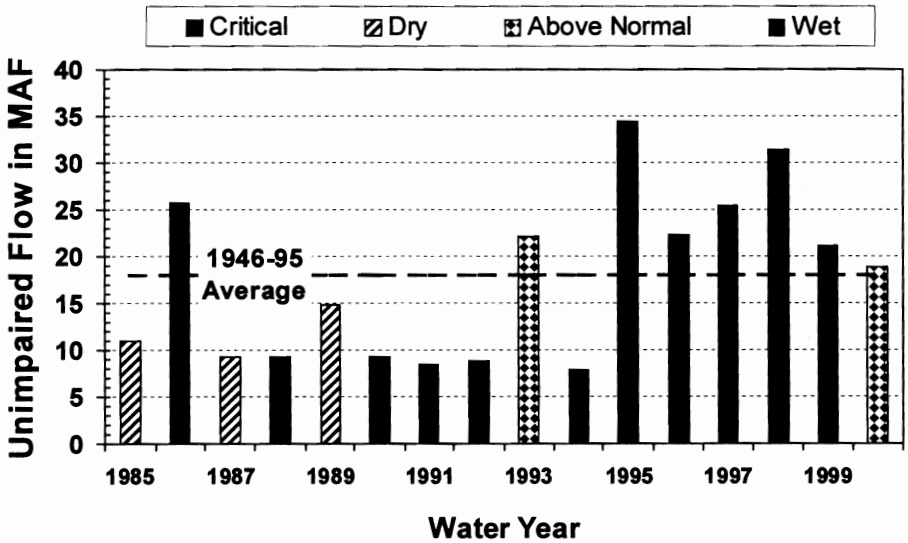

Figure 1 Sacramento River runoff. Sum of Sacramento River above Bend Bridge, Feather River at Oroville, Yuba River at Smartville, and American River at Folsom. 40-30-30 year types are based on observed flow.

Again we had the wetter north-drier south pattern typical of La Niña years. Statewide seasonal precipitation for the water year ending September 30 was 95% of average, ranging from 115% across the middle (Central Coast and San Joaquin River regions) and 110% in the northern Sierra Nevada to a poor 25% in the southeastern desert region (Figure 2).

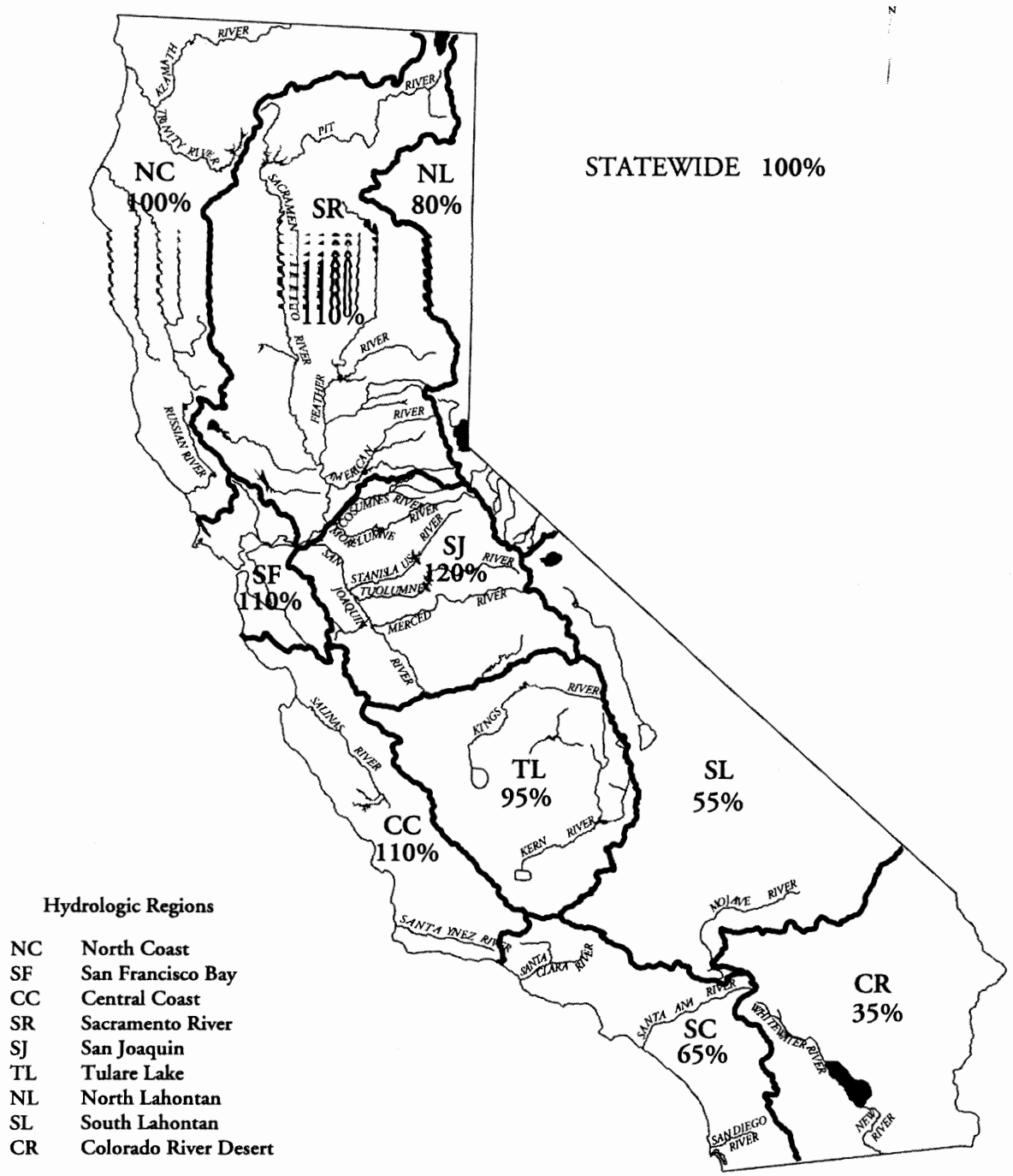

Figure 2 Seasonal precipitation in percent of average to date, October 1 through July 31, 2000

The mountain snowpack water content was 100% of average on April 1, compared to 110% in 1999. But by May 1, the pack had diminished to about 75% of average, compared to 120% last year. Last year the peak snowpack occurred late, in mid-April. This year melting began early, in mid-March, abetted by northeasterly winds, strong sunshine, and warmer weather. We believe sublimation losses were large this year, which may have accounted for the overforecast on the upper Sacramento and Feather River basins in the northern Sierra; in most years those losses are not a significant factor in predicting runoff.

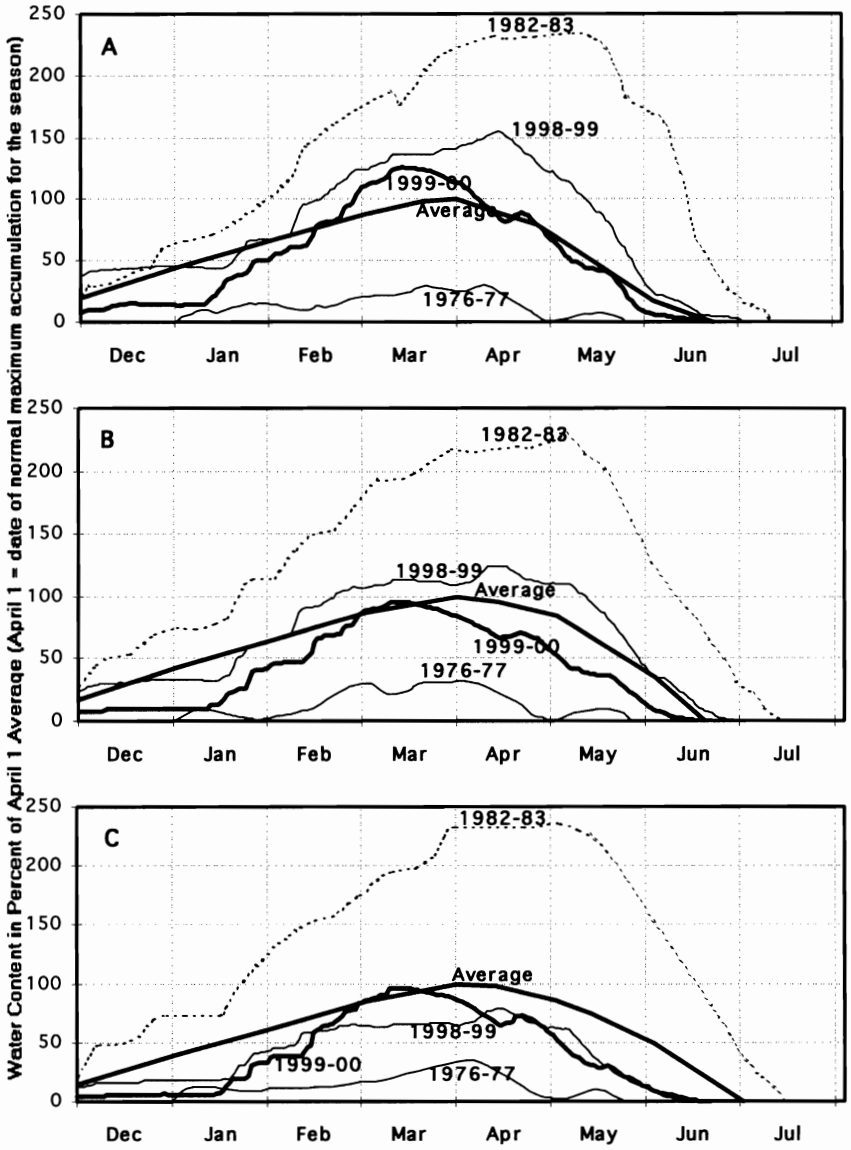

Figure 3 California snow water content, June 19, 2000: (A) Northern Section—Trinity through Feather and Truckee (northern Sierra 8-Station Index is 115% of average); (B) Central Section—Yuba and Tahoe through Merced and Walker (Fresno precipitation is 120% of average); (C) Southern Section—San Joaquin and Mono through Kern and Owens (Bakersfield precipitation is 90% of average. Percent of normal water content for dates shown are not applicable.

The year was a mellow one as far as flood threats. There was some high water on the major rivers, mostly in February and early March, with enough activity to keep flood forecasters busy. The Sacramento River rose just above warning stage in February, then receded. Very few flood stages occurred and flood related problems were at a minimum.

Reservoir storage started well with good carryover from the previous year, generally 110 to 120% of average. As we entered the main irrigation season on April 1, statewide storage was 115% of average, the same as in 1999 and 1998. Most users in the State had adequate water supplies. However, Central Valley Project San Joaquin Valley west side customers had to take deficiencies up to 35% and State Water Project contractors will probably only get 90% of their requests. This was due to Delta constraints on exports. By September 30, statewide storage had decreased slightly to about 110% of average for the date.

Table 1 shows a comparison of hydrologic parameters for water year 2000 and the previous six years. A few of the numbers have been revised from a similar table in last year's PACLIM report to incorporate some revised data.

Table 1 Comparisons of hydrologic parameters for 1994 through 2000

	Percentage of Average (unless noted)						
Year	*2000*	*1999*	*1998*	*1997*	*1996*	*1995*	*1994*
Statewide							
Precipitation	95	95	170	125	110	165	65
April 1 Snowpack	100	110	160	75	95	175	50
Runoff	95	110	175	145	125	180	40
Reservoir storage, Sept. 30	110	118	136	104	120	130	73
Reservoir storage, MAF	----	(25.6)	(29.6)	(22.7)	(26.0)	(28.1)	(15.9)
Regional							
Northern Sierra precipitation	113	110	165	138	123	171	64
8 Station Index, inches	----	(54.8)	(82.4)	(68.7)	(61.3)	(85.4)	(31.8)
Sacramento River	104	117	174	141	123	191	43
Unimpaired runoff, MAF	18.7	(21.1)	(31.5)	(25.4)	(22.3)	(34.4)	(7.8)
San Joaquin River	103	104	183	167	127	217	45
Unimpaired runoff, MAF	(5.9)	(5.9)	(10.4)	(9.5)	(7.2)	(12.4)	(2.5)

Cloud Seeding

It might be of interest to examine cloud seeding projects and where they were operated in California this year. In all, 13 projects operated at least some of the time, mostly seeding with silver iodide to try to provide more rain and snow for water supply and hydroelectric power production. A new avenue of research could evaluate how effective these projects have been in California; however, the job would be difficult. Most of them have been running many years and the broad geographical coverage seems to rule out the traditional target and control area evaluation.

Long Range Weather Forecast Evaluation

A few thoughts about long range weather forecasting. For a number of years we have been trying to keep up with advances in long-range weather forecasting. Some of you are aware that there was a 15-year experiment ending in 1993 with Scripps doing quarterly seasonal forecasts. In the mid-1990s the NWS Climate Prediction Center started a renewed emphasis on such forecasts. I went through four years of CPC forecasts, looking at the 1 month, 1 to 3 month, and 4 to 6 month outlooks (Table 2). I am not exactly sure how best to evaluate these. Most of them show some skill with a small shift in probabilities, which is not enough to be useful for water project operators.

One way to look at these forecasts is to see how often they point the right direction, whether wet or dry. Using northern Sierra Nevada precipitation as a start, I come up with the following table. Interestingly, the better skills seem to be in the longer periods as opposed to those for the next month. We noted the same for Art Douglas, who has continued making the same kind of forecasts formerly produced by Scripps. There is some skill here, but it may just be the effect of very large ENSO signals in three of the four years of my evaluation.

Table 2 Evaluation of the National Weather Service Climate Prediction Center forecasts

	Northern Sierra 4 Years: 1996–1999				
Number of months	*Number*	*Number with signal*	*Right direction*	*Wrong direction*	*Approx. skill R-W/24*
1	47	17	10	7	0.13
1 to 3	48	22	14	8	0.25
4 to 6	47	16	12	4	0.34

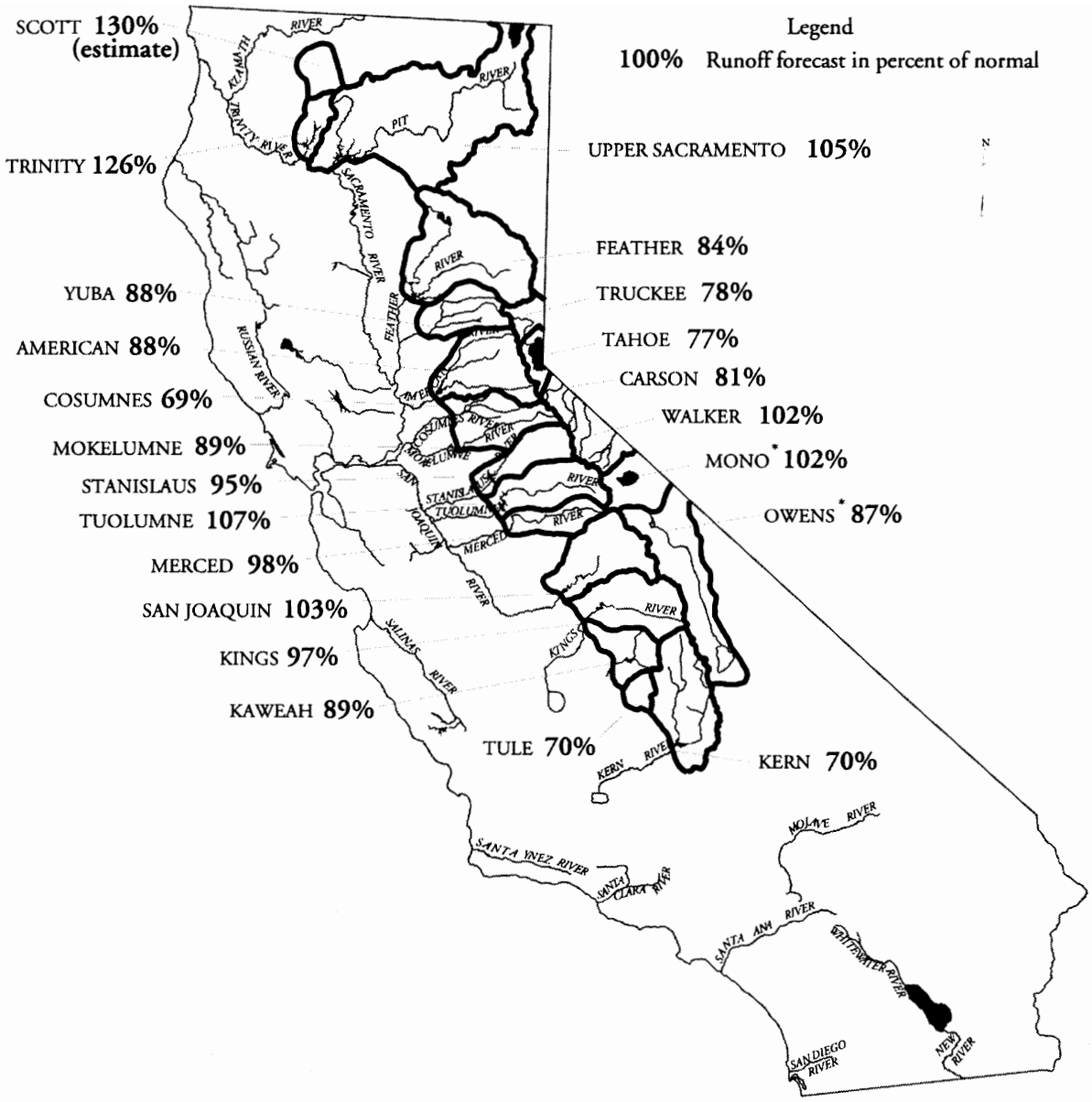

Figure 5 Estimated water year 2000 April through July unimpaired snowmelt runoff

Forecasting Ocean Ecosystem Responses to Various Climate Clocks

Gary D. Sharp, Leonid Klyashtorin, and James Goodridge

Abstract

Regime shifts occur on several time and space scales. Identifying the precursors, or other indicators to provide forecast capability is key to managing anthropogenic effects on natural ecosystems. The Length of Day (LOD) or 1/earth's rotation rate appears to offer some insights into future ecosystem changes. There are several distinct patterns of interest to California in particular, and North Pacific, and Global fisheries, in general, that are closely related to the changes in LOD, as well as the dominant wind-field patterns over the region. We have identified these as useful indicators of Climate Regime Shifts, as well as precursors of fisheries ecosystem responses on decadal scales. We are certain that changing LOD per se, is *not* the direct cause, but is an integrated signal that provides insight into the generic changes in ocean forcing. These forces include wind speed and direction, temperatures along coastal habitats, and upwelling event frequencies, all of which cause ecological cascades on all time scales. We are also becoming convinced that most of the Climate Forcing is initiated by Polar Cold Events, and resulting subsidence—spawning Mobile Polar Highs (MPH). These, in turn, sweep equatorward, to gather surface energy to eventually energize the Trade Winds. If these MPHs are frequent and intense enough, they continue their equatorward transfers. There they encounter moisture laden frontal clouds that result from Equatorial Deep Convection, which enhance their transport of equatorial heat-energy poleward. Regimes shifts can be measured in terms of MPH frequencies and intensities. Of course Equatorial heating and Warm Pool Dynamics are also part of the processes involved, creating periods with more Equatorial Deep Convection (low SOI), and periods of lesser EDC (high SOI). These create Bipolar Ocean Climate regimes, dominated by either East-West or Pole-Equator winds. Transition periods are well studied, in ecological terms, simply because there are usually at least two faunas in each marine ecosystem, one of which benefits from either side of the climate-driven physical processes, changes in precipitation, storage, and water flow rates from rivers and streams, as well as the coastal ocean processes. Many migratory predator species are closely tuned to these changes, and also act as indicators of changes, often only identified after the fact by oceanographers and climate researchers.

Introduction

Growing recognition of climate-components of ecosystem forcing has re-oriented fisheries science to time and space scales encompassing decades, centuries, and millennia. Meanwhile components of aquatic ecosystems live from moment to moment within continuous variabilities imposed upon them, or they are soon removed. The dilemma is not that one scale or another is more relevant, but that all must be accounted for. Many proxy records record population variations on decadal and longer time scales, comparable to varved anoxic sediments in marine environments. Longer term climate indicators point to direct solar forcing within a global setting beset by volcanic and geophysical forcing. Correlations between Length of Day, east and west Pacific SST oscillations and other records lend insights into subsequent ecological responses. ENSO Warm and Cold events are apparently not related to global mean temperatures, but to pole-to-equator gradients. These in turn induce ecological responses on characteristic time scales for known physical phenomena: deep convection from warm ocean regions, passing poleward and eastward into the atmosphere; upper ocean dynamics as a result of cloud mediated ocean surface heat balance; and both gravity and planetary waves—the first within the seasonal cycle, the latter moving upper ocean heat into higher latitudes over periods of more than a decade; and the deep ocean conveyor processes that can take centuries to achieve energy deliveries and related responses. Within all this, the ecological subsystems operate on their daily and seasonal bases, providing challenges to all who would invoke equilibrium processes to explain their changes.

The Medieval Warm period peaked in about AD 1150. The several centuries of climate cooling that followed corresponds with an eventful period in which human populations were vastly changed. Many regions had swollen, crowded human populations as a result of this relatively benevolent warm climatic period. In the last two centuries of the Medieval Warm period Vikings explored the North Atlantic, reaching Iceland, and North America. In AD 990 they colonized Greenland. During this same period highland Peru was in a drought, while coastal Peru was wet and thriving (Thompson and others 1995, 1998). As the cooling ensued, entire regions of Europe and Asia were unable to produce adequate food for their inhabitants, and local famines ensued. Europeans were forced to spread out in search of resource abundances and trade opportunities. The Age of Exploration—and exploitation—began, with mixed results. Starting in the 13th century, bubonic plague spread from China via Genoese merchant vessels, arriving first in Cyprus, then Florence. It was then "traded" over the Swiss Alps, into Germany, France and England, then Poland and Russia, to eventually come full circle, back to China.

Europe was repeatedly decimated by disease and famine. Those who worked the fields and tended the flocks were most affected. Their services became more valued and sought after. The age of feudal self-sufficiency had ended (Braudel 1982). During the resulting social upheavals many people fled to the cities. Situations over the world were not all the same. During the early 1300s, while Europe, China, and Japan experienced repeated famines, the Aztecs founded Tenochtitlan (Mexico City) on the banks of Lake Mexcoco. The highlands of Ecuador and Peru were again wet, and the Inca empire flowered, while the coastal cultures failed. Global cooling progressed, enhanced by periods

of lower solar intensity, and most of the planet's peoples were affected, one way or another.

Since the mid-14th century collapse of the Baltic herring and the advent of the Hanseatic League, shipping records documented the rise and fall of Scando-European fisheries and the epochal shifts from one resource to another, as the environment changed. As fisheries evolved and covered more of the earth's oceans, patterns of exploitation complicated the interpretations of these observations. It is now clear that over-exploitation has its own fingerprints on these fish populations (Sharp and Csirke 1983; Csirke and Sharp 1983; Lluch-Belda and others 1989, 1992).

Among the many links between the only heat source in our galaxy and the earth's oceans lies one of the great scientific problems facing all of us that study population variations. What allows the usually warm, wet earth to cool? Svensmark and Friis-Christensen (1997) have provided a common cause in the relationship of galactic cosmic rays and cloud formation within the high latitudes. We hypothesize that this may well be the critically important link to all scales of climate, ocean variability, and society.

At the end of the two recent Ice Ages a series of human population expansions from one continent to another occurred. The series of climate processes and events that have been recorded by various means over the recent 1,100 years have been very important in their shaping of human society (Figure 1). As Europeans spread out onto the oceans and around the world, the more ancient and sophisticated east Asian cultures had terminated their ocean exploration efforts, and locked themselves away from their neighbors (McDougall 1993). Examination of longer-term proxy records show that observed variations of the relatively short period since the Medieval Warm period were much less vigorous than previous periods of change. As strenuous as the period has been, we have experienced a relatively "Adagio" movement in climate change within the earth's Glaciation-Interglacial themes within the Galactic Fugue. Meanwhile, humanity's growth has crowded the stage with many new noisy instruments. However, we are learning that we do not hold the baton. In fact, we are not really sure what all the external forces are that cause the ebb and flow of earth's climate, or even all the links within the oceans and atmosphere.

The Fugue

Climate change is neither new, nor unexpected. However, it is important to recognize that the earth is warm enough to maintain substantial liquid water. It is a relatively warm, wet planet that experiences occasional sharp excursions into cold states. It cannot be the other way around, or life as we know it would have never evolved. The survival issues of today are much the same as they have been over the several million years that hominids have graced the earth. The result has been that every time there is a protracted benevolent climate period, humans tend to experience "good times." Regionally, local social units are able to obtain abundant food and shelter, to reproduce freely and thrive. As their numbers grew, they spread out over the available terrain.

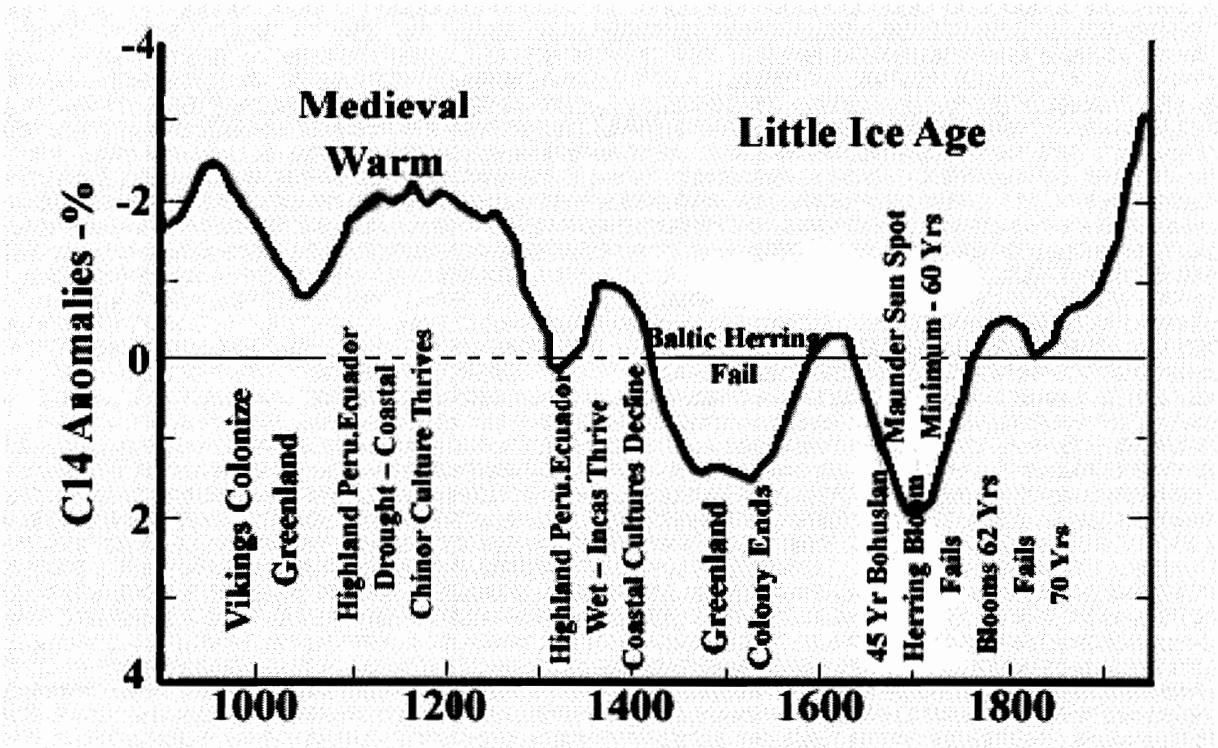

Figure 1 is a plot of the proxy 14C solar activity record of the last 1,100 years. (Note that the axis for the C14 production has been reversed.) The Maunder minimum refers to the period 1645-1715 when very few sunspots where observed. During this period the production of C14 was very high, indicating lower solar activity. The periods of approximate rise and fall of colonies of people in both Greenland (Svensmark and others 1987), and Northern Peru (Thompson and others 1989, 1993, 1995, 1998) since the Medieval Warm Period are noted using text. Baltic herring periods are also indicated for the related period.

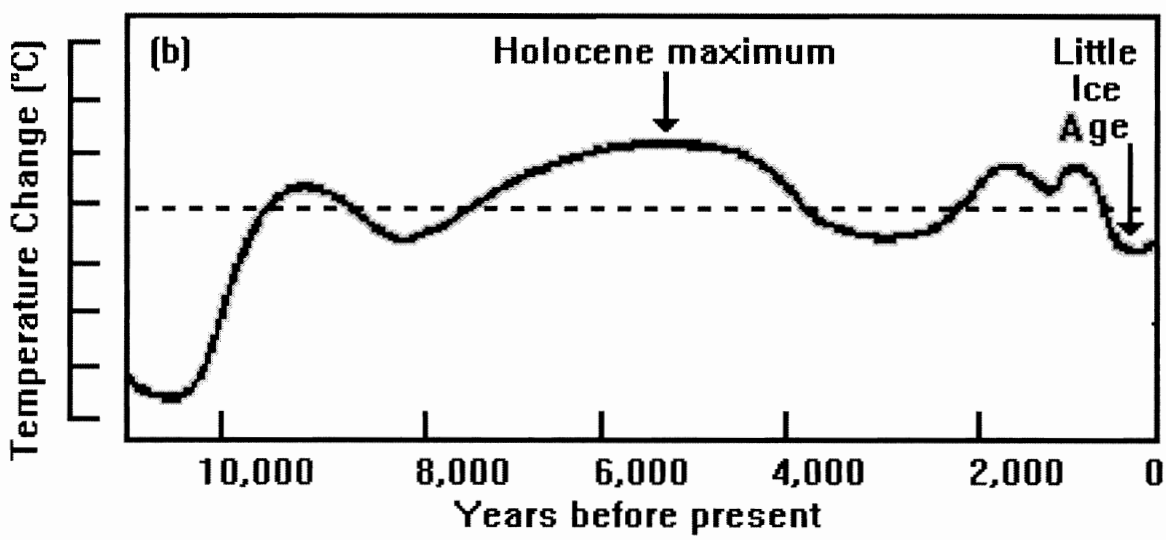

Figure 2 Throughout the Holocene Period there also have been cooler, less benevolent climatic epochs that each caused major societal disruptions.

The recent 11,000 years, the Holocene Period (Figure 2), denotes the warmer period of the deglaciation from the most recent Ice Age. The Holocene is also the context of the general transition of human cultures from mobile hunting and gathering stages to "civilization." The formations of large settlements and agriculture go hand in hand. Each city developed its own modes and specializations. Artisanal skills and services were traded or bartered for living quarters and food.

The Holocene temperature maximum about 5,000 years ago was also the period in which most Old Cultures became civilizations, that is, they settled to build cities, and created trade centers where artifacts from weavers, potters, weapons makers, and other services became available. Hunters, fisherfolk, and tenders of various flocks still provided meat and fish. But now farmers provided much more steady flows of grains and food crops than ever possible before. They were, respectively, less mobile, hence more associated with population centers.Of course, underlying all this there was also a much higher frequency climate variability (Dean and others 1984) that will be discussed, in turn.

The growth of cities and city-states parallels the longer periods of warm, wet climate that affected specific regions. Histories of the rise and fall of these early city-states are partially documented in the writings and scriptures of various scholarly and educated classes that were supported by the trade activities carried out within and between widespread and diverse cultures. Subsistence fisherfolk had long supplied major protein resources for riverside and coastal communities.

They also enjoyed the warm, wet epochs, and thrived. The usual result was for entire waterways to become saturated with settlements and subsistence fisherfolk. The result over several millennia was their inevitable encroachment onto one another's fishing ground. Sometimes major conflicts resulted, particularly as neighboring but disparate cultures grew, and more fish was needed to supply local needs. The emergent civilizations were in direct competition for resources at their spreading boundaries. There were few places around the world where this was not the case, even before the Age of Exploration began, except for some distant offshore islands and Antarctica. For example, the widely separated Pacific Islands were colonized only a few centuries before the Medieval Warm period, and were often well organized into rival clans. Man learned long ago to cope with most decreases in local productivity by shifting either people or food acquisition technologies from any one location to another, wherever opportunity emerged. The result was the spread of humankind over the planet, once ocean navigation was possible. Some extreme devastations occurred of, if not pristine, formerly more productive ecosystems and habitats. Early Russian explorers of Alaska dominated some of the existing cultures, along the Aleutians and Alaskan coastline, but met with violent resistance from the Tlingit of southeastern Alaska and Queen Charlotte Islands, sending them homeward for help (McDougall 1993). As Russia, England and Spain explored the Americas, networks of fishers were found all along the coastal ocean and river shorelines from the Arctic to Tierra del Fuego. They discovered trade systems in place between coastal fishing cultures and upland hunters and gatherers. These isolated cultures used primitive tools and old technology.

The recent 250 years has been one of the most rapidly changing periods in human history. The advent of science, engineering innovations, and the ability to navigate to and from any location on earth made up for most of the negative regional responses to regional climate changes. The ecological consequences have been most severe. The issues are certainly not limited to fisheries, but include large mammals, forests, and many bird populations. The problem is no longer "where to next?" Most options have already been taken. We must change our strategies.

We need to learn to maintain some semblance of habitat diversity so that options will be available for those species that are specialized, and need to be able to move with the changing climate patterns. The see-saw of the Glacial-Interglacial time-scale warming and cooling processes due to various unaccounted for dynamics is among the least discussed public issue. These other forcing phenomena must be accounted for if we are ever to understand, predict, and cope with the inevitably changing patterns, whether on millennial, centennial, decadal, seasonal or daily time scales. Modeling climate using simplistic concepts, using only readily accessed data, is not a legitimate substitute for real science. We need to define the links, event triggers, and monitoring points to give us the ability to track present status within evolving patterns, and identify probable transitions.

One of the problems, of course, is the poor understanding of long-term ocean motion, and its relation to climate change. Among the more insightful and integrative concepts relating ocean motion to climate change was Wallace Broecker's (1987a, 1987b, 1991) thesis about the Ocean Conveyor system. The Ocean Conveyor is driven by thermohaline circulation, primarily related to high latitude air-sea interactions that reflect the multiple roles of polar heat loss, and subsequent subsidence, to force the process of Deep Water formation and surface-to-atmosphere heat transfers. The two major locations of Deep Water formation are the Antarctic continental ice pack edges (Broecker and others 1999), and the winter Greenland Sea, north of Iceland. What are the sources of the surface winds that act to evaporate, thus cool and concentrate the Deep Water?

We believe, also, that Marcel Leroux (1999) has clarified that question, and several others, in his recent book entitled *Dynamic Analysis of Weather and Climate*. He provides the most probable connections via Polar Cooling Events, as manifested by what Leroux labels Mobile Polar Highs (MPHs). These are the results of patterned Polar heat loss, chilling the air, causing subsidence and creating cold dense air, that travels eastward, and equatorward, to interact with the terrain and oceans. Over the oceans, the first consequences are evaporative heat loss as a result of the change of state from either ice or liquid water to water vapor. The frequency and intensity of MPH formation is a consequence of whatever process or processes that regulate radiative energy budgets at the poles. We also respect Broecker's efforts to explain longer-term climate modulations within earth's own ocean-atmosphere system, but find it difficult to explain without dealing with causalities of varying polar heat loss (Figure 3).

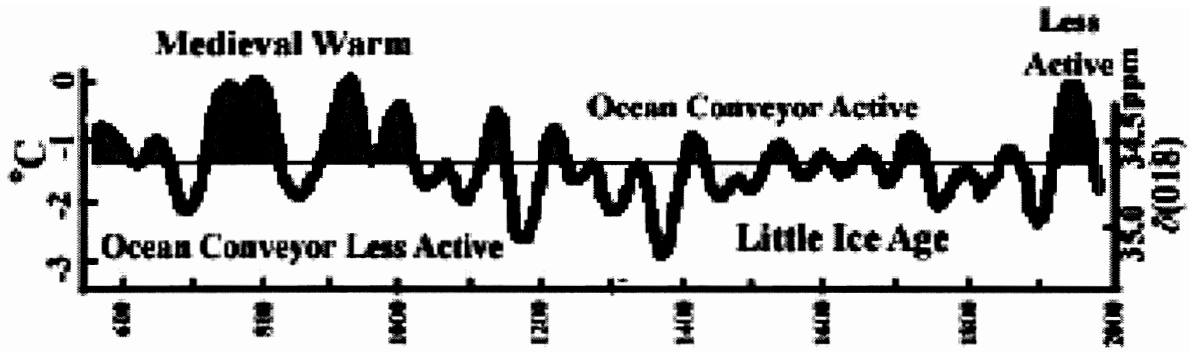

Figure 3 depicts a high resolution time series from Greenland ice cores. These sequentially deposited ice cores contain historical climatic information in the form varying isotopic composition of the ice. The parts per thousand deviation of the concentration of the heavy oxygen isotope ^{18}O contained in the ice layers was compared to standard Mean Ocean Water. Ice layers were laid down at a rate of about 30 cm per year throughout this GISP ice core that was 430 m long. Broecker's periods of Ocean Conveyor activity are noted, along with the climate epochs.

From research on tropical corals we learned that the equatorial temperatures did not vary (Cole and others 2000). Therefore, it is not unlikely that among the major processes to account for the massive changes in earth's heat budget and energy distribution could well be the frequencies and intensities of MPH formation, mediated by polar cloud cover via solar wind (Tinsley 1989; Tinsley and others 1997) and sol-earth magnetosphere modulated galactic cosmic rays (Svensgard and Friis-Lassen 1997). Lean and Rind (1998) reviewed links between climate and solar activity. We, too, recognize that these are complex interactions with both atmospheric processes, oceanographic conditions, solar activity and also non-solar galactic cosmic rays, as described by Svensgard and Friis-Christensen (1997) and others, in their role in cloud nuclei formation. Broecker and others' (1999) recent revisit to the changes in rate of deep water formation, hence the Ocean Conveyor system's transfer of energy and information over the ocean, when considered in light of the theses of Leroux and Svensgard, begins to firm up into a coherent picture.

The southern California sardine-anchovy scale record (Figure 4) and the $\delta^{18}O$ proxy solar activity show notable changes at about 1100 CE, that likely indicate their trends are related. The lower frequency variations have to be dealt with separately, as the time scales have been integrated quite differently. The point being that we believe that there is a coherent link between solar irradiance, electromagnetic modulation of galactic cosmic rays, and cloud formation that is not yet in anyone's climate models, but most likely should be, if credible forecasts are the objective of climate modeling activities. The ultimate question is where are the strongest signals found that can tell us what to expect in clear, interpretable terms. Sharp and McLain (1991a, 1991b) posit that the information is better integrated by various regional species whose life histories are tightly tuned to the variability that they have experienced since the Pleistocene, or even earlier, in some cases. Our choices include ocean fishes and terrestrial plants.

Anderson (1992a, 1992b) discussed the possible roles of solar activity in modulating the frequency of ENSO events, as well as the role of paleoclimate records in defining solar activity. Again, examining the readily available Quinn (1992) records of El Niño Warm Events, it fascinating that so few of our colleagues recognize that this century's ENSO Warm Event frequency has been the lowest since the time of John Goad and the Maunder Minimum. There were 28 ENSO Warm Events in the 20th century, and 29 in the 17th. The 18th and 19th centuries averaged about 48 Warm Events, or one about every two years. The available records from the last half of the 16th century indicate that was a more frequent Warm Event period, too. These records negate whatever has compelled some climate researchers to link ENSO Warm Event frequency with Global Warming. From historical records we can see that the "average" global temperatures, or their trends are not correlated with ENSO frequencies on century scales. Enfield (1989) reviewed the patterns, scientific uncertainty about forcing and known ecological and social effects of the ENSO process with direct and documented authority, leaving speculation to others.

Another myth that has been spread widely, that is certainly not general is that El Niño is a bad thing for humans and ecosystems. From Figure 4 and the information given previously about ENSO Warm Event frequencies for the recent five centuries, the often repeated statement that El Niños are bad for society and marine ecosystems proves to be, in fact, wrong. The 17th and 20th centuries, with their low ENSO Warm Event frequencies, appear to have been much less productive than those with more frequent Warm Events, for both sardines (Warm Ocean favored) and anchovies (Cool-Upwelling favored). What we discover, on close inspection, is that the Comprehensive Ocean Data set (COADS) shows us that higher surface winds equate with periods of warming, hence greater upper ocean mixing, and general ecological production. Lets look at some other widespread oceanic species.

Tropical Tunas and the ENSO cycle

If there were really such a state as "Normal-Ideal" conditions in the tropical ocean there would be a more or less uniform distribution of tropical ocean surface temperatures. The earth and ocean would be warmest at the equator, and temperatures would dwindle poleward. The turning of the earth and the placement of land masses has made this simplified world model subject to other forcing. Hence, the more usual case is that the eastern portions of the equatorial Pacific and Atlantic Oceans exhibit a thinner warm upper layer during most seasons. In the west there is a concomitant thickening of the upper mixed layer, as warm surface waters are evaporated off the eastern tropical oceans by surface winds of the Walker circulation and delivered downstream in the form of moisture and heat. In the Pacific and Atlantic, this portends a warmer western margin, while in the Indian Ocean, the reverse is found. This deepens the oceans' tropical habitat, where tropical tunas thrive. The upper ocean layers rise to high temperatures that only rarely exceed 30 °C. Let's examine some of the better known ocean fisheries.

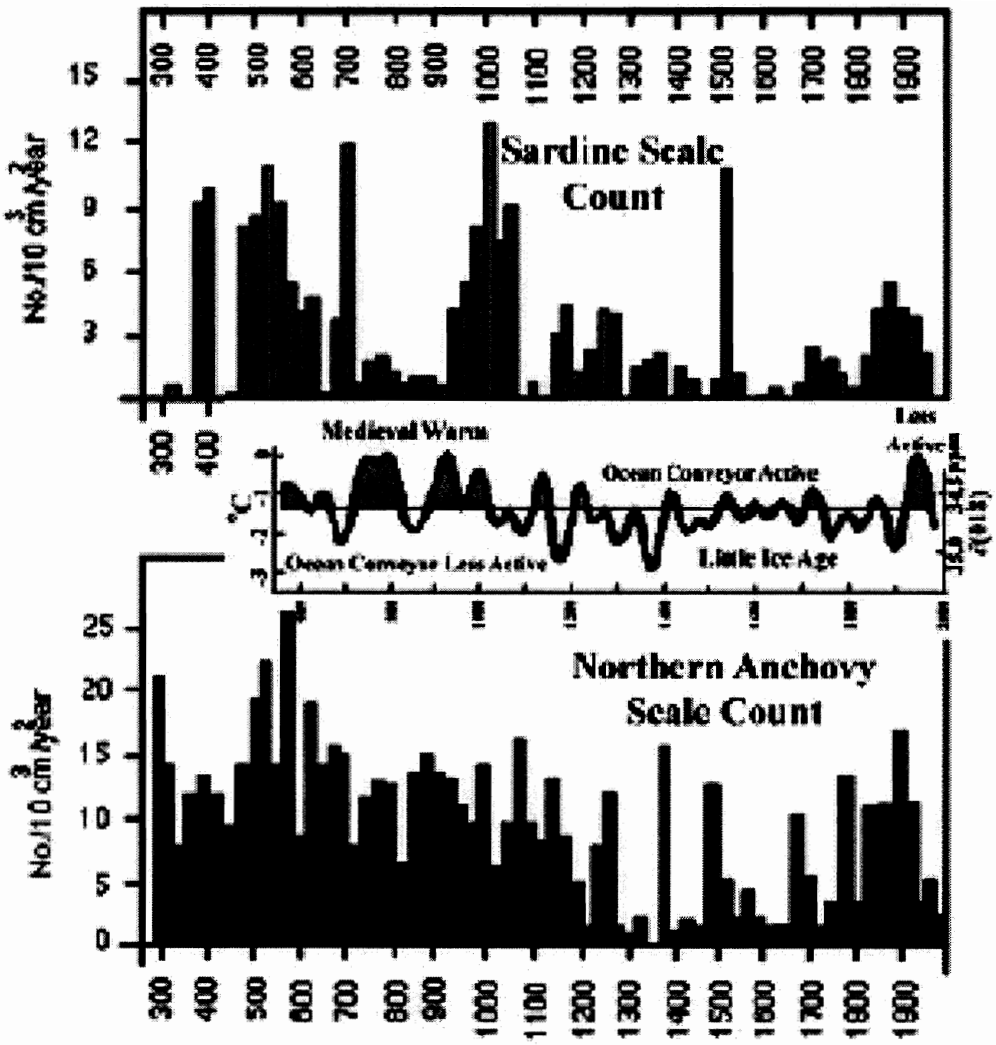

Figure 4 We have embedded the GISP ^{18}O temperature graphic within the Soutar and Isaacs (1974) sardine and anchovy scale records. This shows that the transition from the early abundance period to the lower, more variable abundances of the 11th through 20th centuries is concurrent with the downward shift in global temperatures, indicating a general slowing of surface winds, hence decreasing the long-shore upwelling, hence lowered overall production of the California Current system (Baumgartner and others 1992).

The tropical ocean, where oxygen is often limiting at depth, has been populated and adapted to by several species of tunas, with unique swimming energetics, hence oxygen requirements and temperature tolerances that reflect these trade-offs. If one were to drop a line with an array of hooks into the depths of the western topical oceans, as many as six species of tunas can be caught at any one location. Each species and their size-age groups will, however, have very different depth distributions amongst the hooks. The one general limitation is that there must be adequate oxygen available for them to swim, maintain hydrostatic equilibrium, and grow, or they will be stress-induced into reproduction rather than somatic growth. The larger of the Thunnus species group of tropical tunas tends to drop down into the water column, where, typically, the ocean is cooler,

hence less stressful. In contrast, it has not been widely recognized in the past that the bluefin tunas spend most of their time swimming within a few tens of meters from the surface, at the cooler fringes of the tropical oceans, diving to over 800 meters, or venturing into very cold habitat to feed. Several species of tunas have effectively carved up the global ocean such that there are tunas found in most of the global ocean between the 7-9C subpolar isotherms. This topic has been reviewed fully (Sharp 2000 forthcoming) in the *Ecophysiology of Tunas* (Block and Stevens, editors).

The several species of tropical tunas that inhabit the warm layers respond in different ways, depending upon the patterns that they encounter at different stages in their development. Skipjack tuna (*Katsuwonus pelamis*) are tied to the highly oxygenated upper layers due to their extreme metabolic rates associated with maintaining hydrostatic equilibrium so that they do not sink out of their habitat. In warmer situations there is a generic physiological response in all such organisms, be they fish or other. Their metabolism increases, leaving less energy for growth. The tunas already expend more of their available food energies on swimming than on growth, because they are more dense than seawater. The skipjack tuna is a cosmopolitan species, found in all the tropical oceans. The more energy they expend, the less they have for growth, hence the fish in the warmer habitats tend to be relatively smaller at age, and then tend to develop reproductive capabilities earlier rather than building bigger bodies. The characteristic life history strategies for each region are direct reflections of typical upper ocean habitat temperatures. In the Pacific Warm Pool, these fish become adult and reproductively active at much earlier ages and much smaller sizes than individuals from cooler but still tropical (> 23 °C) surface temperatures. Lehodey and others (1997) rediscovered that skipjack tuna respond to Warm Pool dynamics, by expanding with their natal habitat boundaries, and contracting during cooler periods.

Now, if we focus on the eastern extremes of the tropical oceans, the usual upper ocean upwelling tends to bring oxygen poor cool water near the surface. This happens for the simple reason that the cooler source waters underlie some of the more productive tropical surface waters on earth. Due to the relatively high primary production, the nighttime metabolism of the plankton tends to extract most of the available oxygen. This reduces the availability of oxygen rapidly with depth, and excludes most of the species of tunas found in the oxygenated western tropical oceans. This means that the same fishing experiment within the eastern tropical ocean will yield fewer species. This is observed everywhere except in the eastern Indian Ocean, where everything is complicated by the merger of two major ocean bodies, filtered through a shallow sea environment. This means that we should be able to forecast certain responses to physical forcing processes.

For example, if a stifling or reversal of the Walker Circulation surface winds occurs, the depth distributions of upper ocean tropical water evens out between the east-west extremes, the primary production patterns reverse, tending to allow more species to invade the eastern oceans, and for those species usually constrained to depths that make them unavailable to surface fishing gear to spend more time near the surface. The western Pacific seine fisheries will (and do) start to observe more large yellowfin in their

catches during ENSO Warm Events as soon as the signature Kelvin wave is released, and the thermocline structure emerges. To the east, the deepening of the thermocline and suppression of primary production allows more species access, providing more habitat and making the usually vulnerable tunas less visible, hence less vulnerable to surface fishing techniques. Catch rates tend to decline rapidly, as the Kelvin wave arrives, and *in situ* heating occurs due to increased cloudiness. The deeper fishing longline tuna gear exhibits generally opposite trends, to those enjoyed by the surface seine gear, and must change distribution to enable their gear to be effective. Locating cooler, oxygen-rich water at hook depths is their objective.

In extreme situations of ENSO warming, the expansion of tropical tuna habitat poleward is notable, and makes available to usually temperate ocean fisheries some portion of the tropical tunas and associated species such as marlins, dolphin fish (*Coryphaena* spp.), and some jacks (*Seriola* and others). These invasions by tropical predators can cause havoc in local fisheries where small pelagics and other coastal species can be preyed upon by these voracious predators species. In the so-called Cold regimes, these same coastal regions tend to exhibit strong upwelling, hence more local production, and abundances of secondary predator species from anchovies to jellyfishes can bloom. Beyond the usual local predator populations, toward the poles, and seaward, there are entire arrays of usually excluded predators. Offshore of the eastern boundary currents lie the more tropical and subtropical elements of the oceanic environment. During local warming, and warming associated with cloud and water vapor transport of the ENSO tropical ocean heat resources, these predator fields are often overlain onto the coastal environment, suppressing upwelling production, and causing the local fauna to submerge. By making vertical dives, the invaders from offshore can devastate local coastal resources.

On the other hand, during extreme cool events, coastal upwelling can become more intense as well as more frequent, tending to transport more of the production offshore, leaving little behind for emergent fish larvae, or birds, and can in this fashion also devastate local production. It is, in fact, the balance between extremes, the transitional processes, and the dynamic interactions between the various ecological components and compartments that is important, and links these systems into an interactive, sustainable whole. The worst things that happen during any one phase or stage of the ENSO cycle is often good news for another set of ecosystem participants. Extreme climate changes, such as the recent millennial cooling, result in a general decreased overall production along California's coast (Figure 4) compared to previous warmer times.

Climate dynamics are the "reset" buttons for the patterns of ecological winners and losers. Enzel and others (1989) showed the dramatic consequences of ENSO Warm Events on the rainfall patterns across the southwest desert of North America, and the long-standing records of rise and fall of the water levels of Mono Lake, in response to the larger scale atmospheric patterns and dynamics. In the higher latitudes, still farther downstream from the Warm Pool, Dean and others (1984) showed that the region west and at the mid-latitudes of the Great Lakes expressed not only the influences of the Pacific Warm Events, but also those of the movement of the Bermuda High, northwestward from its contemporary position, to affect the region, as well as periods when the

North Pacific (Aleutian) High would shift eastward, to dominate the regions climate. They called this a "triple-junction" zone, in which the lake sediments provided insights into the rather rapid shifts between Northern forests, balmy summers that brought another flora, and the more dry periods resulting from extra-energetic Warm Pool processes. Again, Leroux's MPHs play a very particular role, or lack thereof, in this region, leading to three rather than only two binary (On–Off) states. The passage of Polar Highs across a cold dry North American plains, has quite different consequences from those flowing over a warm, wet plain. And, then, a period of fewer MPHs allows warm, humid periods, dominated by shifts of the Bermuda High well inland, to transport unusual amounts of warm moist air across a larger region, leading to another dynamic state, and unique ecological responses. In each case, the frequencies and intensities under each generic climate situation defines the ecological status for the larger region. The next question is, of course, "So what?"

The contemporary problem is that for nearly 50 years much of the world's population has lived within a very narrow range of climate variability, leading to a general apathy, or expectation that global climate is generally as benign as that we have experienced. This is simply not the usual case. This poses several dilemmas. Declaring that humanity's economic health is the primary measure of success has not worked well. Historically, we humans have tended to homogenize our environments, removing many of the options that were in place before we began tinkering with these usually dynamic and supportive environments. The worst case scenarios include our treatments of forests, freshwater lakes, rivers and tributaries, and, of course, the failure to manage the living resources of our major grasslands and oceans. Our support systems have shown their limitations. People have again begun to compete for basics—food and water. History provides rich clues and the most fruitful pathways toward better understanding of what to expect and how to cope with these changes. To thrive humanity must learn to cope with change, as a proactive component of earth's ecosystem, without destroying the underlying system complexity that provides options during different climate states.

The Time Keepers

In the early development of the natural sciences ancient Chinese and Persian astrologers observed the skies, and debated cosmology, confounding correlation with cause and effect. The Greeks converged on them, and Alexander the Great attempted to bring all their knowledge into one location, at the library in Alexandria. The basis for modern science was concentrated, for study. Whatever was not hastily removed, was subsequently burned by conquerors in the 3rd century BC. This was not the first time in history that occurred, as ancient China's historical literature was similarly ordered burned by an anti-Confucianist, anti-scholar Emperor. Eventually, the advent of Europe's renaissance led to an unusual period of transition from looking outward, toward the moon, sun, and stars to discover cause and effect, to measuring earthly phenomena. This led to innovations of instrumental measurements of atmospheric phenomena, and the definition and refinement of the scientific method. The role of the Catholic Church in suppressing progress is notable, as the stories about Copernicus and Galileo attest. The transition between astrology and astronomy was subtle, reaching its zenith with the invention of

the telescope, at the dawn of the 17th century (Table 1), and serious time-keeping devices in the mid 18th century. The rapid evolution of astronomy after the discovery of the optical telescope is portrayed in the following exemplary 11-year timeline.

The continuing evolution of galactic observations and scientific theory during the 1620–1740 period led to the description of Physical Laws that govern "coelestial" motions and interactions with our known world. The parallel or co-evolution of empirical science, measurement tools, and theories to explain physical phenomena that took place during the 16th through18th centuries. Both sequences of developments were important, and direct consequences of the period of relative cool climate after nearly a thousand years of more optimal climate conditions. Two related but distinct families of science evolved. One branch followed the age-old practice of observing coelestial phenomena, that continues to this day, but evolved most quickly in the short 20-year period. The second branch—the more diverse of the two—was the birth of empirical science, or the "Scientific Method" first defined by Sir Francis Bacon.

John Goad, a 17th century natural historian, recorded his observations over a lifetime (1616–1691) in which his hometown, London, underwent some of the more serious consequences of the urbanization associated with the post Medieval Warm cooling period, including the Maunder Minimum and the Little Ice Age. From the end of the Medieval Warm Period in the late 12th century there was a series of excursions downward from long-term high temperatures, reaching lows in the early 18th century, and finally trending upward from about 1850 or so, depending upon where on earth you might locate records. The general results of this cooler climatic shift, along with a general expansion of global trade and sharing of disease vectors, included severe famine as people moved off the farms and into the cities (Braudel 1982). There was general political chaos as a result of sporadic disease outbreaks and great numbers of deaths, along with continuous debilities associated with urban crowding and pollution.

Goad's (1686) tome, *Astro-Meteorologica; or Aphorisms and Discourses of the Bodies Coelestial, Their Nature and Influences*, was a chronicle of such socially devastating events, various climatic and weather phenomena, as well as of solar, lunar, and comet phenomena. He classified each by their astrological characteristics (Figure 5), using symbols and terms that were well understood at the time, but which seem arcane to those of us brought up with calendars and timelines at hand. On page 444, near the end of his treatise, we find in Goad's words a particularly poignant statement, which we will refer to as - John Goads' Goad i.e., "It grieveth me to see learned men to speak of pressures of aire and thereby solve problems concerning the ocean's ebb and flow."

Table 5 The rapid evolution of astronomy after the discovery of the optical telescope is portrayed in this exemplary 11-year timeline

Year	*Event*
1608	Hans Lippershey, optical telescope
1609	Lippershey and Janssen, the compound microscope
1609	Johannes Kepler, 1st and 2nd laws of planetary motion
1609	Thomas Harriot, maps moon using a telescope
1609	Johannes Kepler, notion of energy
1609	Galileo Galilei, builds a telescope
1610	Galileo Galilei, observes the phases of Venus
1610	Galileo Galilei, observes moons of Jupiter
1610	Galileo Galilei, observes craters on the moon
1610	Galileo Galilei, observes stars in the Milky Way
1610	Galileo Galilei, observes structures around Saturn
1611	Fabricius, Galileo, Harriot, Scheiner, sunspots
1611	Johannes Kepler, principles of the astronomical telescope
1612	Simon Marius, Andromeda galaxy
1613	Galileo Galilei, principle of inertia
1615	S. de Caus, forces and work
1618	Francesco Grimaldi, interference and diffraction of light
1619	Johannes Kepler, 3rd law of planetary motion
1619	Johannes Kepler, explains why a comets tail points away from the Sun

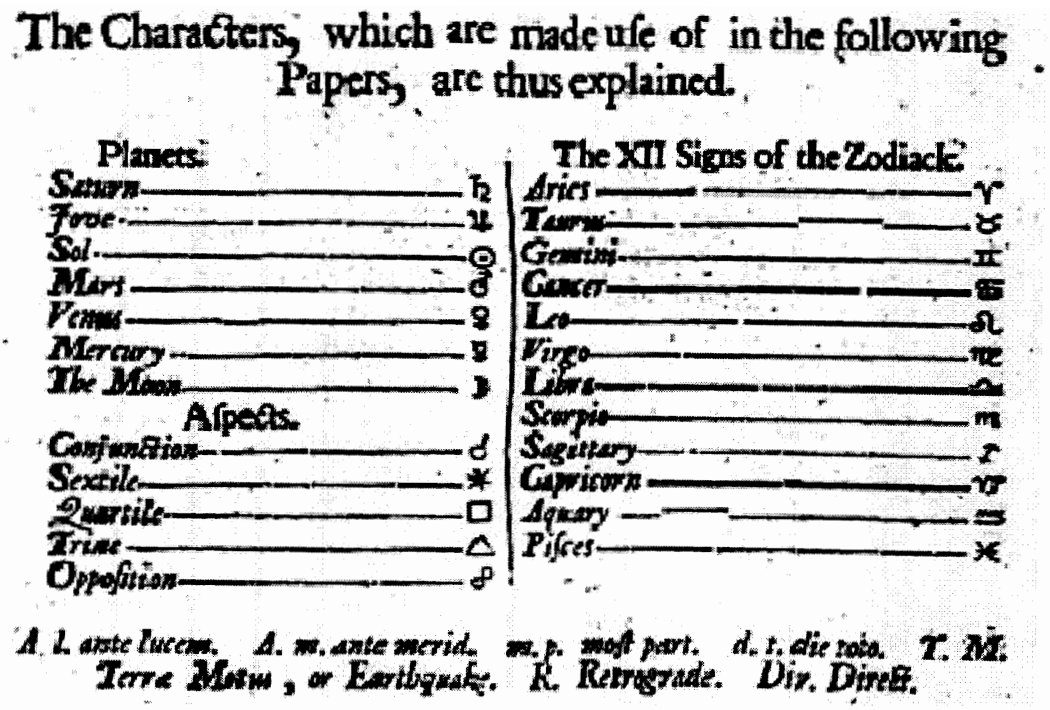

The Characters, which are made use of in the following Papers, are thus explained.

Planets.		The XII Signs of the Zodiack.	
Saturn	♄	Aries	♈
Jove	♃	Taurus	♉
Sol	☉	Gemini	♊
Mars	♂	Cancer	♋
Venus	♀	Leo	♌
Mercury	☿	Virgo	♍
The Moon	☽	Libra	♎
Aspects.		Scorpio	♏
Conjunction	☌	Sagittary	♐
Sextile	✶	Capricorn	♑
Quartile	□	Aquary	♒
Trine	△	Pisces	♓
Opposition	☍		

A. l. ante lucem. A. m. ante merid. m. p. most part. d. t. die toto. T. M. Terræ Motus, or Earthquake. R. Retrograde. Dir. Direct.

Figure 5 is a digital copy of the key provided in the first page of Goad's (1686) chronicle. It provides readers with the code to decipher Goad's heavily symbol-laden text.

Goad was amongst the last of the millennia-old convention of fundamentalist astrology-based observers. Their prime intent was to explain the events and processes that affected society through careful and prodigious observations of various categories of events. Among the many observations that he documented, from his own and the log-books of trading vessels, were the monstrous comets recorded by sailors and landlubbers, alike, that were "Greater than the Sun" lasting more than a month in the night skies. These natural historian-astrologers attempted to explain and forecast future events through careful logging of the relative positions of the various "coelestial bodies." This shift from "looking upward" for explanations, to a more intense measurement of local phenomena, defines the transition from natural historian's traditional astrologically based empiricism, to another era during which instruments were beginning to be invented to measure various physical phenomena. These new styled measurements were, in turn, studied and related to local weather patterns. This was by no means the end of astronomy, or astrology. It was merely another stage in human efforts to classify natural events and processes. As discussed earlier, this was a period of intellectual progress, which continues today.

The scientific and technological developments and resulting societal progress were shared amongst many of the same early researchers as those who helped make the transition from astrology to astronomy. In the 20th century, air travel and rocket warfare propelled the next phases. The tools and measurements that were made possible by the efforts of these early scientists surely facilitated the exploration of the surface of our own planet, at first on foot, and then by sailing vessels. John Harrison's chronometer was the key to navigation to, from, and return to any place on earth. Within the last half of the

20th century, we invoked our historical passion for things extra-terrestrial, flinging ourselves into the skies, to reach and walk on the moon, and eventually to the outer reaches of earth's atmosphere from which to look down upon our domain to see mostly—water...

Water, Water, Everywhere—But From Where?

Liquid water is the basis of life, as we know it. Yet, we still know less about the earth's oceans, beyond wading depths, than we do about the moon's surface. What is more important? The earth's size and surface temperature distribution—as a result of earth's orbital parameters—provide a harmonious environment for liquid water. But, where did all earth's water originate?

With all the attention given to large visible phenomena in the night skies in history, little attention has been given to the smaller objects that occur at various intervals within the largely emptiness of space. Small, abundant water-laden comets seem to have become a controversial theme within the space research communities. They may account for the large volumes of water that are present in earth's oceans (Frank and Huyghe 1990; Frank and Sigwarth 1997). Often, the rabid controversies over such seemingly simple theories usually emerge from within research communities where funding is competitive and ideas are graded by peers who are competing for the same research funds. John Harrison's lifelong quest to build the better timepiece, and thereby lay claim to the elusive royal reward, was similarly thwarted by a competing group of astronomers (Sobel 1996). In this contemporary example we see that even posing the idea that frequent small inputs from small "ice comets" was simply out of tune with even more difficult to accept theories that had taken on auras of truth, by consensus, rather than factual support. Recently, Frank and Sigwarth (1997) reasserted their hypothesis, stimulating a major re-examination of the Visible Imaging System (VIS) aboard the POLAR space craft. Hannegan and others (1998) review the data, and test the validity of the hypothesis using their new stratospheric-mesospheric circulation model and observations from the more recent UARS satellite. They found that the existing water vapor in the stratosphere was very low in concentration, at least 100 times smaller than initially proposed by Frank and Sigwarth (1997), and inadequate according to their model. Orders of magnitude are at issue, not the existence of water comets, or other sources.

The fact that no one really knows where the earth's water supply originated has never really been conceded by the challengers. Frank pointed out that daily comet deliveries over an extended time could easily account for all the liquid water available on earth to fill its oceans. Once you have oceans, you can have life, and climate. The existence of ice comets is an important finding. The fact that they arrive regularly is also interesting. But do we know, yet, if there are periods when our solar system encounters more frequent ice accretions or debris from other fellow travellers within our Galaxy?

By introducing these and other possible sequences of events, our intent is to prepare the reader for various sojourns, some into space, and others to look into known and hypothesized interactions, and an eventual understanding of the world about which we each strive to understand many complex processes, which may not at all be what they seem,

from up close. The point is to more fully appreciate that the many interactive, often invisible parts are much more complex than they may appear from inside our local environment. For example, Leonid Klyashtorin (1997, 1998) provided stimulus to each of our convergent mental models about longer-term patterns and cycles that effect ocean ecosystems. He pointed out that Length of Day records were correlated with Pacific and Atlantic Ocean fisheries production. He also made the observation that each of the LOD cycles comprised two distinct periods where surface winds have been predominantly Zonal (E-W) or Meridional (N-S). We are beginning to understand more the over-riding wind-related forcing of the upper ocean, and the resulting responses of ocean ecosystems. We start with observed trends in two ocean faunal systems in Figure 6.

Length of Day is not the cause of anything, but understanding it's underlying dynamics will lead toward long sought answers. Links from physical forcing to ecosystems are the domain of those of us watching and trying to explain the behaviors and variabilities of eastern Boundary Currents, and high latitude shelf or demersal fisheries, from where a great proportion of the sea fish protein that humans need derives. Studies of Length of Day related phenomena have established that the atmosphere provides significant forcing of changes in polar motion and earth's rotation rate (1/Length of Day), but that there are observable, often large variations in these rotation elements which cannot be explained solely by the atmosphere's interactions (Gross and others 1996). In Figure 7, the major fisheries catches of entire regional ecosystems switch with each change in dominant wind field forcing regime to another, over 20- to 50-year production cycles.

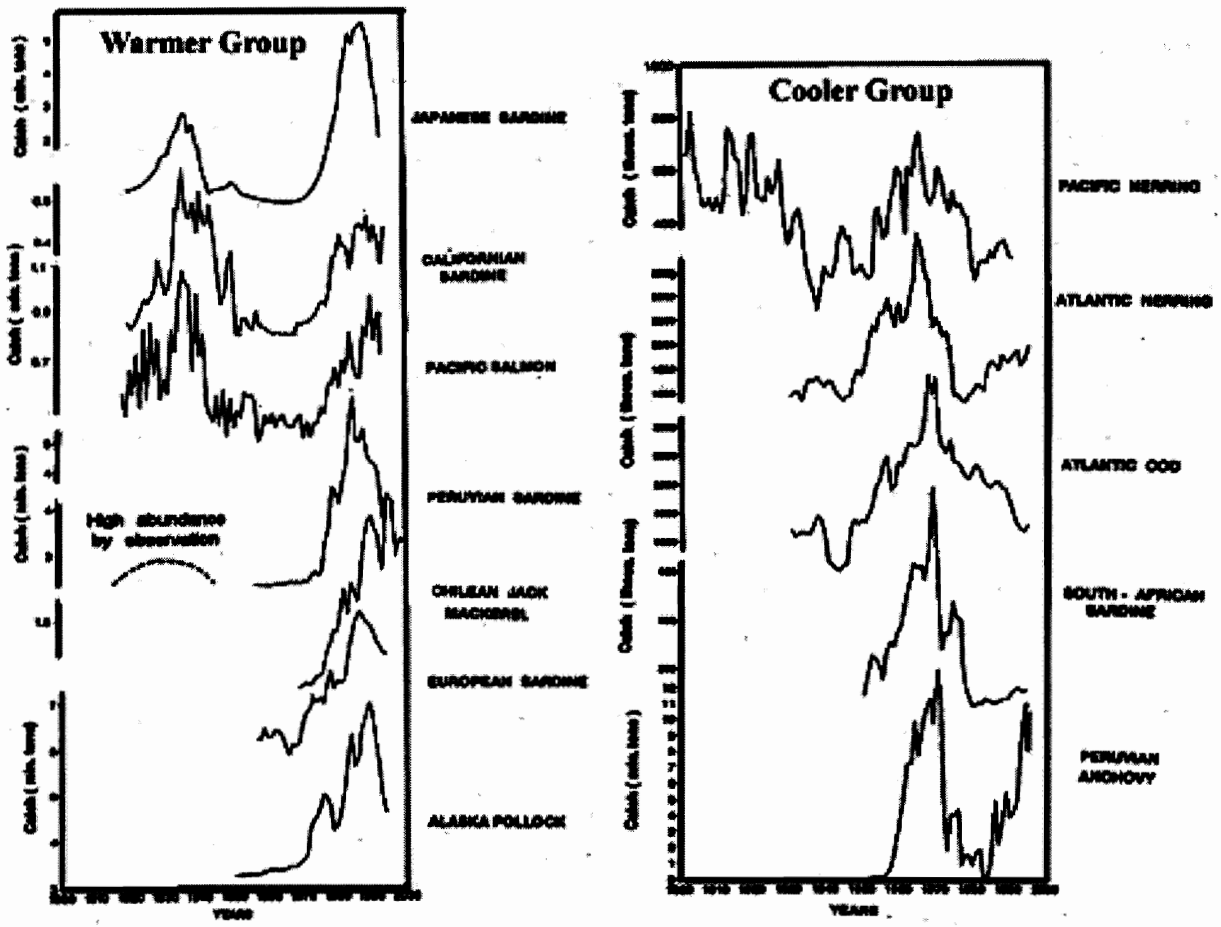

Figure 6 shows the official annual catch records for major fisheries of the Atlantic and Pacific Oceans for the recent century. Each species is associated with either a Warm or Cold ocean climate regime. The patterns of blooms and busts are coherent within and between oceans, for the northern hemisphere.

Explaining these dynamic patterns by tracing the forcing backward from the regional ocean ecosystem dynamics into the oceans and atmosphere and beyond, has been the quest of many fisheries ecologists and other scientists for decades (Hjorth 1914; Russel 1939; Southward and others 1975; Cushing 1982; Sharp and Csirke 1983; Ebbesmeyer and others 1991; Francis and Hare 1994). All have searched for general mechanisms that induce the transitions from one faunal assemblage, to another, as the various species from each are favored, or not, by the dominant physical forcing along shore, cross-shelf, or the open ocean. Recent convergences of interests by fisheries researchers, climate scientists, and climatologists have provided many clues, and now, more understanding of where the ultimate forcing is initiated.

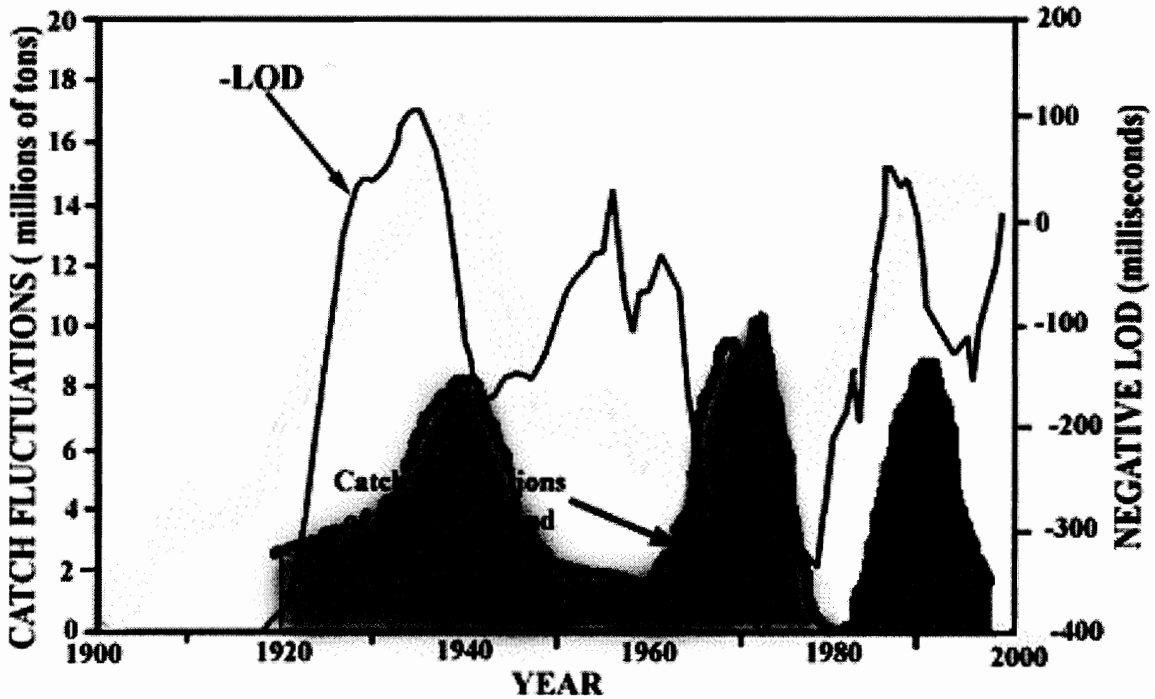

Figure 7 The relation between Klyashtorin's Atmospheric Climate Indices, ACI (WE = West-East) and ACI (C = North-South), and the major fisheries species production in the Atlantic and Pacific Oceans (from Figure 6) suggests that the patterns that we have observed over the recent century are forced by atmospheric processes, that affect the ocean habitat in very characteristic fashions, leading to very specific opportunities for the fish species from the two different faunal assemblages.

Recent research supports the fact that the oceans explain a large part of the remaining variations in the earth's rotation, at periods of a year and less. Marcus and others (1998) clearly shows that residual non-atmospheric LOD changes are of oceanic origin. Of course there is a contribution from the storage of water mass on land and in ice, but this appears to be less important at short periods (less than a year), and is probably more important at longer periods. Figures 8 and 9 show the results of Goodridge's similarly structured analysis of the LOD and Pacific-wide atmospheric patterns, as measured using the difference between sea level pressure at Tokyo and San Francisco, and upwelling off the coast of California.

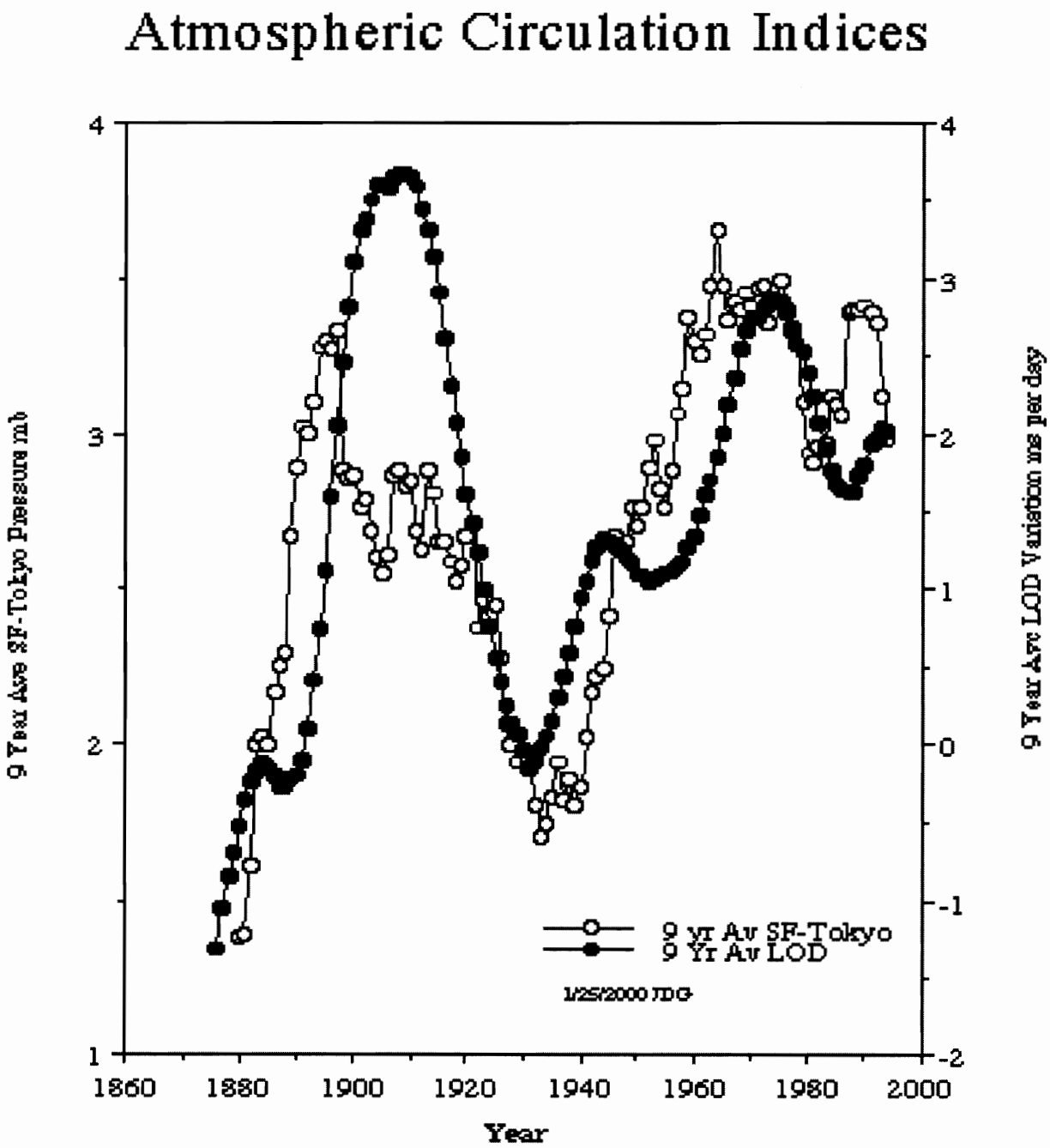

Figure 8 The running nine-year means seal level pressure differences between San Francisco, California, and Tokyo, Japan, are plotted against similarly averaged measures of Length of Day. There has been a parallel shift from Warm Western Pacific Ocean - Cold Eastern Pacific Ocean see-saw pattern, over the recent century, as indicated by the shorter record in Figure 8.

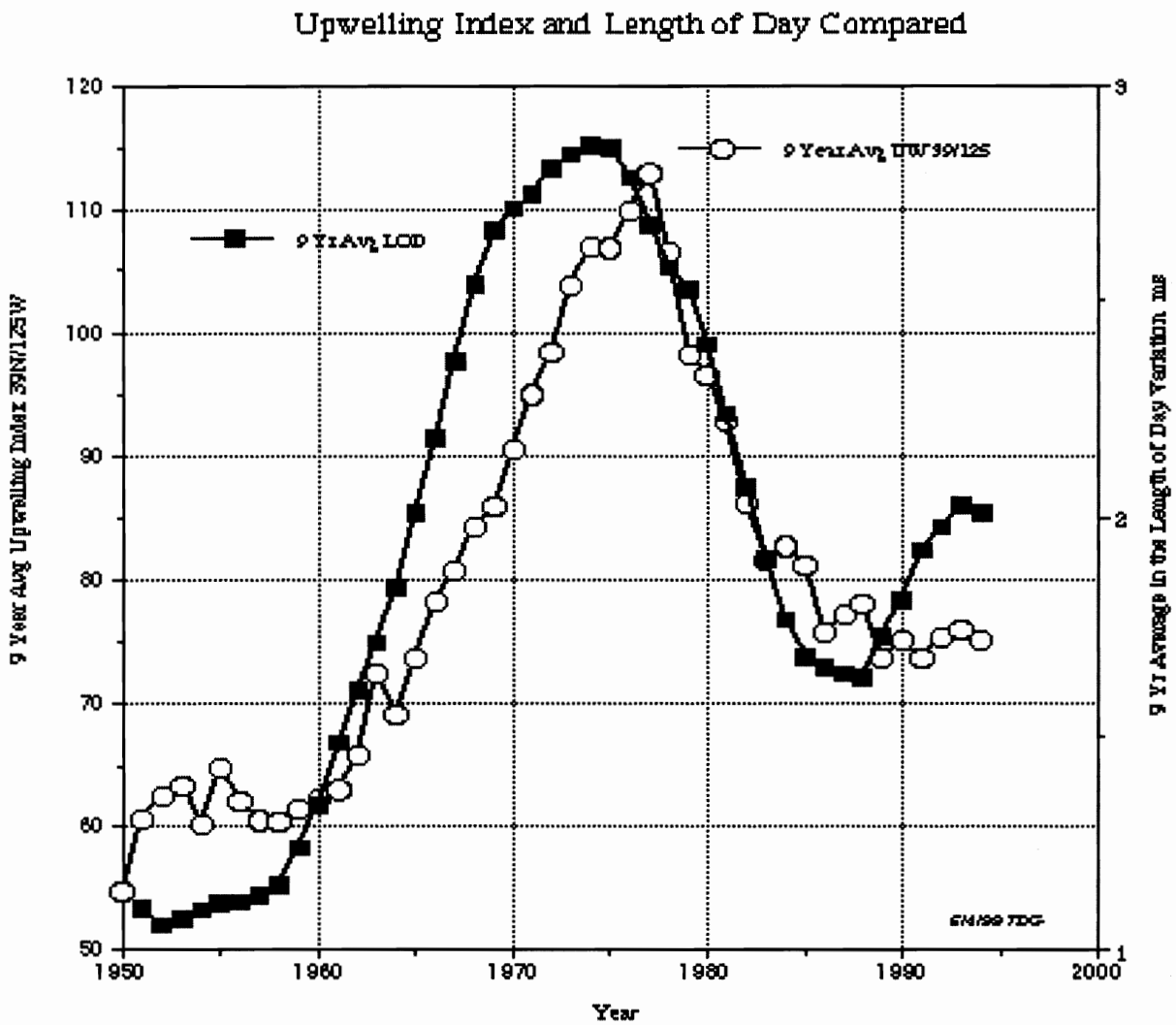

Figure 9 The 50-year record of the Bakun Upwelling Index off San Francisco, California, is compared to the Length of Day record for the same period. Given that we know that surface winds drive the regional Upwelling, the link between the forcing into the upper ocean - that has dramatic consequences on both primary production and habitat temperatures, hence fisheries production - begins to clarify. The Klyashtorin LOD study, with his ACI dominance analyses, provides a more coherent picture of the globally coherent patterns of ecological regime changes. It also provides a pathway to forecasting them.

Conclusions

The most notorious of the major fisheries species oscillations are those of the Eastern Boundary Currents, and Northwest Pacific–Sea of Japan in which the faunal switches involve anchovies and sardines (California, Peru-Chile, Benguela-Namibia, Spain-Morocco, and Japan-Sea of Japan). The first major modern sardine recolonization after a collapse was described by Kondo (1978) as he documented the revival of the Sea of Japan sardine population from two refuge colonies along the western shores of Japan. Valdivia (1978) provided the first insights into the links between ENSO and the Peruvian

anchoveta catch, as well as a series of ecological responses. Sharp and Csirke (1983) revisited similar pattern changes in distribution, species composition and abundances all over the globe. Kawasaki (1983; Kawasaki and others 1991) initiated studies of the apparent synchrony of sardine population cycles in the Pacific Ocean, and beyond. This stimulated many authors to document their regions' patterns of fish population rises and declines, along with descriptions of these Pacific fishes habitats, and their physical forcing (reviewed by Sharp 1988; Sharp and McLain 1992; Bakun 1996). More recently, Schwartzlose and others (1999) review and discuss the fluctuations of sardines and anchovy populations in the various ecosystem contexts around the world. Klyashtorin's studies have tied these observations to several others, and made forecasting of regional dynamics possible from *a priori* climate observations.

The North Pacific's high latitude fisheries have been studied thoroughly, with more recent attention paid to climate dynamics, winds, tides and other non fishery-related ocean and ecosystem forcing (Lluch-Belda 1989, 1992; McFarlane and Beamish 1992; Beamish 1996; Mantua and others 1997; Francis and Hare 1994; Anderson 2000). A fascination with the newly-named Pacific Decadal Oscillation (PDO) and the North Atlantic Oscillation (NAO), has grown out of these studies. The most direct linkages between these two "regional" manifestations of a truly more hemispheric dynamic has also been made by Marcel Leroux (1998). Our next point is that the PDO and NAO are hindcast or a posteriori "statistical" artifacts resulting from static conceptualizations of dynamic processes that are in continuous or "dynamic" motion. Forecasting from these data sets is limited to near-term, regional responses, while tracking the Vangengeim-Girs Atmospheric Climate Indices offers the opportunity for proactive fisheries management decisions to be made, well in advance of crises.

Why all the commentary about MPHs? It is possible that monitoring and tracking the Mobile Polar High phenomena may provide the best resolution to various dilemmas in short-term climate forecasts and longer-term climate changes as well. Tracking the variable intensities and frequencies of MPHs is another important key to understanding both climate-scale variability and seasonal weather. The MPHs gather energy as they progress, and shift their directions to affect the Trade Winds, thus affecting the Vangengeim-Girs Index. In the Southern Hemisphere, the Indian Ocean provides a unique path of least resistance for MPHs traversing Antarctica's icy edges, onward across the equator, to affect the Asian monsoon, and downstream ecosystems. Some of these stronger MPHs eventually interact with highly energized, moist tropical atmosphere that result from the deep convection along the Inter-Tropical Convergence. This links the MPH activity with the ocean's Warm Pool in the western Pacific and eastern Indian Ocean. Poleward transfers of equatorial heat (energy stores) result.

This all ends up being directly related to earth's long-term Length of Day variations, too, as the interactions are all about water vapor moving from the earth surface into the atmosphere. These processes eventually involve various energy swaps resulting from the contrary motions of the lower atmosphere over seasonal terrain and longer-term dynamic ocean systems that, in turn, affect the more equatorward ocean and atmosphere. Better understanding will lead to useful prediction capabilities. Large scale prox-

ies such as LOD, not unlike local ecological responses, integrate many useful, important signals for which we now have only limited operational monitoring systems. While we are trying to enhance our ability to monitor the subsurface oceans, and track the ecological responses to their changes, we need more insight into global climate dynamics and their disparate forcing. Perhaps it is time to refocus on those process integrators that nature has provided to tell us when climate regime changes will occur (or have already begun to change) rather than waiting for the changes to become obvious. Scientific credibility requires that every available piece of information be used.

References

Anderson JJ. 2000. Decadal climate cycles and declining Columbia River salmon. In: Knudsen EE, Steward CR, MacDonald DD, Williams JE, Reiser DW, editors. Sustainable fisheries management: Pacific salmon. New York (NY): CRC, Lewis Publishers. p 467–84.

Anderson RY. 1992a. Long term changes in the frequency of occurrence of El Niño events. In: Diaz HD, Markgraf V, editors. El Niño: historical and paleoclimatic aspects of the Southern Oscillation. Cambridge University Press.

Anderson RY. 1992b. Possible connection between surface winds, solar activity and the earth's magnetic field. Nature 358:51–3.

Anderson RY. 1992c. Solar variability captured in climatic and high-resolution paleoclimatic records: a geological perspective. In: Sonnet CP, Giampapa MS, Matthews MS, editors. The Sun in time. Tucson (AZ): University of Arizona Press.

Baumgartner TR, Soutar A, Ferreira-Bartrina V. 1992. Reconstruction of the history of Pacific sardine and northern anchovy populations over the past two millennia from sediments of the Santa Barbara Basin, California. CalCOFI Report 33:24–40.

Block B, Stevens ED. The ecophysiology of Tunas. San Diego (CA): Academic Press. Forthcoming.

Braudel F. 1982, Civilization and capitalism, 15th-18th century. Three volumes. New York (NY): Harper and Row.

Broecker WS. 1987a. Unpleasant surprises in the greenhouse? Nature 328:123–6.

Broecker WS. 1987b. The biggest chill. Natural History 10:74–82.

Broecker WS. 1991. The great ocean conveyor. Oceanography 4:79–89.

Broecker WS, Sutherland S, Peng T.-H. 1999. A possible 20th-century slowdown of Southern Ocean deep water formation. Science. 286(5442):1132–5.

Cole JE, Dunbar RB, McClanahan TR, Muthiga NA. 2000. Tropical Pacific forcing of decadal SST variability in the western Indian Ocean over the past two centuries. Science 287:617–9.

Csirke J. 1980. Recruitment in the Peruvuian anchoveta and its dependence on the adult population. In: Saville A, editor. The assessment and management of pelagic fish stocks. Rapp. p 307–13.

Dean WE, Bradbury JP, Anderson RY, Barnosky KW. 1984. The variability of Holocene climate change: evidence from varved lake sediments. Science U.S. 226:1191–4.

Dessler AJ. 1991. The small comet hypothesis. Reviews Geophysics 29:355–82.

Enzel Y, Cayan DR, Anderson RY, Wells SG. 1989. Atmospheric circulation during Holocene lake stands in the Mojave Desert: evidence of regional climatic change. Nature 341:44–7.

Ebbesmeyer CC, Cayan DR, McLain DR, Nichols FH, Peterson DH, Redmond KT. 1991. 1976 step in the Pacific climate: forty environmental changes between 1968-1975 and 1977-1984. In: Betancourt JL, Tharpe VL, editors. Proceedings of the Seventh Annual Pacific Climate (PACLIM) Workshop, April 1990. Interagency Ecological Studies Program Technical Report 26. Sacramento (CA): California Department of Water Resources. p 115-126.

Enfield DB. 1989. El Niño, past and present. Rev. Geophys 27(2):159–87.

Francis RC, Hare SR. 1994: Decadal-scale regime shifts in the large marine ecosystems of the North-east Pacific: a case for historical science. Fish Oceanogr 3:279–91.

Frank GA, Sigwarth JB, Craven JD. 1986. On the influx of small comets into the Earth's upper atmosphere, II Interpretation. Geophysical Research Letters 13:307–10.

Frank LA, Huyghe P. 1990. The big splash. New York (NY): Avon, Birch Lane Press. 255 p.

Frank LA, Sigwarth JB. 1997. On the influx of small comets into earth's atmosphere. In: Proceedings of the 1997 International Symposium on Instruments, Methods, and Missions for the Investigation of Extraterretrial Organisms. San Diego, California. SPIE 311:238–48.

Gross RS, Marcus SL, Eubanks TM, Dickey JO, Keppenne CL. 1996. Detection of an ENSO signal in seasonal length-of-day variations. Geophysical Research Letters 23:3373–6.

Hannegan B, Olsen S, Prather M, Zhu X, Rind D, Lerner J. The dry stratosphere: a limit on cometary water influx. Geophysical Research Letters 25(10):1649–52.

Hjort J. 1914. The fluctuations in the great fisheries of northern Europe viewed in the light of biological research. Rapp. P-v. Reun. Cons. Int. Pacific. Fisheries Research 37:115–25.

Kawasaki T. 1983: Why do some fishes have wide fluctuations in their number? A biological basis of fluctuation from the viewpoint of evolutionary ecology. In: Sharp GD, Csirke J, editors. Proceedings of the Expert Consultation to Examine Changes in Abundance and Species Composition of Neritic Fish Resources. FAO Fish. Rep. 291(3):1065–80.

Kawasaki T. Regime shift and climate change. Beyond El Niño, Prog. Oceanogr. Forthcoming.

Kawasaki T, Tanaka S, Toba Y, Taniguchi A, editors. 1991. Long-term variability of pelagic fish populations and their environment. Tokyo: Pergamon Press.

Klyashtorin LB. 1997. Pacific salmon: climate-linked long-term stock fluctuations. PICES Press 5:2–34.

Klyashtorin LB. 1998. Long-term climate change and commercial fish production in the Atlantic and Pacific. Fisheries Res. 37:115–25.

Lean J, Rind D. 1998. Climate forcing by changing solar radiation. Journal of Climate 11(12):3069–91.

Lehodey P, Bertignac M, Hampton J, Lewis A, Picaut J. 1997. El Niño Southern Oscillation and tuna in the western Pacific. Nature 389:715–8.

Leroux M. 1998. Dynamic analysis of weather and climate, Wiley/Praxis series in Atmospheric Physics. J Wiley & Sons. 365 p.

Lluch-Belda D, Schwartzlose RA, Serra R, Parrish R, Kawasaki T, Hedgecock D, Crawford RJM. 1992. Sardine and anchovy regime fluctuations of abundance in four regions of the world oceans: a workshop report. Fish. Oceanogr. 1(4):339–47.

Lluch-Belda R, Crawford JM, Kawasaki T, MacCall AD, Parrish RH, Schwartzlose RA, Smith PE. 1989. World-wide fluctuations of sardine and anchovy stocks: the regime problem. S Afr J Mar Sci 8:195–205.

McDougall WA. 1993. Let the sea make a noise. New York (NY): Avon Books. 793 p.

Morgan TH, Shemansky DE. 1991. Limits to the lunar atmosphere. J Geophysical Research 96:1351–67.

Moum JN, Caldwell DR, Paulson CA. 1989. Mixing in the equatorial surface layer and thermocline. J. Geophys. Res. 94 C2:2005–21.

Parker KS, Royer TC, Deriso RB. 1995. High latitude climate forcing by the 18.6-year Lunar Nodal Cycle and historical recruitment trends in Pacific halibut. Special publication. Can Fish Aquat Sci 121:447–59.

Quinn WH. 1992 A study of Southern Oscillation-related climatic activity for AD 622-1990 incorporating Nile River flood data. In: Diaz HF, Markgraf V, editors. El Niño: historical and paleocliatic aspects of the Southern Oscillation. Cambridge Press. p 119–50.

Royer TC. 1993. High latitude oceanic variability associated with the 18.6-year Luni-Solar Tide. Journal of Geophysical Research 84(4):639–44.

Russel ES. 1939. An elementary treatment of the overfishing problem. Rapp Proc-Verb Cons Int Explor Mer 110:5–14.

Schwartzlose RA, Alaheit J, Bakun A, Baumgartner TR, Cloete R, Crawford RJM, Fletcher WJ, Green-Ruiz Y, Hagen E, Kawasaki T, Lluch-Belda D, Lluch-Cota SE, MacCall AD, Matsuura Y, Nevarez-Martinez MO, Parrish RH, Roy C, Serra R, Shust KV, Ward MN, Zuzunaga JZ. 1999. World-wide large-scale fluctuations of sardine and anchovy populations. S Afr J Mar Sci 21:289–347.

Sharp GD. Tuna oceanography: an applied science. In: Block B, Stevens ED, editors. The ecophysiology of tunas. San Diego (CA): Academic Press. Forthcoming.

Sharp GD, Csirke J, editors. 1983. Proceedings of the expert consultation to examine the changes in abundance and species composition of neritic fish resources; San Jose, Costa Rica; 18-29 Apr 1983. FAO Fish Rep Ser 291. volumes 2-3. 1294 p.

Sharp GD, McLain DR. 1993a. Comments on the global ocean observing capabilities, indicator species as climate proxies, and the need for timely ocean monitoring. Oceanogr 5(3):163–8.

Sharp GD, McLain DR. 1993b. Fisheries, El Niño-Southern Oscillation and upper-ocean temperature records. Oceanogr 6(1):13–22.

Sobel D. 1996. Longitude. Penguin USA. 184 p.

Soutar A, Isaacs JD. 1974. Abundance of pelagic fish during the 19th and 20th centuries as recorded in anaerobic sediments of the Californias. Fish Bull 72:257–73.

Soutar A, Crill PA. 1977. Sedimentation and climatic patterns in the Santa Barbara Basin during the 19th and 20th centuries. Bull Geol Soc America 88:1161–72.

Southward AJ. 1974a. Changes in the plankton community in the western English Channel. Nature 259:5433.

Southward AJ. 1974b. Long term changes in abundance of eggs in the Cornish pilchard (*Sardina pilchardus* Walbaum) off Plymouth. J Mar Biol Assn.UK NS 47:81–95.

Svensmark H, Friis-Christensen E. 1994. Variation of cosmic ray flux and global cloud coverage—a missing link in solar-climate relationships. Journal of Atmospheric and Solar-Terrestrial Physics 59:1225–32.

Thompson LG, Davis ME, Mosely-Thompson E, Sowers TA, Henderson KA, Zagorodnov VS, Lin P-N, Mikhalenko VN, Campen RK, Bolzan JF, Cole-Dai J, Francou B. 1998. A 25,000-year tropical climate history from Bolivian ice cores. Science 282:1858–64.

Thompson LG, Mosely-Thompson E, Davis M, Lin P-N, Yao T, Dyurgerov M, Dai J. 1993. Recent warming: ice core evidence from tropical ice cores with emphasis on central Asia. Global and Planetary Change 7:145–56.

Thompson LG, Mosely-Thompson E, Davis M, Bolzan JF, Dai J, Yao T, Gundestrup N, Wu X, Klein L, Xie Z. 1989. Holocene-late pleistocene climatic ice core records from Qinghai-Tibetan Plateau. Science 246:474–7.

Thompson LG, Mosely-Thompson E, Davis ME, Lin P-N, Henderson KA, Cole-Dai J, Bolzon JF, Liu K-B. 1995. Late glacial stage and holocene tropical ice core records from Huascaran, Peru. Science 269:46–8.

Tinsley BA. 1996. Correlations of atmospheric dynamics with solar wind-induced changes of air-earth current density into cloud tops. Journal of Geophysical Research Atmospheres 101(D23, 29):701–29, 714.

Tinsley B, Brown GM, Sherrer PH. 1989. Solar variability influences on weather and climate: possible connections through cosmic ray fluxes and storm intensification. J Geophysical Research 94(14):783–92.

Valdivia J. 1980. The anchoveta and El Niño. Rapp PV Réun CIEM 173:196–202.

Pollen Analysis of Late Pleistocene-Holocene Sediments from Core CL-73-5, Clear Lake, Lake County, California: A Terrestrial Record of California's Cismountane Vegetation and Climate Change Inclusive of the Younger Dryas Event

G. James West

Abstract

The Younger Dryas was an abrupt cold event that occurred during the transition from Glacial to non-Glacial climates at the end of the Pleistocene. Its expression is most resolved in the fossil and isotopic records of the North Atlantic region. Pollen frequency and ratio changes from Clear Lake sediments are used to examine the vegetation and climate of the Clear Lake region since the last Glacial Maximum. This new record provides for a higher resolution examination of the transition from Glacial climates to the Holocene not available from previous studies. A reversal in the pine pollen frequencies and ratios of pine-oak values suggests that the Younger Dryas event is reflected in the fossil record for California's North Coast ranges.

Introduction

The transition from late Glacial Maximum (22,000 years ago) climate of the Late Pleistocene to Holocene climatic period appears to have occurred in a step-like manner with several reversals. Many plants and animals responded to these climate shifts by dislocations in their ranges, extirpation, and, in some cases, even extinction. One of the most significant climatic reversals during this transition has been termed the Younger Dryas (YD). The YD was a major cooling event that occurred sometime between 11,700 to 10,200 years BP (Taylor and others 1997). First recognized in the fossil plant records of northwestern Europe, the YD cooling has been documented in numerous fossil records in northeastern North America and appears to have been global in extent. The YD cooling apparently ended as abruptly as it began.

Further down the air stream, the eastern Pacific borderlands' record of the YD is uneven and, with little exception, not well defined. Fossil isotopic records from near shore deep marine basins appear to provide the most explicit YD record (Kennett and Ingram 1995) and fossil and isotopic records from the higher latitudes (Grigg and Whitlock 1998) and the Great Basin (Benson and others 1997) provide additional evidence. In many of the cismountane California terrestrial pollen records, the transition from the Pleistocene to the Holocene is missing (Davis 1999), not highly resolved (Adam 1988), or obscured by inverted ^{14}C dates of the shallow meadow-marsh-pond sediments of high elevation west slope Sierran fossil sites of YD age (Davis and Moratto 1988). Cryoturbation of YD age

sediments of west slope Sierran meadows is the probable cause of the reversed order of the radiocarbon dates and sedimentary disconformities, a condition that does not appear in the later Holocene sediments. For cryoturbation to occur, YD temperatures had to be cold enough to freeze (probably repeatedly) the meadow, marsh, or pond deposits of these shallow Sierran sedimentary basins. If these deep freezes did occur, the YD climate must have had a significant affect on California's cismountane vegetation.

As part of the Anderson Flat Archeological Project on the east side of Clear Lake, pollen analysis of two USGS sedimentary cores from Clear Lake was undertaken to clarify late Pleistocene-Holocene regional environments. Adam's (1988) earlier study of Clear Lake cores CL–73–4 and CL–73–7 emphasized the long-term aspects of vegetation and climate change and how such changes correlated with other long-term records that cover the late Quaternary. In the present study of core CL–73–5, the emphasis has been to provide a higher resolution pollen record of the late Pleistocene-Holocene vegetation-climate transition noted by Adam (1988), and in particular to examine the pollen frequencies-ratios of YD age sediments.

Methods

USGS recovered core CL–73–5 (core 5) by a truck mounted drilling rig from a barge using Shelby and Ostenberg samplers. The location of core 5 is near the south shore of the main body of Clear Lake north of Mount Konocti (Figure 1). Core slugs were retrieved and extruded into rigid plastic tubes which were sealed with plastic endcaps and waxed to prevent moisture loss. In the USGS laboratory the cores were split lengthwise, inspected, logged and photographed. A 1-cm slice was removed from the middle of each core segment for X-ray radiography. For pollen analysis, USGS cut equal sized samples from the core at 10-cm intervals wherever core recovery and preservation allowed. Descriptions of the recording and sampling procedures are provided in Beaver and others (1976). David Adam, USGS, arranged to provide the samples and copies of the records from core 5.

Pollen extraction was undertaken at the Department of Anthropology, University of California, Davis. Standard methods for Quaternary age sediments including hydrofluoric acid digestion, acetylation, and hydroxide dissolution of humates were used (Faegri and Iversen 1975). Slides prepared from the extracted samples were mounted in AQUA-MOUNT medium. Counting was done with a Nikon Labophot phase contrast microscope with a 40X objective and 10X eyepieces. Identification of pollen grains was based on type slides made from collections at the Tucker Herbarium, University of California, Davis and the Jepson Herbarium, University of California, Berkeley, and on illustrations and keys in standard pollen texts. Plant and pollen nomenclature follows Hickman (1993), Adam (1967), and Faegri and Iversen (1975).

Four tablets (Batch #414831), each containing about 12,100 exotic *Lycopodium* spores, were added to each sample to determine absolute pollen abundance by weight and volume (Stockmarr 1971). Because of inadequate temporal constraints, pollen influx values were not determined.

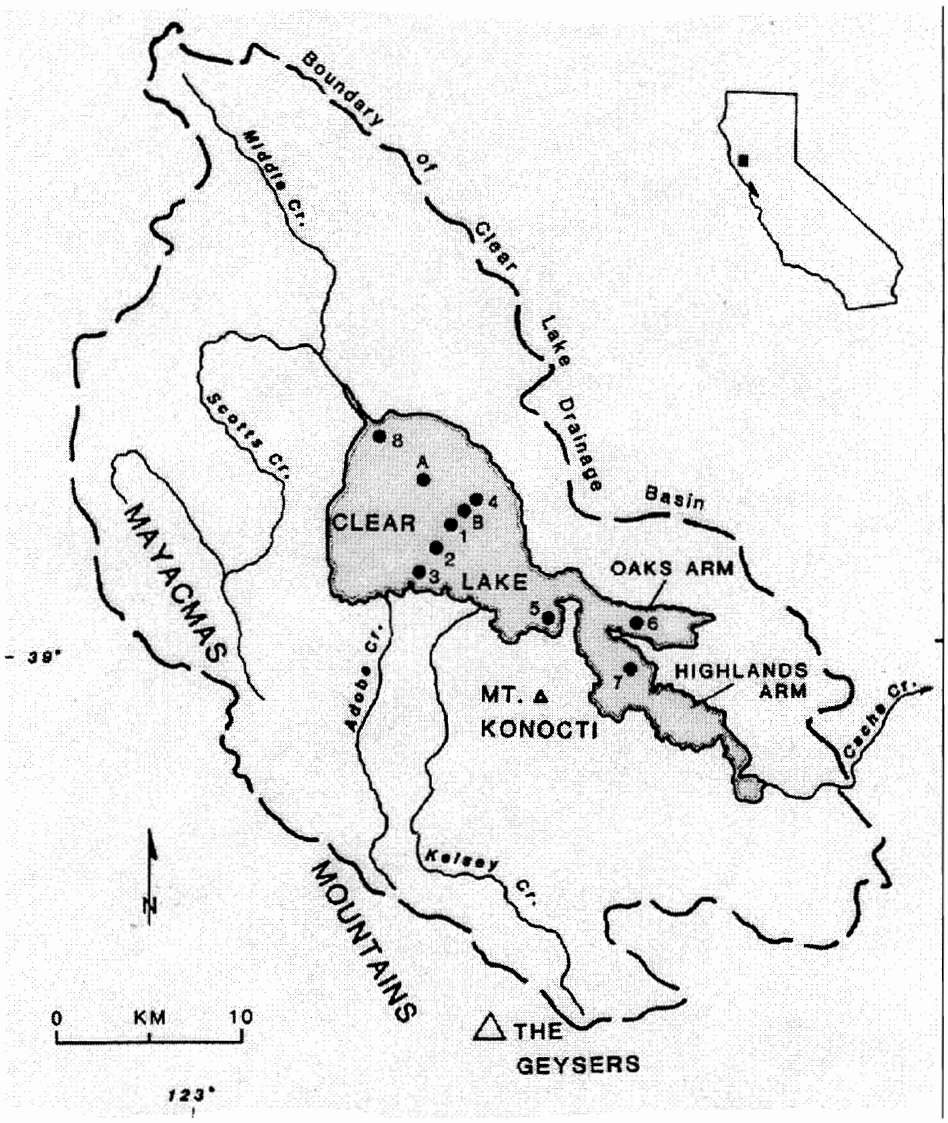

Figure 1 The Clear Lake drainage basin showing geographic features and core locations in the lake. Numbered sites refer to the series of U. S. Geological Survey cores taken in 1973 and are designated by the prefix CL-73-. Lettered sites refer to the two cores taken in 1980. (from Sims 1988).

Seventy-four samples from core 5 were counted. A minimum of 200 arboreal pollen grains or 200 *Lycopodium* spores were counted for most samples. The algae *Botyrococcus* was counted but the abundance of the algae *Pedistrium* was so great that it was not counted.

The pollen diagram for core 5 was produced by TILIA (Figure 2). Unlike Adam (1988), the aquatic-emergent fossil pollen types are outside the pollen sum as are the microspores of *Isoetes* (quillwort). However, the inclusion of pollen grains from aquatic-emergent plants in the sum has very little effect on the data since those types are scarce. Based on previous studies (Adam and West 1983) the *Quercus*:(*Quercus* + *Pinus*) ratios were determined for core 5 and are presented in Figure 3.

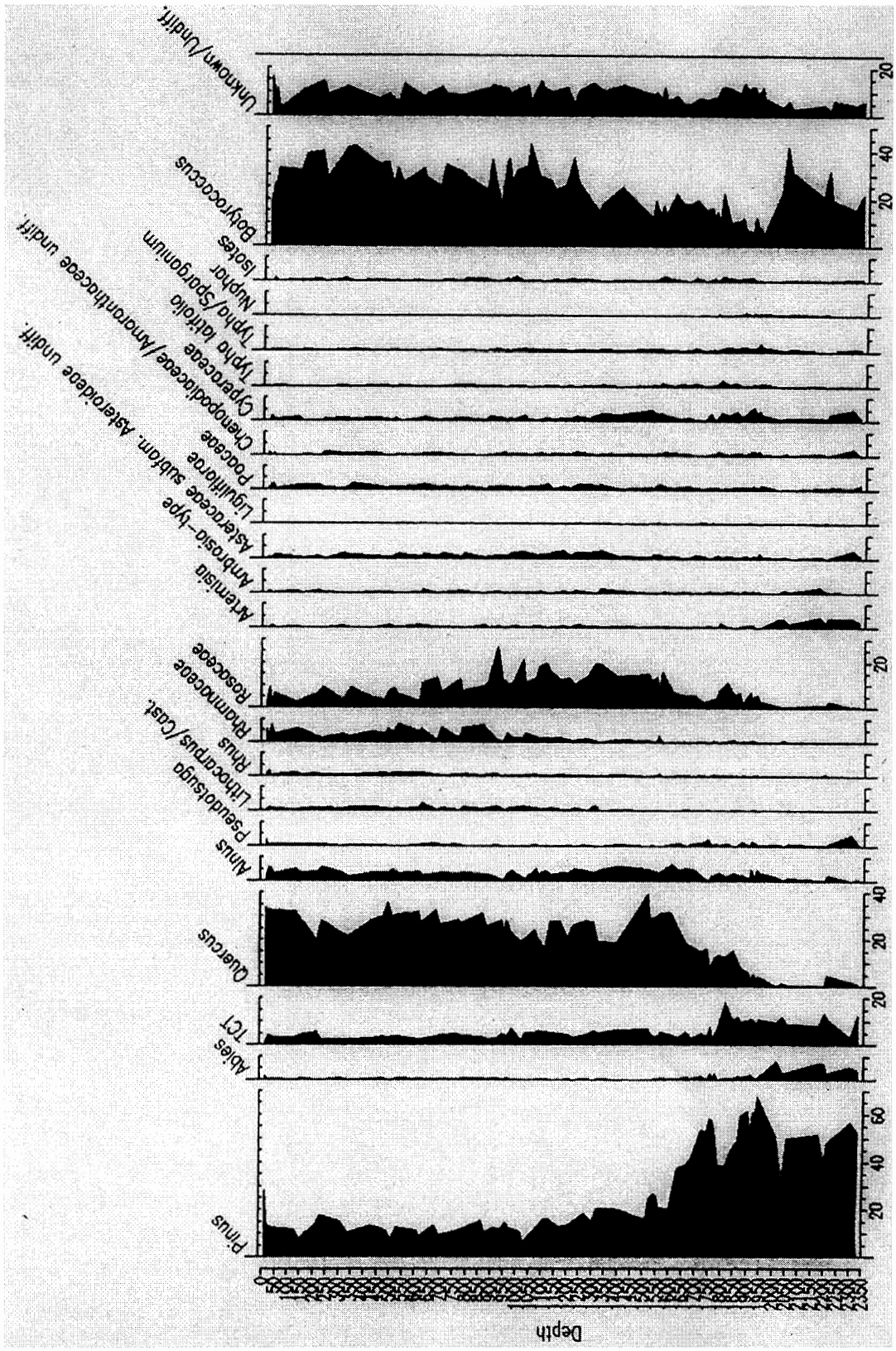

Figure 2 Relative pollen values for core CL-75-5, Clear Lake, Lake County, California

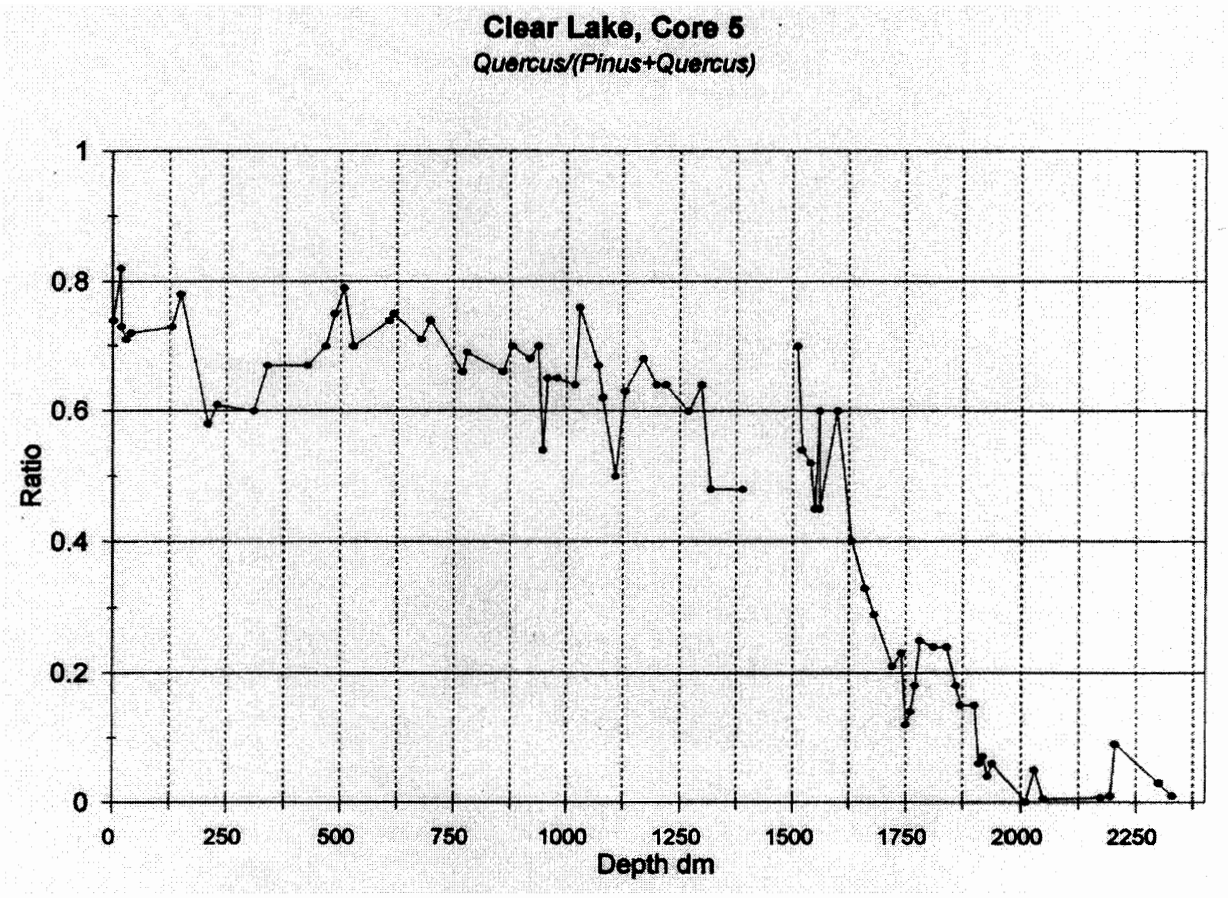

Figure 3 Ratio of Oak to Pine pollen values (*Quercus/Pinus* + *Quercus*), core CL–75–5

Results

Sediments

Core 5 is from the west side of Buckingham Peninsula near the south shore of the main body of Clear Lake. Depth at the core site of the water in October 1973 was 7.6 m. Average depth of water in the main part of the lake is about 9 m (Sims 1976).

Sediments for core 5 are described in Sims and Rymer (1975a). Recovery of sediments was about 94%, with significant gaps in recovery between 14 to 15 m and 22.15 to 22.6 m. The sediments consist of olive gray to dark olive gray (5Y4/2 to 5Y3/2) mud with seven inter-bedded volcanic ashes. Extensive bioturbation has undoubtedly obscured many of the sedimentologic features. No peat deposits are present, suggesting that the sediments were deposited in depths of water >2 m.

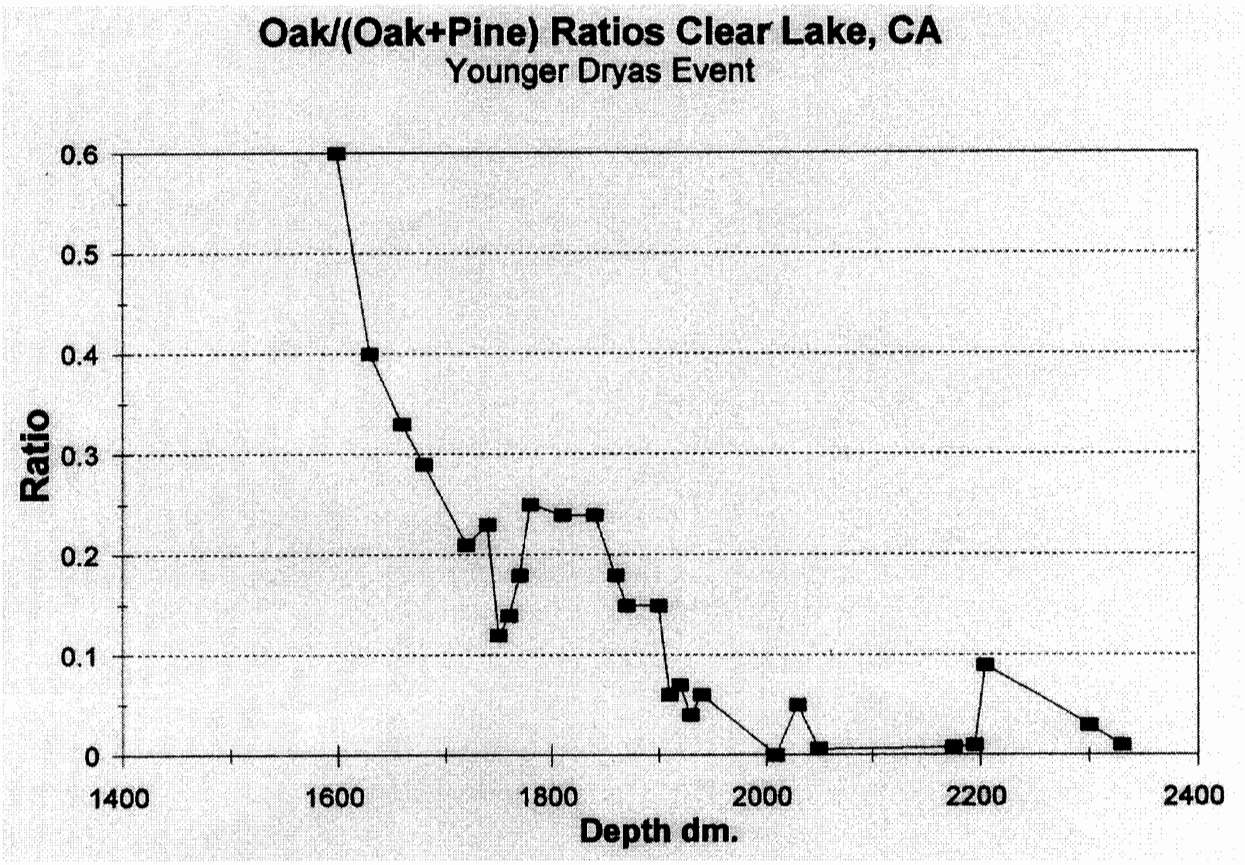

Figure 4 Ratio of oak to pine pollen values for the Late Pleistocene-Younger Dryas event, core CL–75–5

Pollen

Fifty-three pollen types were identified: 15 arboreal, 29 non-arboreal, and seven aquatic-emergent, and two spore types. Unknown and undifferentiated pollen grains averaged about 12% and ranged from 5% to 22% of the pollen sum. A large percentage of the unknown grains are likely derived from non-arboreal taxa (shrubs and herbs). Pollen preservation was generally good. Raw pollen counts are presented elsewhere (West n.d.).

Major Pollen Types

Pinus (Pine) grains were counted as wholes and thirds. While five species of pine grow in the region, no effort was made to distinguish individual species or classes of pine. Gray pine (*P. sabiniana*) is the most common pine in the Clear Lake basin today. With the exception of sugar pine (*P. lambertiana*), all the pines in the region are in the subgenus Diploxylon.

Abies (Fir) grains are discontinuously present in the section, but are most prominent between 2,010 and 2,330 cm with values between 3% and 10%. Seven species of fir occur in California. The grains are most likely derived from white and red firs (*A. concolor*, *A. magnifica*) that grow in higher elevation conifer forests to the north of Clear Lake, such as those at Snow Mountain. Another likely candidate is grand fir (*A. grandis*). Grand fir is presently restricted to the coast as far south as the Russian River, where it grows at lower elevations (generally <2,000 ft) in more temperate habitats than stands of white fir (Griffen and Critchfield 1972). Adam (1988) identified needles from Grand fir in full glacial age sediments from cores 1 and 4. Of the four other fir species, their ranges are restricted either to western Monterey County (*A. bracreata*) or to high northwestern mountane regions and are less likely candidates.

Quercus (Oak) pollen grains are representative of more than one species. Seven species of oaks are found in or immediately adjacent to the Clear Lake basin today. Blue oak (*Q. douglasii*) is the dominant oak in the basin. No attempt was made to separate out the oaks on the basis of their pollen.

TCT (Taxodiaceae, Cupressaceae and Taxaceae) pollen grains are combined together because of the difficulty in distinguishing the various taxa. Incense cedar (Libocedrus decurrens) and cypress (*Cupressus* spp.) are probably the main contributors, but occasional grains of redwood (*Sequoia sempervirens*) were observed. Other possible contributors to the TCT category are the yews, particularly nutmeg (*Torryana california*) and the Pacific yew (*Taxus brevifolia*).

Alnus (Alder) pollen grains are present throughout the section. Four species of alder grow in California. The most likely contributors are white (*A. rhombifolia*) and red (*A. rubra*) alders, although mountain (*A. tenuifolia*) and Sitka (*A. sinuata*) alders could have been contributors in times of colder climates.

Lithocarpus and *Chrysolepis* (tanoak, Chinquapin) grains are very similar and were not distinguished in this study. Both taxa occur in Lake County.

Rhus (Sumacs) grains are most likely derived from *R. trilobata* (skunkbrush) and *Toxicodendron diversilobum* (poison oak).

Rhamnaceae (Buckthorn family) pollen grains are from shrubs and small trees, many of which are major components of Chaparral communities. Species in the Clear Lake area include coffeberry (*Rhamnus californica* Esch.) and the California lilac (*Ceanothus* spp.).

Rosaceae (Rose family) pollen grains are from a large family of herbs, shrubs and small trees. Chamise (*Adenostoma fasciculatum* H.&A.), western mountain mahogany (*Cercocarpus betulodies*), *Prunus* spp., and toyon (*Heteromeles arbutifolia*) are prominent Rosaceae types in the Clear Lake basin. Berry bushes (*Rubus* spp.) are common Rosaceae members on the moist areas of the Clear Lake shoreline.

Compositae (Sunflower family, Asteraceae) were divided into four types: high-spine, low-spine, Liguliflorae, and *Artemisia* following Martin (1963). Only *Artemisia* and the high and low-spine Compositae were in high enough values to be plotted. *Artemisia* (sagebrush) pollen grains are derived from sagebrush shrubs or herbs. There are at least 15 species, as well as a number of sub-species, that occur in California. Specific identification was not possible, but *A. tridentada*, *A. californica*, and *A. douglasiana* are likely contributors.

Poaceae (Gramineae, grass) grains, because of limited variation, were not divided into sub-types.

Polygonaceae (Buckwheat family) grains were sorted to Polygonaceae and *Eriogonum* species. *Polygonum californicum* grains were encountered at 9.78, 12.69, and 16.6 m, but have not been entered in tabular form or on the pollen diagram. A single *Rumex* sp. grain was noted in a sample from 5.08 m.

Umbelliferae (Carrot family, Apiaceae) grains were present in small numbers in most samples. The Umbelliferae family is large and most are herbs, many of which are found growing in areas with moist soils.

Cyperaceae (Sedge family) grains are most likely derived from *Scirpus* spp. (tules) growing on the shallow lake margins.

Typha latifolia (cattails) grains are relatively most abundant below 15 m. Cattails prefer water depths of <1 m.

Salix (willow) grains are found in most samples. Willows grow on the moist shoreline of Clear Lake.

Isoetes (quillwort) megaspores are present discontinuously in the profile. Quillwort species are common aquatic plants in lakes and ponds.

Botyrococcus, an algae, is abundant throughout the section, particularly at 20.5 m and above 13 m.

The algae *Pedistrium* was not counted but it is the major portion of the detritus remaining after pollen extraction. Several types noted in Adam (1988) were observed.

Less Common Pollen Types

Douglas fir (*Pseudotsuga menziesii*) grains are discontinuously present but occur most frequently in the upper 5 m and there is a small peak at 23 m. The closest stand of Douglas fir is on the slopes of Mount Konocti, immediately south of the core 5 locality. Regionally isolated trees are found in favorable environments as far south and east as the western drainages of Lake Berreyssa in Napa County.

Other arboreal types of note are redwood (*Sequoia sempervirens*), coast and mountain hemlock (*Tsuga heterphylla*, *T. mertensiana*), and buckeye (*Aesculus californica*). Redwood and coast hemlock are restricted to near coastal areas, although a few redwood stands are present in eastern Mendocino and Napa counties. Mountain hemlock is found in higher subalpine sites to the north. Buckeyes, on the other hand, are a common small tree or shrub on the slopes, canyons and borders of streams in the Clear Lake basin.

Discussion

Age Determination

Core 5 has two radiocarbon age determinations:

Sample #1981 (core 5)	10.82 m	10,400 ± 350	W-3296
Sample #2373 (core 5)	21.75 m	24,080 ± 1,000	W-3220

Robinson and others (1988) argued that old carbon from lake sediments and springs beneath Clear Lake add about 4,200 years to the apparent age of each Holocene radiocarbon age determination and that a significant component of younger carbon makes the dates older than 20,000 years unacceptable for core 4. Fredrickson and White (1988) and White and King (1993) also have questioned the early Holocene radiocarbon age determinations from the Mostin site (CA–Lak–380/381), in which the archaeology is more compatible with a middle Holocene period cultural pattern.

The Holocene age radiocarbon dates for core 5 appear to be too old for the pollen record. The transition from high pine values to high oak values has been dated elsewhere in the North Coast ranges as occurring >8,500 years ago (West 1993) and most likely occurred between 10,000 and 13,000 years ago. Subtracting the 4,200 years proposed by Robinson and others (1988) would make the radiocarbon dates compatible with the upland pollen records (West 1993) and, as proposed by Fredrickson and White (1988), the archaeology at the Mostin site. The "corrected" radiocarbon age determination gives an assumed lineal sedimentation rate of approximately 175 cm/1,000 yrs for core 5. While this rate is a crude estimate, the uniformity of the sediments (some of which may be due to bioturbation) and data from other cores (Adam 1988) suggest an accuracy of ± 1000 years. Because of the old-carbon effect, calibration of the radiocarbon dates to absolute years does not appear to be wise. Clearly, additional dating of the sediments based on the AMS radiocarbon dates of arboreal pollen grains contained within them is warranted.

The Pollen Record

The pollen record from core 5 shows some distinct shifts and trends in the relative frequencies of both arboreal and non-arboreal pollen grains (Figure 2). A very distinct successional pattern is evident in the transition from the Pleistocene to the Holocene. The

lowest level pollen spectra between 1,950 and 2,350 cm are characterized by very high pine, fir, and TCT values. Artemisia is the most important non-arboreal contributor. Oak is virtually absent with values <5%. These pollen spectra have congruence with other Modesto Age spectra from core 4 (see below), Sacramento, and Laguna de las Trancas (West 1998).

Pine pollen values vary in a pattern that may be reflecting significant climatic events; in particular, pine values of >50% occur below 1,650 cm, while above 1,650 cm they are about 15% to 20%. The transition from the higher pine values of >50% to the lower values above 1,650 cm is not uniform, as there is a marked reversal that peaks at about 1,750 cm to 60%. This abrupt shift would appear to mark the YD.

The rising trend in oak pollen values through time reverses in a number of places, with the most notable trend between 2 and 4 m. Beginning from an absence at 21 m, oak values peak between 15 to 16 m at 35% to 40%, then fluctuate between 20% and 35% above 16 m. Oak/(oak + pine) values (Figure 3) and their shift at the Pleistocene-Holocene transition are similar to that observed in cores 4 and 7 by Adam (1988). Using the corrected sedimentation rates noted above, the shift from oak to pine occurred between 9K and 10K. (For estimated dates based on the corrected radiocarbon/sedimentation rates, "K" will be used to indicate 1,000 years BP to avoid confusion with other dating schemes.) The reversal in oak-pine values between 2 and 4 m occurred roughly 1.1K to 2.3K years ago.

Tanoak, sumac, and buckthorn pollen values increase above 13 m. (approx. 7.4K) and Rosaceae pollen values are highest between 6 and 16 m. (approx. 3.4K to 9K). There appears to be an inverse relationship between Rosaceae and buckthorn pollen values—Rosaceae pollen values decline as buckthorn pollen values increase—suggesting that buckthorn replaced Rosaceae types.

Cyperaceae, cattail, and willow pollen grains are generally more abundant below 10m. (>5.7K). Quillwort spores also are more prominent in the lower part of the profile.

The algae Botyrococcus has high values between 20 and 23.3 m (approx. 12.5K), exhibits a sharp drop at 19 to 19.5 m. (approx. 11K), then lineally increases above these levels to values generally exceeding those between 20 and 23.3 m. The sharp drop in Botyrococcus occurs with the initial increase in oak and decrease in pine-fir-*Artemisia* values. These changes may reflect changes in water quality during the transition from late glacial climates to Holocene conditions.

Comparison with other Clear Lake Pollen Records

The overall trend in the pollen record from core 5 compares favorably with cores 4 and 7. For comparison with core 5, the designated (Adam 1988) late Pleistocene and Holocene pollen zones A, B, C and D for core 4 and A7, B7, C7 and D7 for core 7 are pertinent.

Core 4

Zone A extends from the top of the core to a depth of 20 m. Oak pollen is the dominant pollen type having an average value of almost 60%. Pine and TCT frequencies are less than 20%. Rhamnaceae pollen is present in only minor amounts in the bottom of this zone but rises in frequency above 13 m similar to the trend seen in core 5. Tanoak is present in low frequencies above a depth of 16 m; a similar trend is seen in core 5. Not noted in cores 4 and 7 was the trend seen for Rosaceae pollen, since Adam (1988) did not distinguish Rosaceae pollen in his diagrams.

Zones B, C, and D are characterized by pine pollen frequencies of 45% to >60%. Similar pine pollen frequencies were observed below 16 m in core 5. Cyperaceae pollen frequencies are comparable to those observed in core 5. Adam (1988) noted a significant increase of TCT pollen (32%) in zone C; a congruent but lesser increase occurs in core 5, which had TCT values ranging between 15% to 20%, suggesting that zone C may be similar in age to the lowest samples examined in cores 5. Fir pollen is present (2% to 5%) in zones B and D; it is also present in most of the zones below D in core 4. Fir pollen values range from 3% to 10% (average 6.6%, $n = 8$) between 20.1 and 23.3 m in core 5, which is approximately the same depth of pollen zones B through D. *Artemisia* also is most prominent at the same depths in core 5, corresponding to increases observed in zone D.

Pollen concentration and percentage values for core 4 suggest a sequential shift through time in the late Pleistocene to the Holocene from TCT to pine to oak (Adam 1988; Figure 14). The successional sequence from core 5 appears to overlap only the latter part of this transition, since TCT and *Artemisia* values never reach the values observed in zone E of core 4.

Core 7

Zone A7 (0 to 6.8 m). Average oak values for zone A7 are 42%, similar to the frequencies observed above 16 m in core 5 (30% to 45%). Oak pollen percentages verses depth reach their highest values in the middle part of this zone. In core 5, oak pollen percentages show a distinct linear increase from about 16 m to 5 m, decline, then increase in the upper 2 m. These results may be due to the closer sampling interval in core 5 or, more likely, are representative of a regional pollen rain like the trends observed for the oak pollen spectra in core 4. Pine values are about 16%, the same as observed above 13 m in core 5. Like the other profiles, Rhamnaceae pollen is common in the upper part of the zone.

Zones B7, C7 and D7 do not compare as well with cores 4 and 5 because of the high frequencies of pollen from aquatic-emergent plants. Core 7 is from the Highlands Arm of the lake and, as suggested by Adam (1988), may have been subject to local tectonic or other geomorphic events.

Comparison with other North Coast Range Records

No direct comparison with the Clear Lake record can be made since the other North Coast Range records are from small landslide lakes, marshes, forest hollows, and spring mats. These sediment and pollen traps respond to much more local conditions, whereas the Clear Lake records are far more complacent, reflecting a more regional pattern in which most local high-frequency variations in the pollen rain have been filtered out because of a much larger catchment. West (1985, 1990, 1993) has described the late Pleistocene-Holocene vegetation shifts based on 12 upland pollen records which indicate more complex localized changes during the Holocene, but the changes have similar secular successional trajectories most likely resulting from climatic forcing.

On the other hand, the shifts in Rosaceae and Rhamnaceae pollen values are more local in character as representative of the Clear Lake basin, yet Rosaceae pollen frequencies also peak in the mid-Holocene record from Cedar Lake in Shasta County (West 1989). From the same locality, unlike the Clear Lake records, high pine values precede increased frequencies of TCT. A different TCT pollen source, Port Orford cedar (*Chamaecyparis lawsoniana*), is a likely source, whereas in the Clear Lake basin other taxa are obvious contributors. At Lily Pond on the interior side of the North Coast Ranges, Rhamnaceae pollen frequencies increase after about 5000 BP, suggesting a time-transgressive expansion of buckthorn chaparral (West 1983, 1993).

In the upland areas of the North Coast ranges, oak values, like those reflected in the Clear Lake records, increase rapidly at the end of the Pleistocene and peak during mid-Holocene times. Only one record from Clear Lake, core 7, has a mid-Holocene peak, suggesting that core 7 is reflective of a more local pollen rain. A somewhat different pattern is seen in the Sierra Nevada (Anderson 1990; Byrne and others 1993; Davis and Moratto 1988).

The records of oak pollen frequencies for central and northwestern California are not fully compatible with one another since they are from different climatic regions, vegetation distributions, oak species, pollen taxonomic attribution, and depositional and diagenic environments. There are some 18 oak (*Quercus*) species plus hybrids and varieties in California, of which nine are predominately tree size, and two of these trees grow only in southern California and the islands (Hickman 1993; Pavlik and others 1991). The remaining smaller shrub oaks are predominately found within the State's chaparrel communities. In some high elevation Sierra Nevada localities, the range of shrub oaks expanded during the early Holocene, while in the higher elevations of the North Coast ranges tree oaks apparently became more abundant during the mid-Holocene when oak pollen reached its highest values about 5,000 years ago. Nonetheless, it is clear that oaks are an important, if not the dominant, arboreal taxa in large areas of low to mid-elevation central and northwestern California during most of the Holocene.

It appears that California's oaks are favored by inter- and intra-glacial conditions. California oaks rapidly expand their ranges during transitional climatic shifts from glacial (cooler) to warmer conditions when there is limited competition from other taxa. How-

ever, there are other secular changes in the climate that also are occurring in the transition from the Pleistocene to the Holocene. The basis of some General Circulation Models suggests that seasonality in the mid-latitudes was greater during the very late Pleistocene-early Holocene (COHMAP 1988). As a shift occurred away from greater to lesser seasonality, oaks were favored in many areas of California; but as conditions became more equitable, in some places oaks were favored and in other regions they were not. Other taxa expanded at the expense of oaks. During the late Holocene in the North Coast ranges at elevations higher than Clear Lake, oaks decreased with a corresponding increase in Douglas fir (West 1990). Euro-American land-use patterns may be altering the historic pattern of oak regeneration (Byrne and others 1993).

Conclusions

The changes in pollen frequencies observed in core 5 suggest that significant regional vegetation changes have taken place in the Clear Lake basin in the last 20,000 years. Arboreal plant communities dominated by pines-firs-TCT were replaced by oak woodland and chaparral. This shift is interpreted as signaling the transition from glacial (Pleistocene) to inter-glacial (Holocene) climate which occurred in California between 10,000 and 13,000 years ago. However, the successional transition was not unidirectional and at least one major reversal is indicated. The increase in pine values and declines in oak, Rosaceae and TCT values exhibit a pattern that may reflect the YD's cold climatic event on the region's vegetation. While precise dating remains a problem, the observed shifts in pollen frequencies provide additional support for a YD hemispheric scale cooling.

On a regional scale, during the Holocene, chaparral communities became more pronounced and their composition changed. In the early Holocene chaparral community, Rosaceae spp. (most likely dominated by chamise) were most prominent, but by mid-Holocene times members of the Buckthorn family (probably Ceanothus spp.) increased and significantly changed the composition of this community. Sumac also became more conspicuous.

Higher pollen values for aquatic-emergent plants and quillwort spores in the late Pleistocene-Holocene transition and YD times suggest shallower water levels. In other areas of western North America at the same latitude, lake levels during the late Pleistocene (ca. 13 to14.5 kyr) were high, then dropped in the YD, and many lakes dried up during the Holocene (Benson and Thompson 1987; Benson and others 1997). In contrast, the Clear Lake levels appear to have risen during the Holocene. Also, as indicated by the increase in the algae *Botyrococcus*, productivity of the lake co-occurred at about the time of high pine-fir-*Artemisia* values (20 to 23.3 m) in late Glacial times and during the Holocene at the time when the composition of the chaparral shifted. Fluctuations in lake levels appear to be partly the result of geomorphic changes in the Clear Lake basin, but sufficient moisture must have been available to raise the lake level during the late glacial and the early mid-Holocene, about the same time as the high *Botyrococcus* values.

The observed changes and trends in the vegetation undoubtedly are linked, to a greater or lesser extent, to shifts in climatic regimes. The high pine, fir, TCT and sagebrush val-

ues suggest the late Pleistocene was cooler and, probably, more seasonal than today. Unlike upland areas (West 1990), small stands of Douglas fir were present. As the climate warmed, pine and fir decreased rapidly as oak trees increased reflecting the new climatic regime. Pine rapidly increased again as a result of the cold Younger Dryas event that lasted for about a millennium. As a result of the cold, the expansion of oaks was slowed and a slight reversal occurred. TCT species declined to modern levels. Following the YD, during the early Holocene, temperatures again rose rapidly and chamise chaparral quickly invaded slopes that were formerly occupied by pine-fir-TCT dominated communities. Oak trees, virtually absent during late glacial times, resumed their rapid expansion over the Clear Lake basin. Sometime during the early mid-Holocene parallel shifts occurred—tanoak-chinquapin expanded its range and buckthorn moved into the existing chaparral communities. Oak trees continued to expand throughout the basin because of increased moisture or more favorable precipitation patterns. Lake levels went up. Finally, while initially the dominance of oaks declined a bit, modern-day plant communities stabilized during the last few thousand years reflecting our current climatic regime. Again the habitat for Douglas fir had small increases.

Charcoal, obviously derived from fires in the basin, is present in all the core samples examined. While no evidence is present to suggest changes in fire frequency, some of the charcoal may be representative of fires purposely or inadvertently set by Native peoples. If so, this interaction would have affected the basin's vegetation by enhancing fire tolerant or fire dependent species, particularly chaparral taxa, thus adding another variable to the causes responsible for the evolution of the vegetation of the Clear Lake basin. However, the observed major changes, which are congruent with earlier interglacial periods (Adam 1988), appear to be the result of climatic forcing.

References

Adam DP. 1967. Late Pleistocene and recent palynology in the central Sierra Nevada, California. In: Cushing EJ, Wright HE, Jr., editors. Quaternary Paleoecology, New Haven (CT): Yale University Press. p 275–301.

Adam DP. 1988. Palynology of two Upper Quaternary cores from Clear Lake, Lake County, California. U.S. Geological Survey Professional Paper 1363.

Adam DP, West GJ. 1983. Temperature and precipitation estimates through the last Glacial Cycle from Clear Lake, California, pollen data. Science 219(4581):168–70.

Anderson RS. 1990. Holocene forest development and paleoclimates within the central Sierra Nevada, California. Journal of Ecology 78:470–89.

Beaver CK, Adam DP, Sims JD, Rymer MJ. 1976. Sampling procedures and catalogue of samples for eight boreholes at Clear Lake, Lake County, California. U.S. Geological Survey Open File Report No. 76-157.

Benson LV, Burdett J, Lund S, Kashgarian M, Mensing S. 1997. Nearly synchronous climate change in the Northern Hemisphere during the last glacial termination. Nature 388:263–6.

Benson LV, Thompson RS. 1987. Lake-level variation in the Lahonton Basin for the past 50,000 years. Quaternary Research 28(1):69–85.

Byrne R, Mensing S, Edlin E. 1993. Historic distribution of oaks from pollen analysis, oaks 'n' folks. Integrated Hardwood Range Management Program, University of California 8(2):1–2, 6–7.

COHMAP. 1988. Climatic changes of the last 18,000 years: observations and model simulations. Science 214:1043–52.

Davis OK. 1999. Pollen analysis of Tulare Lake, California: Great Basin-like vegetation in central California during the full-glacial and Early Holocene. Review of Palaeobotany and Palynology 107:249–57.

Davis OK, Moratto M. 1988. Evidence for a warm dry Early Holocene in the western Sierra Nevada of California: pollen and plant macrofossil analysis of Dinkey and Exchequer meadows. Madroño 35(2):132–49.

Faegri K, Iversen J. 1975. Textbook of pollen analysis. New York (NY): Hafner.

Fredrickson DA, White GG. 1988. The Clear Lake Basin and early complexes in California's North Coast ranges in early human occupation in far western North America: the Clovis-Archaic Interface. In: Willig JA, Aikens CM, Fagan JL, editors. Nevada State Museum Anthropological Papers 21:75–86.

Grigg LD, Whitlock C. 1998. Late-Glacial vegetation and climate change in western Oregon. Quaternary Research 49:287–98.

Hickman JC, editor. 1993. The Jepson manual: higher plants of California. Berkeley (CA): University of California Press.

Kennett JP, Ingram BL. 1995. A 20,000-year record of ocean circulation and climate change from the Santa Barbara basin. Nature 377:510–4.

Pavlik B, Muick PC, Johnson SG, Popper M. 1991. Oaks of California. Cachuma Press and California Oak Foundation.

Robinson SW, Adam DP, Sims JD. 1988. Radiocarbon content, sedimentation rates, and a time scale for core CL-73-4 from Clear Lake, California. In: Sims JD, editor. Late Quaternary Climate, Tectonism, and Sedimentation in Clear Lake, Northern California Coast Ranges. Geological Society of America Special Paper 214. p 151–60.

Sims JD. 1976. Paleolimnology of Clear Lake, California, U.S.A. In: Horie S, editor. Paleolimnology of Lake Biwa and the Japanese Pleistocene, 4. p 658-702

Sims JD, editor. 1988. Late Quaternary climate, tectonism, and sedimentation in Clear Lake, Northern California Coast Ranges. Geological Society of America Special Paper No. 214.

Sims JD, Rymer MJ. 1975. Preliminary description and interpretation of cores and radiographs from Clear Lake, Lake County, California: Core 5. U.S. Geological Survey Open File Report No. 75-381.

Stockmarr J. 1971. Tablets with spores used in absolute pollen analysis. Pollen et Spores 13(4):615–22.

Taylor KC, Mayewski PA, Alley RB, Brook EJ, Gow AJ, Grootes PM, Meese DA, Saltzman ES, Severinghaus JP, Twickler MS, White JWC, Whitlow S, Zielinski GA. 1997. The Holocene-Younger Dryas transition recorded at Summit, Greenland. Science 278:825–7.

West GJ. 1983. Pollen analysis of sediments from Lily Pond, Lower Letts Valley, Mendocino National Forest, California: a record of Holocene vegetation and climate. In: Charles Slaymaker C, editor. The archaeological test excavations of CA-COL-76 and CA-COL-81, Fouts Springs, Mendocino National Forest, California. Report on file Mendocino National Forest, Willows.

West GJ. 1989. Late Pleistocene-Holocene vegetation and climate. In: Prehistory of the Sacramento River Canyon, Shasta County, California. Basgall ME, Hildebrandt WR, editors. Center for Archaeological Research at Davis, Publication 6. p 36-50

West GJ. 1990. Holocene fossil pollen records of Douglas Fir in northwestern California: reconstruction of past climate. In: Proceedings of the Sixth Annual Pacific Climate (PACLIM) Workshop. Betancourt JL, MacKay AM, editors. Interagency Ecological Studies Program Technical Report 23. California Department of Water Resources. p 119–122.

West GJ. 1993. The Late Pleistocene-Holocene pollen record and prehistory of California's North Coast ranges. In: White G, Mikkelsen P, Hildebrandt WR, Basgall ME, editors. There grows a green tree: papers in Honor of David A. Fredrickson. Center for Archeological Research at Davis, Publication 11. p 219–35.

West GJ. 1998. A Late Glacial age pollen biozone for central California. In: Wilson R, Tharp VL, editors. Proceedings of the Fourteenth Annual Pacific Climate (PACLIM) Workshop; 6-9 Apr 1997. Interagency Ecological Program Technical Report 57. Sacramento (CA): California Department of Water Resources. p 23–35.

West GJ. n.d. Pollen analysis of two Late Pleistocene-Holocene cores from Clear Lake, Lake County, California. In: White G, editor. Anderson Flat Archaeological Project. Anthropological Studies Center, Sonoma State University, Rohnert Park. p 54–67.

Abstracts

Oral Presentations

The Western Winter of 1999–2000

Kelly Redmond
Western Regional Climate Center, Reno NV

For the first time in a quarter century, La Niña lingered through a second year. The general precipitation pattern approximately resembled the "canonical" La Niña winter pattern, and the previous winter, but with significant differences. Most of the western states were drier than average, and the Southwest experienced another extremely dry winter. This region has recently experienced a noteworthy multi-year sequence of climatic anomalies of different types, following on the heels of two wet decades. A variety of environmental and social consequences are occurring there on several time scales. Only the Pacific Northwest and parts of the Sierra Nevada experienced a wet winter. An unusual feature of this La Niña dominated winter was the uncharacteristic temperature pattern: warm nearly everywhere, especially to the north; the exceptions occurred along the Pacific Coast. The possibility of a recent, or ongoing, phase change of the Pacific Decadal Oscillation reached the level of a public discussion, demonstrating the wider awareness of climate in recent years. One item of particular note was a Southwest monsoon that was both extraordinarily wet and badly needed. The dry conditions in the Southwest (punctuated by a wet summer) contrasted sharply with the wet conditions of the Northwest (highlighted by investigations of a world record snowfall), and reiterated the extreme diversity of climate behavior in this region.

Water Year 2000—A February Save

Maurice Roos
California Department of Water Resources, Sacramento, CA

Water year 1999-2000 was the second La Niña year in a row. Looking at total season amounts, it was about as close to average as one could expect in California. This in itself was unusual. Most of the State was in the normal range of precipitation this year. The statewide snowpack water content on April 1 was average also, about 10% below last year's 110% peak. But the southern Sierra pack was about 30% greater than last year, which will provide better supplies in the Fresno to Bakersfield area.

The total seasonal amounts mask some strong monthly departures. Most of the rainy season was dry, especially in the south, where extreme drought prevailed until January. December was extremely dry. We were saved from a bleak water

supply outlook by a wet February, double the monthly average. In fact most of the rain and snow fell during a 60-day period from about mid-January to mid-March.

For the Sacramento River system (the four rivers) the forecasted runoff is slightly under 20 million acre-feet, about 110% of average. It is not certain if the runoff year will be "wet" or slip into the "above normal" category. If it remains wet, this would be six years in a row, unprecedented in the instrumental record. The reconstructed record from three rings indicate a 6 year run of wet years in 1801–1806 and also 1601–1906.

The year was a mellow one as far as flood threats. There was some high water on the major rivers, mostly in February and early March, with enough activity to keep flood forecasters busy. But very few flood stages occurred and flood related problems were at a minimum.

Reservoir storage started well with good carryover from the previous year, generally 110% to 120% of average. As we entered the main irrigation season on April 1, statewide storage was 115% of average, the same as in 1999 and 1998. Most users in the State should have adequate water supplies. However, Central Valley Project west side customers will still have deficiencies.

The Effects of Galactic Cosmic Rays on Weather and Climate on Multiple Time Scales

Ed Mercurio
Natural Sciences, Hartnell College, Salinas, CA

Galactic cosmic rays (GCRs) appear to be a major forcing agent on weather and climate with good correlations to observed effects on multiple time scales ranging from weekly through glacial-interglacial. Effects of GCRS are used to explain observations in the fields of meteorology, climatology, paleoclimatology and paleoecology in this presentation. Svensmark and Friis-Christensen (1997) describe GCRs as "a missing link in solar-climate relationships."

The ionization of the lower atmosphere by GCRs is the meteorological variable subject to the largest solar cycle modulation (Svensmark 1998). Evidence is presented that a primary effect of an increase in levels of GCRs is a decreasing of the temperature of and an increasing of the strength of the stratospheric polar vortex. This has widespread effects on atmospheric circulation including ENSO. Other effects of increases in levels of GCRs include increasing amounts of and albedo of clouds, increasing precipitation, increasing vorticity area indices and increasing relative humidities. Secondary effects arising from these include a colder, more oscillating tropical Pacific, and changes in surface temperatures, levels of glaciation and equabilities. GCRs are modulated by solar magnetic and geomagnetic fields. Their levels are inversely related to the strength of the fields.

Variations in solar magnetic field structure are used to explain the origin of approximately weekly, monthly, quasibiennial, decadal, bidecadal, multidecadal,

and millennial scale climatic periodicities including the modulation of ENSO frequencies and amplitudes. Changes in geomagnetism are used to explain glacial-interglacial periodicities. Channell and others (1998) have correlated changes in geomagnetism to obliquity of the earth's orbit. Obliquity, inclination of the earth's orbital plane with relation to the invariable plane of the solar system and inclination of the earth's orbital plane with relation to the plane of the solar equator are used as the primary parameters to calculate a hypothetical curve of geomagnetism that would result over the last three million years. Higher geomagnetism and lower levels of GCRs are attributed to a greater sum of these factors. This curve is compared to glacial-interglacial chronologies derived from ice core and deep sea core records along with a 412,000-year geomagnetic periodicity modulated by the earth's orbital eccentricity. Effects of high levels of GCRs are used to explain glacial climates, including ENSO. The cycle of the changing time of the year of the earth's maximum B angle is used to calculate a 13,000 year periodicity of geomagnetism. It is used to explain the origin of Bond Cycles and many Heinrich Events.

Changes in the earth's geography and topography are used to explain ice age periodicities. Sulfurous volcanic gasses and anthropogenic factors are shown to affect climate primarily through effects on the stratosphere. Predictable changes in levels of GCRs are used to predict climate changes of the future. The effects of GCRs on weather and climate are used to explain (1) variations in the earth's rotation rate, (2) characteristics of prehistoric biological communities and their variations with glacial-interglacial chronology, (3) the uniqueness of the Holocene, (4) causes of Quaternary megafaunal extinctions, and (5) effects of resulting climates, environments, and theft changes on human prehistory.

Changes in the Onset of Spring in the Western United States

Daniel Cayan
Climate Research Division, Scripps Institute of Oceanography, La Jolla, CA

Fluctuations in spring climate over the western United States have been consequential, with changes in both the onset of plant development and in the timing of snowmelt runoff over the region. These changes are described using a network of observations of plant phenology and daily streamflow from snowmelt. Two measures of spring's onset are considered: (1) the timing of the first bloom of lilac and honeysuckle bushes from a cooperation phenological network that was maintained from 1957-1994 and (2) the timing of the first major pulse of snowmelt recorded in mountainous streams. Although springtime plant development and snowmelt runoff are controlled by factors such as latitude and orography, the first bloom of lilacs and honeysuckles and the spring snowmelt pulse also contain year-to-year fluctuations from their long-term average timing, with typical anomalies of one to three weeks from long-term averages. First bloom anomalies and spring runoff timing anomalies both exhibit considerable spatial coherence, with regional patterns that cover most of the West. Fluctuations in the lilac first bloom are highly correlated to those of honeysuckle and these are also significantly correlated to fluctuations in spring snowmelt pulse, suggesting that they may each

respond to a common climate-related cause. Anomalous temperature exerts the greatest influence upon both interannual and secular changes in the onset of spring in these networks. Earlier spring onsets since the late 1970s are a remarkable feature of this record, which reflects the unusual spell of warmer-than-normal springs over the western United States during this period. This warm episode is clearly related to larger scale conditions across the North Pacific and North America, but whether it is purely an expression of natural variability or also a symptom of global warming is not certain.

Climate Change Sensitivity Analysis of Two California Headwaters: American River and Russian River

Normal L. Miller[1], Jinwon Kim[1], and Michael D. Dettinger[2]
[1]Regional Climate Center at Berkeley National Laboratory, University of California
[2]Geological Survey at the University of California, San Diego

A preliminary climate change study using the HadCM2 as initial and lateral boundary conditions to the Regional Climate System Model were used to generate forcing for the Precipitation Runoff Modeling System at the American River headwater and TOPMODEL at the Russian River headwater. The atmospheric 2xCO2 environment produces an increase in stream flow at the American River headwater during January to April (approximately double), a decrease from May to July (approximately half), and an increase from July to November (approximately triple). The large increase during January to April can be attributed to temperature increase in the HadCM2 scenario causing early snowmelt and increased runoff. The loss of winter snowpack in turn reduced the spring and early summer stream flow. The increase toward late summer is due to the high water vapor that the HadCM2 produced during the summer season. The Russian River headwater, which does store snowpack, showed an increase in stream flow from December to February, and a decrease from February to May, with a small increase during the summer months. Both the Sierra Nevada headwater and the northern coastal headwater show a shift in the timing of peak stream flow. For the American, this shift is from May-June to February-March and for the Russian the shift is from March to February.

Linkage Between Anti-sprawl Land Use Policies and Climate Changes

Bonnie C. Gee
Department of Geography, University of Montana

Technological and non-technological response strategies are discussed in the Intergovernmental Panel on Climate Change's 1995 report, *Economics and Social Change*. The non-technological strategies suggested are cost-effective energy conservation and efficiency improvements, CO_2 mitigation, and forestry options. Land use policies can be used to implement these strategies.

I will discuss three non-technological land use policies that are linked to the earth's CO_2 budget. One policy links developer incentives with increased housing density and energy efficient design. A second policy links tax and cash incentives with planted open space retention in the form of forests, parks, agricultural lands, and wildlife preserves. A third policy links community design with less driving through the use of convenient walkways, bikeways, rapid transit and mixed use zoning that provides desired services in close proximity to housing.

The data presented illustrate the use of these policies in three locations with anecdotal results. While there is good conceptual understanding of the connection between the earth's CO_2 budget and its vegetative cover, as well as the heat island effect when urban areas are concretized, there is little long-term quantitative assessment of the relationship between suburban sprawl and the greenhouse effect. The results stress the need to assess the effect of anti-sprawl land use policies on the earth's CO_2 budget.

Effects of Recent Precipitation Variability in Northern California on CALFED

Lawrence H. Smith
U.S. Geological Survey, Sacramento, CA

Probably the driest decade on record in northern California occurred from 1985 to 1994. During this period winter run salmon (*Oncorhynchus tshawytsha* [wr]) and delta smelt (*Hypomesus transpacificus*) were declared threatened species under the Endangered Species Act and biological opinions helped limit subsequent freshwater exports from the Sacramento-San Joaquin Delta to the smallest amounts since the 1976–1977 drought These conditions increased public desire to find a long-term solution to the problems of the Delta. CALFED was created in December 1994 by agreement among State and federal agencies and stakeholders to seek public consensus on a 30-year solution. Since then northern California has experienced six consecutive wet years, and CALFED is trying to reach consensus on a solution for the third time during this period. These attempts appear to relate better to two-year political cycles than to hydrologic variations.

Drought Issues in the Western United States

Kelly Redmond
Western Regional Climate Center, Reno NV

Aridity and dryness are defining characteristics of large parts of the West. These are linked to, and often confused with, drought, which can be broadly defined as a lack of water to meet needs or demands. This perspective views drought as a relative phenomenon, defined by its effects, and exhibiting different faces simultaneously on a variety of time scales. No single index can adequately capture the full status of drought, even if given a (well-motivated) desire to distill its considerable complexity into simple numbers. Drought has the greatest economic effect of

all climatic phenomena, exceeding floods and severe weather. The factors which lead to western drought or dry periods are to a significant degree associated with behavior in the Pacific Ocean. Aside from smaller-scale regional droughts, the West has not been affected by a major drought for nearly 50 years. As planning horizons slowly lengthen, it is becoming increasingly important to better understand the long-term context of dry and wet periods over periods of hundreds of years to millennia. Climate change and climate stationarity thus emerge as strong elements of the discussion about what the future will bring. The Western Drought Coordination Council, an activity of the Western Governors Association, and the followup National Drought Policy Commission, have recently led to much greater attention to this issue regionally and nationally. An operational Drought Monitor has proven to be the locus for a weekly dialog and a number of stimulating email discussions. Research needs deriving from these activities will be addressed, and in particular two complementary themes relevant to PACLIM: (a) the use of long proxy records to reconstruct drought histories and (b) the effects of long-term climate variability (on several scales) on how human and natural systems function.

Update of Winter (DJF) 1901–2000 PAPA Trajectory Index (PTI) Time-series, computed with the Oscurs Model, is Examined for Anticipated Shift in Decadal North-South/Wet-Dry Oscillation Patter in the Gulf of Alaska

W. James Ingraham Jr.
Alaska Fisheries Science Center-NMFS-NOAA, Seattle, WA

Sea surface drift trajectories with start-points from Ocean Weather Station PAPA (50°N, 145°W) were simulated using the OSCURS (Ocean Surface Current Simulations) model for each winter (Dec. 1 to Feb. 28) from 1901 to 2000. To reveal decadal fluctuations in the oceanic current structure, the trajectories were smoothed in time with a five-year boxcar filter. The drift from Ocean Weather Station Papa has fluctuated between north and south modes about every 20 years over the last century. The time-series has been updated with year 2000 calculations. Development of OSCURS was motivated by the need in fisheries research for indices that describe variability in ocean surface currents. These synthetic data, although derived from empirical modeling and calibration with satellite-tracked drifters, provide insight which far exceeds their accuracy limitations. OSCURS daily surface current vector fields are computed using empirical functions on a 90 km ocean-wide grid of monthly mean sea level pressures (1900–1945) and daily sea level pressures (1946–1997); long-term-mean geostrophic currents (0/2000 db) were added. The model was tuned to reproduce trajectories of satellite-tracked drifters with shallow drogues from the eastern North Pacific. Additional start points were selected in the Bering Sea and their time series examined for insight into the 1989 regime shift controversy.

The Extratropical Northern Oscillation Index (NOIx): A New Index of Environmental Variability for the Northeast Pacific

Phaedra M. Green, Franklin B. Schwing, and Tom Murphree
Pacific Fisheries Environmental Laboratory, SWFSC/NMFS, Pacific Grove, CA

Prior studies of annual cycles and warm and cold ENSO events have shown that the North Pacific High (NPH) pressure system is an important indicator of climate variability in the northeast Pacific Ocean (NEP). On a basin scale, this stems from the NPH's role in the north Pacific's Hadley-Walker atmospheric circulation, which links the NEP to the tropics. On a smaller scale, this stems from the NPH's role in surface wind stress over much of the NET, which drives coastal upwelling in the Monterey Bay National Marine Sanctuary.

A strong correlation between the Southern Oscillation Index (SOI) and NPH on interannual to decadal scales led us to develop a North Pacific equivalent of the SOI. The extratropical Northern Oscillation Index (NOIx) is the sea level pressure anomaly from climatology at the annual mean position of the NPH (35°N, 135°W) minus the pressure anomaly at Darwin, Australia. It relates variability in the teleconnections between equatorial and midlatitude Northern Hemisphere regions. The NOIx seems to be a better indicator of NEP variability then the SOI due to the proximity of the NPH, plus a connection to a tropical location (Darwin) that encompasses zonal and meridional processes, including variations in the north Pacific trade winds. We explore the connection between the NOIx and a number of atmosphere and ocean variables (SST, winds, and precipitation) for regional to global scales and evaluate the utility of the NOIx as an index of ecosystem climate change in the Sanctuary and for the NEP.

Regional Effects of ENSO and the PDO in the Upper Colorado River Basin Hydroclimate

Hugo G. Hidalgo and John A. Dracup
Civil and Environmental Engineering Dept., University of California, Los Angeles, CA

This study investigates the effects and possible links between the Pacific Basin climate, acting as a forcing mechanism, and the response of hydroclimatic variables in the Upper Colorado River Basin (UCRB). It builds on recent research on interdecadal climatic variation in the Pacific Basin and its effects on the North American physical environment.

Previous research has shown episodic changes in North Pacific climate conditions over relatively short periods of time, also known as climatic regime shifts. The most well known of these climate regime changes occurred in 1976–1977, when physical and environmental variables exhibited a significant change in their characteristics compared to pre-1977 conditions. This event seemed so strongly evident in physical records for some regions, that many researchers initially

reported this shift as a single event. Recently, other researchers suggested that this is just one realization of an interdecadal recurring climatic pattern, with widespread effects around the Pacific Basin. Additional significant changes were recorded in 1924–1925 and 1946–1947. These changes are associated with sign reversals of the north Pacific sea level pressure (SLP) and sea surface temperature (SST) fields. The atmospheric component of these variations is obtained in the leading principal component (PC) of the North Pacific SLP, also known as the north Pacific pressure index (NPPI). Variations of the oceanic component, which contain the longer memory, are represented by the leading PC of the SLP field, named (inter) decadal Pacific oscillation (PDO). These regime shifts produce changes in the mean and/or the variance on physical records such as glacial mass, streamflow, marine populations, ecological response variables, and fires around the North Pacific Basin.

For the UCRB, our preliminary results suggest that the 1976–1977 climatic regime shift is particularly strong in several hydroclimatic variables (i.e. streamflow, precipitation, tree rings and Palmer Drought Severity (PDS) indices) as shown by a change in the frequency of extreme events. Also, significant changes in the mean in annual averages of streamflow, PDS indices, and with less intensity in total precipitation could be detected in 1976–1977. Average annual temperature was the only variable that showed all three steps (1924–1925, 1946–1947, 1976–1977) in the mean coincidental with the PDO. Compared to the more complicated mechanisms that carry moisture from the ocean to the basin, a strong temperature link may be related to a more direct atmospheric teleconnection between the Pacific and the UCRB. Links between the PDO and El Niño Southern Oscillation (ENSO) are still under research. Work in progress is aimed to study the modulation of the response of extreme events caused by the combination of both effects.

The Pacific Decadal Oscillation and Flood Frequencies in the United States

Michael Dettinger and Daniel Cayan
U.S. Geological Survey, Scripps Institution of Oceanography, La Jolla, CA

Interdecadal variations of the climate of the North Pacific Ocean basin have been categorized by an index of sea-surface temperature patterns called the Pacific Decadal Oscillation (PDO). The PDO tracks climate variations that in part are distinct from, and complementary to, the tropical climate variations of the El Niño-Southern Oscillation (ENSO) process. Together the PDO and ENSO climate variations make significant contributions to year-to-year streamflow variability in North America. To identify possible PDO influences on the occurrence of floods, statistics describing the magnitude of floods with 5-year to 50-year return intervals have been analyzed in daily streamflow series from over 1100 gaging stations in undisturbed river basins across the conterminous United States. In 34% of the flow records analyzed, the estimated magnitudes of 20-year floods, calculated from annual maximum daily flows in years during which a 5-year moving averaged PDO index is positive, are significantly different (at 99% confidence level) from the corresponding flood magnitudes during years in which the smoothed PDO index is negative. Larger and smaller floods (with between 5-year and 50-year return inter-

vals) are similarly influenced. To use such statistics for prediction of flood probabilities, and in recognition of the rapid response of atmospheric circulations and fluxes to sea-surface temperature variations, the corresponding statistical analyses were repeated with a version of the PDO index that can be estimated from immediately antecedent sea-surface temperature variations. Flood frequencies were well correlated with this "nowcast" of the decadal PDO variations, which encourages a new set of long-lead forecasts of flood-frequency variations in rivers throughout the country.

Circum-North Pacific Climate Variability and a Tree-Ring Reconstruction of the Pacific Decadal Oscillation

Rosanne D'Arrigo[1], Ricardo Villalba[2], and Gregory Wiles[3]
[1]Tree-Ring Laboratory, Lamont-Doherty Earth Observatory
[2]IANIGLA-CRICYT, Mendoza, Argentina
[3]Wooster College, Wooster, OH

Instrumental studies have recently described the existence of decadal-scale oscillatory modes of atmosphere-ocean variability for the Pacific sector. The climatic regime shift around 1976 is one noteworthy example of this decadal scale climatic variability in the Pacific, and was shown to have affected climate along the western Americas. Meteorological data for the Pacific and western Americas are short, limiting analyses of decadal-scale climate variability. Here we document the existence and stability of decadal-scale oscillations using temperature and precipitation-sensitive tree-ring series from the circum-Pacific region spanning the past four centuries. A reconstruction of the Pacific Decadal Oscillation index is described based on western North American tree-ring records covering the period AD 1790–1980. Evaluation of tree-ring records from the circum-Pacific, including Hokkaido, Kamchatka, and the western coasts of the two Americas, reveals a shift towards more pronounced interdecadal variability in the pre-instrumental period before about 1850.

The Influence of Climate on the Decorative Styles of Neolithic Pottery

L.G. Riddle
Scripps Institution of Oceanography, University of California, San Diego, CA

I examined one aspect of Neolithic pottery decorative traditions: the relationship between ceramic decorative styles and whether the local climate is moist throughout the year or has extended seasonally dry periods. TFUs study does not consider the symbolic meaning of the decorations, just the methods used to apply the decorations to the pottery.

To accomplish this, I examined the regionality of Neolithic ceramic decorative styles in various regions of the Northern Hemisphere (North America, Japan,

Western Europe, the Middle East, and North Africa) and the influence of climate on those styles. The study is in three parts. Part one is an examination of the decorative style of the pottery of the eastern United States. Part two examined that of the western United States. The final part of the study examined some stylistic similarities between decorative styles in North America and similar climates in other regions of the world. It also proposes some reasons for those similarities.

Climate appears to have a definite influence upon the choice of decorative ceramic surface methodology in Neolithic societies. In the temperate and subtropical climate zones of the Northern Hemisphere, pottery decorative methodologies appear to be separated along the "Cs"/"Cf" division in the Trewartha system. The "Cs" and drier climates have painted surfaces and the "Ct" and wetter climates have tooled surfaces.

Tree-Ring Records of Drought in the West Since AD 1000

M.K. Hughes and G. Funkhouser
Laboratory of Tree-Ring Research, University of Arizona, Tucson, AZ

The western United States are rich in natural records of past climate variability. In particular, the region has a unique concentration of tree-ring records of 1000 years and longer. They contain clear, extractable climate signals whose precise nature depends on whether their growth is limited primarily by moisture availability (near tree species' lower elevational limits) or a combination of temperature and moisture availability (near their upper limits). We have gone back to the raw data (on which these records are based) and recalculated the record of common ring growth patterns for each site-species combination. Short series have been excluded from these reworked chronologies and only the most conservative methods were used to remove non-climatic noise. This has been done to enhance the retention of information concerning decadal to century time scale fluctuations. Once reprocessed, the array of site chronologies has been used to build regional networks that we have used to reconstruct spatiotemporal variations of Palmer Drought Severity Index and November-April precipitation since AD 1000. That is to say, the results may be viewed as annual maps of these variables, or as almost 1,000-year time series for each of the points on the 2-by-3 degree grid reconnected. One network of sixteen 1,000-year and longer chronologies was developed using no individual sample with less than 500 annual rings. This has been used to investigate multi-decade to century-scale variation in the climate of the region. One of the most striking features of these reconstructions is the existence of several robust modes of quasi-periodic variation, for example in a multi-grid-point mean for the Four Corners Region. The strongest modes of variation had periods of 71.4 years (6.1% of total series variance), 286 years (5.1%), 31.7 years, 125 years (3.3%) and 21.5 years (2%). The decadal-to-century scale portion of this series resembles a reconstructed principal component of the global annual surface temperature field (Mann and others 1998) that relates primarily to conditions over the Atlantic Basin.

Another network of twenty-seven 1,000-year and longer chronologies has been developed relaxing this minimum segment length to 100 annual rings. This was done to provide better spatial detail and to allow study of variation in the properties of interannual to decadal variability in the climate of the region since AD 1000. Maps and time series analogous to those derived from the 16-site dataset have been produced. A subset of the 27-site dataset, comprising those that extend to AD 1988, has been used to develop reconstructions of the Southern Oscillation Index and the Pacific Decadal Oscillation back to AD 1000. The reliability and implications of these reconstructions will be discussed.

Reference: Mann ME, Bradley RS, Hughes MK. 1998. Global-scale temperature patterns and climate forcing over the past six centuries. Nature 392:779–87.

Cell Dimensions—A Possible Source of Age-independent Proxy Data from Larch Tree Rings

Irina P. Panyushkina, Malcolm K. Hughes, Eugene A. Vaganov, and Martin A. Munro
Laboratory of Tree-Ring Research, The University of Arizona, Tucson, AZ

Ring width and maximum latewood density of annually dated conifer tree rings have long been established as premium sources of information on aspects of past climate variability on interannual to multidecadal time scales. Both ring width and maximum latewood density vary not only in response to climate, but also show a long-term trend that is related to tree age and size. A trend-removing procedure carries with it the risk of also removing low-frequency (that is, century to millennial-scale) climate information. There is currently vigorous controversy about continental to global scale variability in temperature over the last 1,000 years, focusing on the nature of low-frequency century- to millennium-scale changes in surface temperature. Hughes and others (1999) have established a well-calibrated reconstruction of early summer temperature in far northeastern Eurasia (Yakutia), which now extends back to the sixth century BC, and is well replicated back to the sixth century AD. This larch ring width based reconstruction is from a region whose climate is linked to that of the northern Pacific Basin and shows a dramatic decrease in temperature in the years following 1976. We report analyses of time series of microanatomical features of larch tree rings, namely tracheid cell sizes and double cell-wall thicknesses from those Yakutia sites and comparison summer temperature reconstructions from tree-ring width and cell wall thickness chronologies for the last 350 years. Certain of these show climate relationships comparable in strength to those known for ring width and maximum latewood density, but differ in one important respect. There appears to be little, if any, age-size related trend in the cell size variables, potentially obviating the need for detrending, and possibly increasing the utility of these tree rings in tracking century to millennial-scale change.

Reference: Hughes MK, Vaganov LA, Shiyatov S, Touchan R, Funkhouser G. 1999. Twentieth-century summer warmth in northern Yakutia in a 600-year context. The Holocene 9:603–8.

Using Dendroclimatic Anomalies and Downscaling for Centennial-Scale Climate Estimates

Rachael Craig[1], Leila Shiozawa[1], Marina Timofeyeva[1], and Hal Fritts[2]
[1]Kent State University, Kent, OH
[2]Laboratory of Tree-Ring Research, The University of Arizona, Tucson

We report a new method for reconstructing annual high-resolution gridded time series of temperature and precipitation for any period that tree ring anomaly records are available. These reconstructions can be calculated for any area in western North America. We illustrate their application to the changing spatial distribution of selected plant species that occur in the Sonoran Desert. We also illustrate the application of the technique for calculating hydrologic variables at the same time and space scale so that an independent reconstruction of river discharge is available. This provides a new link between dendroclimatic data and paleoclimate modeling. The method also allows new methods of applying paleoclimate proxies for testing the validity of climate models.

This reconstruction procedure relies on the Kent State University Local Climate Model to calculate mean climate (temperature and precipitation) at each grid cell. The model has been extended to also calculate the variance of climate at the same grid cells. A quasi-Monte Carlo simulation of climate is achieved by perturbing each cell by the appropriate tree ring anomaly value for each year in succession. These form the basis of paleovegetation and paleohydrologic reconstructions that are possible using these annual climate reconstructions as the driver.

Pollen Analysis of Late Pleistocene-Holocene Sediments from Core CL-73-S, Clear Lake, Lake County, California: A Terrestrial Record of Climate and Vegetation Change Inclusive of the Younger Dryas Event

G. James West
Bureau of Reclamation, Sacramento, CA

The Younger Dryas was an abrupt, cold event that occurred during the transition from Glacial to non-Glacial climates at the end of the Pleistocene. Its expression is most resolved in the fossil and isotopic records of the North Atlantic region. Pollen frequency and ratio changes from Clear Lake sediments are used to examine the vegetation and climate of the Clear Lake region since the last Glacial Maximum. This new record provides for a higher resolution examination of the transition from Glacial climates to the Holocene not available from previous studies. A reversal in the pine pollen frequencies and ratios of pine/oak values suggests that the Younger Dryas event is reflected in the fossil record for California's North Coast ranges.

Climatic Variability in the Northwestern Great Basin During the Last Millennium: Geochemical Records from Harney and Alkali Lake Sediments

Hong-Chun Li and Teh-Lung Ku
Department of Earth Sciences, University of Southern California, Los Angeles, CA

The Harney and Alkali lakes are hypersaline and alkaline closed-basin lakes located in southeastern Oregon and northern California, respectively. A 24-cm deep trench and a 76-cm deep trench were excavated in 1997 at the edges of Harney and Alkali lakes, respectively. From these trench sections, 149 samples were collected from Harney Lake, and 114 samples from Alkali Lake, for analyses of $\delta^{18}O$ and $\delta^{13}C$, XRD, carbonate and salt contents. The $\delta^{18}O$ of lake sediments serves as an indicator of lake level fluctuations. The carbonate/salt contents and carbonate mineralogy of the sediments give information on changes in lake water chemistry.

Based on ^{210}Pb and ^{137}Cs distributions, the 24-cm-thick deposit of Harnay Lake records the lake history during the past 350 years. The $\delta^{18}O$ data indicate that Harnay Lake dried up around AD 1920, in good agreement with the historic record. Before AD 1910, the lake had $\delta^{18}O$ values of –6.5‰ to –3.8‰ (PDB). Desiccation of the lake began in 1910 due to human activities and dry climate in the region, as shown by a 5‰ increase in $\delta^{18}O$. A broad $\delta^{18}O$ peak between 1660 and 1760 shows a slow drop in lake level, corresponding to the arid climate of the middle Little Ice Age. Five wet episodes occurred around AD 1905, 1880, 1840, 1800 and 1770. $\delta^{13}C$ values range from –2.4‰ to 0.2‰ (PDB), indicating that lake productivity has been low for the past 350 years. The XRD analyses show calcite as the main carbonate mineral, but aragonite and dolomite became significant when the lake dried up.

The 76-cm thick Alkali Lake deposit represents a 780-year sedimentary record based on the chronology determined by ^{210}Pb and ^{137}Cs profiles. Before AD 1280, Alkali Lake level was relatively low, indicated by high salt and carbonate contents and a minor $\delta^{18}O$ peak. Between 1280 and 1380 the lake became relatively deep, as shown by the light $\delta^{18}O$ values of –6.6 to –5.6‰ (PDB). From AD 1400 to 1560, an increasing $\delta^{18}O$ trend (from –4.8 to –1.49‰) indicates a continuous drop of lake level caused by moderately dry climate. Since 1600, calcite has become a dominant mineral, constituting 30 to 60 wt.% of the lake sediments. Two major wet episodes occurred between 1560 and 1660 and between 1740 and 1820, corresponding to wet intervals in the early and late parts of the Little Ice Age. The arid climate between 1660 and 1740 was well indicated by the high salt and carbonate contents and heavy $\delta^{18}O$ values of the lake sediments. Alkali Lake has turned to hypersaline and alkaline since 1860 under both natural and human-induced conditions. Since then, the $\delta^{18}O$ and $\delta^{13}C$ have remained relatively constant, with values of –2 ± 0.5‰ and 0.2 ± 0.2‰, respectively. No $\delta^{18}O$–$\delta^{13}C$ covariance exists during this period, reflecting high salinity and alkalinity of the lake

water. In contrast, strong $\delta^{18}O$–$\delta^{13}C$ covariance existed in sediments deposited before AD 1860 under a closed lake condition. The $\delta^{13}C$ values are found to range from –1.4‰ to 2.2‰, reflecting low lake productivity over the past 780 years.

Climate for the 21st Century and Beyond from a Calibrated Solar-Output Model

Charles A. Perry[1] and Kenneth J. Hsu[2]
[1]U.S. Geological Survey, Lawrence, KS
[2]ETH, Zurich, Switzerland

The debate on the cause and the amount of global warming and its effect on global climates and economics continues unabated. One helpful key to estimating future climate may be found in examining the timing of significant events in world history with a climate change model. Although the causes of climate change are not completely understood, an important causal candidate is changing total solar output. Examination of cycles in various climate-proxy data shows a tendency for the data to emulate a fundamental harmonic sequence of a basic solar-cycle length (11 years) times 2N, (where N = 1, 2, 3... 13).

A simple additive model for total solar-output variations was developed by simply superimposing a progression of fundamental harmonic cycles with slightly increasing amplitudes. These cycles begin with the basic solar-activity cycle having an observed total variation in luminosity of 0.1% and end with the full glacial cycle of about 90,000 years with an estimated total variation of 0.6%. Geophysical evidence of significant climatic events was used to calibrate the timeline of the model. Then the model is compared with archaeological and historical evidence of warm or cold climates during the Holocene. The historical evidence of periods of several centuries of cooler climates worldwide called "little ice ages," similar to the period AD 1300 to 1850 and reoccurring approximately every 1,300 years, corresponds well with fluctuations in the solar-output model amplitudes. A more detailed examination of the climate sensitive history of the last 1,000 years further supports the validity of the model. Extrapolation of the model into the future suggests a gradual cooling during the next few centuries with intermittent minor warm-ups and a return to near little-ice-age conditions within the next 500 years. This cool period then may be followed by a return to altithermal conditions similar to the previous Holocene Maximum in approximately 1,500 years.

La Niñas Persistence May Be Part of Larger Climate Pattern

William C. Patzer
Jet Propulsion Laboratory, Cal Tech, Pasadena, CA

Imagery from the U.S.-French TOPEX/Poseidon satellite show that La Nina's persistence may be part of a larger climate system. A giant horseshoe pattern of higher than normal sea-surface heights that began developing in early 1999 is dominating the entire western Pacific and Asiatic oceans. This pattern certainly resembles the characteristic horseshoe pattern of the Pacific Decadal Oscillation (PDO)—higher than normal sea-surface heights (warmer than normal sea surface temperatures) connecting the north, west and southern Pacific, contrasting with a cool wedge of lower than normal sea-surface heights (cooler than normal sea surface temperatures) off the coasts of the Americas and spreading into the eastern equatorial Pacific. This is a dramatic switch in the Pacific Ocean sea-surface height pattern of the past 20 years. Since 1976, the Pacific Ocean has been locked in a "warm phase" of the PDO-exhibiting a reversal of the present warm and cool regions; the horseshoe has been cool and the wedge warm. Since the PDO waxes and wanes approximately every 20 to 30 years, the emergence of this very strong pattern could indicate a "phase shift" in the PDO from the El Niño friendly "warm phase" of the past 20 years to a more La Niña friendly "cool phase" in the coming few decades.

Although it is too early to definitively label these changes in basin-wide conditions as a strong, multiple-year Pacific Decadal Oscillation "phase shift," the current TOPEX/Poseidon data suggest that simple labels or explanations such as a continuing La Niña/El Niño climate condition could be misleading. These interpretations have significant implications for our understanding of global climate.

Model of Saguaro Establishment Using Dendroclimatic Anomalies and Kent State University Local Climate Model

Rachael Craig[1], Leila Shiozawa[1], Marina Timofeyeva[1], Julio Betancourt[2], and Hal Fritts[3]
[1]Kent State University, Kent, OH
[2]Desert Laboratory, U.S. Geological Survey, Tucson, AZ
[3]Laboratory of Tree-Ring Research, The University of Arizona, Tucson, AZ

We use the 360-year (1602-1961) tree-ring temperature and precipitation anomalies at Yuma, Arizona, in a quasi-Monte Carlo perturbation of gridded (15 km x 15 km) solutions of the KSU Local Climate Model throughout the Sonoran Desert. From this series we calculate the time sequence of Saguaro establishment in each grid cell. Establishment requires several years of good climatic conditions. The rule we use is at least five consecutive years of climate within 5% and 95%

quantities of modern climate range. We find that the suitability of cells for establishment varies greatly over this area even when it is assumed that the climate perturbations are homogeneous. Some cells never suffer a population crash; some suffer only a few in the entire period, and others have only a few episodes of establishment, separated by up to 100 years of unsatisfactory conditions. Thus, our approach predicts great differences in population structure from one area to another, something that is also observed where careful measurements are available (Pierson and Turner 1998).

The memory imposed on the climate simulations by way of the anomaly record yields an establishment series radically different from that created by Monte Carlo simulations where year-by-year independence is assumed. For instance, a cell where no establishment would be predicted in a Monte Carlo analysis is predicted to have four major establishment episodes using the anomaly record.

Saguaro can live up to 250 years and those that are observed today, or have been recorded, may have been established many years previous to observation. The first records date from about 1900, so Saguaro established around 1650 may be represented in our database. Thus, it is of interest to determine which years in our reconstruction produce an establishment pattern that corresponds most closely with the recorded distribution. We have made year-by-year calculations of type I and II errors to identify the years that may have experienced major establishment events. The total area suitable for Saguaro establishment (five years of good climate) varies by about 50% during this time, from about 250,000 km^2 to nearly 350,000 km^2. If 10 years were required for establishment the pattern is very similar although smoothed accordingly and about 25,000 km^2 less area is suitable at any one time.

Poster Presentations

Regional Scale Variability in Spring Snowmelt Runoff in the Western US

D.R. Cayan, D. Peterson, and M. Dettinger
Scripps Institution of Oceanography, U.S. Geological Survey

Spring and early summer snow fed watersheds throughout the western United States are characterized by streamflow pulses with "cycles" lasting from a few days to a few weeks. Examination of these intraseasonal (<30 day) fluctuations in a large set of USGS stream gage records finds a surprisingly coherent pattern of streamflow pulses over most of the high elevations in the western United States. The coherent events often have time scales of 15 to 25 days. A typical event begins first in the mountains along the far west and propagates eastward, so that pulses in Sierra Nevada streams lead those in the Rockies by 4 to 5 days. These fluctuations are controlled by regional weather patterns such that warm high pressure systems produce more snowmelt and runoff and cool, cloudy low pressure systems retard the streamflow.

National Water Resources, Lunar Tidal Resonance, Sunspots, and Nonlinear Climate Response

Thor Karlstrom
U.S. Geological Survey (retired), Seattle, WA

Natural climate and geophysics cycles typically show some wavelength variability, interrupted series that come and go, and abrupt 180 degree phase changes, all characteristics of complex nonlinear systems. Half-cycle smoothing of the annual U.S. hydrologic indices of Langbein and Slack (1980) and of sunspots adjusted to timing elements of the lunar resource model (Karlstrom 1995 cf) reveal the following correlations.

Correlations with the harmonically strong 24/1 (11,583-year) resonance of the 278-year Subphase Cycle (plus its own 2/1 and 3/1 resonances) reveal generally poor, but locally excellent, phasing with the Sunspot series that include abrupt 180° phase changes near AD 1780 and 1989. These shifts, in turn, are associated with lower frequency turning points of the resonance model. Weak to very strong correlations of the hydrologic records with the 11,583-year cycle and, therefore, also with its 23,167-year double. This is best attested to in the Eastern Region and in the combined U.S. records, and poorest in the Western Region. No correlation with the 11-year cycle in Northwest and Southwest sectors of the Western Region, but strong phasing in the Southwest with a 15.4-year ('Joseph') cycle, and in the Northwest with the half cycle of 7.7-year, which appears to contribute to the repeated opposing climatic trends of the two sectors. In contrast, correlations with the 'double five' 25/1 (11.2-year) resonances of the 278-year Subphase Cycle show (1) very strong phasing with the average 11.12-year Sunspot Cycle along with its double Sunspot (Hale magnetic) Cycle; (2) a generally strong phasing of the hydrologic records the Hale Cycle, but a much weaker tendency for phasing with its single; and (3) weak to strong phasing of the hydrologic records, but not the Sunspot record, with a 7.4-year cycle that is alternately in and out of phase with the 11.12-year sunspot cycle, thus emphasizing the expression of the double cycle in the climate records; and (4) a positive subharmonic cycle throughout the Southwest record, but not in the Northwest sector, where the cycle abruptly changes sign following 1942, thus seemingly explaining the pronounced anti-phasing of most recent climatic trends in the two sectors. This phase shift also originates near a lower frequency turning point of the resonance climate model.

The above data strongly suggest a dynamic climate system characterized by nonlinear responses to both external lunar tidal- and solar- effects. The persistence and spatial distribution of the derived cycles are directly testable by similar analyses of hydrologic data collected since 1979 and prior to 1911. For example, similar half-cycle analyses of Colorado Plateaus runoff records reveal the persistence of the Hale Cycle and its 3/1 7.42-year resonance back at least to the late 1860s. The use of these and other cycles in predicting future trends, however, is limited by nonlinear tendencies for abrupt phase changes, and additional work is neces-

sary to determine whether such changes can be anticipated through recognizable precursor elements.

Singleleaf Pinyon Pine: Assessing Its Usefulness for Dendroclimatic Reconstruction in Southern California

Judith A. King and Glen M. MacDonald
Department of Geography, University of California, Los Angeles

Severe drought is recurrent in semi-arid Southern California, with several major events occurring during the 20th century. The region's instrumental record extends only 100 years. However, a longer-term record is necessary to allow identification of the periodicity and magnitude of past droughts and to assess the probability of future extreme drought events. Ring-width records from climatically sensitive trees allow us to create a detailed local record of variability in precipitation and drought occurrence.

Singleleaf Pinyon Pine (*Pinus monophylla*) has been successfully used to reconstruct past moisture availability in the Great Basin. This species is unique as it occurs in drier habitats than any other long-lived tree species. The goal of our research is to assess the usefulness of this species in the reconstruction of past climate in southern California. The new site chronologies from this species will temporally and spatially expand the existing tree-ring record for the Los Angeles Basin.

Currently, more than 150 individual trees (two cores per tree) at locations in the mountains of Southern California have been sampled and are being analyzed. These sites represent Ventura, Los Angeles, San Bernardino, and Riverside counties. Using the 100-year instrumental record as a calibration period, we are assessing the usefulness of *P. monophylla* for the dendroclimatic reconstruction of past climate.

Preliminary analysis of *P. monophylla* ring width series indicates that this species attains ages of over 500 years. Annual growth is variable and missing rings are frequent. However, accurate crossdating is possible, given a large sample size. Based on these preliminary results, we believe it will be possible to construct a dendroclimatic model of past precipitation and drought in southern California.

A Century-Length Tree-Ring $\delta^{13}C$ Chronology from Southeastern Arizona

Steven W. Leavitt[1], William E. Wright[1], Austin Long[2], and Harold C. Fritts[1]
[1]Laboratory of Tree-Ring Research, The University of Arizona, Tucson, AZ
[2]Dept. of Geosciences, The University of Arizona, Tucson, AZ

A 100-yr $\delta^{13}C$ chronology was developed from ponderosa pine tree rings collected at ca. 2400 m in the Santa Catalina Mountains near Tucson. Three subdivisions from each year were analyzed separately: two initial equal segments occurring before (and including) the false-latewood band produced during arid June conditions (pre-1 and pre-2), and the third segment after the false-latewood band when cambial growth is renewed by July-August southwestern monsoon precipitation (post-F). Sites were well represented and replicated by sampling four radii from each of nine trees. Tree rings were pooled, using two subsets of the nine trees to develop segments of chronology in the first and second half of the century, with an overlap from 1940–1960 to identify and adjust for isotopic offset (ca. 1‰). A similar low-frequency pattern is exhibited by the individual pre-1, pre-2 and post-F chronologies, with high $\delta^{13}C$ at the beginning of the century, a secondary minimum around 1920–1930, a second maximum around 1950–1960, and a decline to lowest values after 1980. At least a portion of this pattern can be related to atmospheric changes in $\delta^{13}C$ of CO_2. Although also correlated among chronologies, the high-frequency fluctuations of the time series show their respective strongest correlations with climate parameters and ocean-atmosphere proxies (SOI) in different months and seasons.

The Influence of Climate on Environmental Conditions and Lower Food Web Production in Northern San Francisco Bay Estuary, 1975–1993

P.W. Lehman
Department of Water Resources, Sacramento CA

Causes of the many changes in environmental conditions and biological variables in the northern San Francisco Bay Estuary between 1975 and 1993 are unclear. Streamflow and variables directly affected by streamflow, including nutrients and salinity, varied with climatic conditions that produced wet conditions in the late 1970s and early 1980s and drought conditions in the late 1980s and early 1990s. An increase in water transparency, wind velocity, water temperature and precipitation after 1980 was superimposed on this wet and dry pattern, but differed among regions and seasons. The largest cumulative change occurred upstream during the spring when water transparency, water temperature, wind velocity, and precipitation simultaneously increased after 1980. These physical changes upstream were accompanied by a decrease in organic carbon and phytoplankton and zooplankton biomass. Significant cross correlation among trends in environmental and biological variables calculated using time series analysis was used to

develop a conceptual model of how lower food web production could have been influenced by natural changes in environmental conditions produced by climate.

Climate Change in the Monterey Bay National Marine Sanctuary Based on the Extratropical Northern Oscillation Index (NOIx)

Frank Schwing, Phaedra Green, and Tom Murphree
Pacific Fisheries Environmental Laboratory, SWFSC/NMFS, Pacific Grove, CA

The extratropical Northern Oscillation Index (NOIx) is a new index of climate variability in the northeast Pacific. It is an analog to the well-known Southern Oscillation Index (SOI) and captures variability in atmospheric forcing over the north Pacific, and tropical-extratropical coupling. We analyze monthly time series of these indices since 1950 to identify a variety of local and remote climate signals of significance to the Monterey Bay National Marine Sanctuary (MBNMS).

The SOI and NOIx have a similar overall appearance, but clearly reflect distinct climate patterns and a different set of individual climate events. Interannual variations indicating El Niño (EN) and La Niña (LN) events can be seen in both series, however the NOIx displays a number of positive and negative extrema not evident in the SOI. While the SOI is often associated with its negative extremes indicative of EN events, LNs occur about twice as frequently as ENs in both indices. Both types of event were twice as likely to be followed by another EN as a LN. The classic biennial oscillation between EN and LN states is not evident.

The NOIx identifies climate shifts in 1970, 1977, l983, and 1991 that may be ecologically important to the MBNMS. Large-scale anomaly fields during these climate regimes suggest likely mechanisms for the development and global propagation of climate change signals. Correlations with a variety of physical and biological time series from the Sanctuary and along the west coast indicate the NOTx may be a reliable index of the effects of climate variability in the MBNMS.

Forecasting Pacific Basin Ecosystem Responses to Various Climate Clocks

Gary D. Sharp[1], James Goodridge[2], and Leonid Klyashtorin[3]
[1]CCORS, Monterey, CA
[2]Mendocino CA
[3]Vnirov, Moscow

Regime shifts occur on several time and space scales. Identifying the precursors, or other indicators to provide forecast capability is key to managing anthropogenic effects on natural ecosystems. The Length of Day (LOD) or 1/earth's rotation rate appears to offer some insights into future ecosystem changes. There are several distinct patterns of interest to California in particular, and North Pacific fisheries, in general, that are closely related to the changes in LOD, as well as the dominant

wind-field patterns over the region. We have identified these as useful indicators of both Climate Regime shifts, as well as precursors of fisheries ecosystem responses on decadal scales. We are certain that LOD per se, is *not* the direct cause, but is an integrated signal that provides insight into the generic changes in ocean forcing, such as wind speed and direction, temperatures along coastal habitats, and upwelling event frequencies, all of which cause ecological cascades, on short and longer time scales. Transition periods are well studied, in ecological terms, simply because there are usually at least two faunas in each marine ecosystem, one of which benefits from either side of the climate-driven physical processes, changes in precipitation, storage, and water flow rates from rivers and streams, as well as the coastal ocean processes. Many migratory predator species are closely tuned to these changes, and also act as indicators of changes, often only identified after the fact by oceanographers and climate researchers.

Appendix A: Agenda

Seventeenth Annual PACLIM Workshop
Wrigley Institute for Environmental Studies
Two Harbors, Santa Catalina Island, California
May 22–25, 2000

PACLIM is a multidisciplinary workshop broadly focused on climate phenomena occurring in the eastern Pacific and western America. Its purpose is to understand climate effects in this region by bringing together specialists from diverse fields, including both physical and biological sciences. Time scales range from weather to paleoclimate.

Our theme sessions this year are equally diverse and deal with upcoming issues, like climate change, decadal changes in the North Pacific, and paleoclimatic reconstructions in the eastern Pacific and western North America. In addition, the future of the PACLIM Workshop itself will be discussed.

The atmosphere of the Workshop is intentionally informal, and room and board are provided for the participants. The Workshop is organized by a committee of representatives from several organizations, but historically it has been spearheaded by U.S. Geological Survey scientists. Held annually, the Workshop has benefited from funding and other forms of support from several agencies, public and private. This year's PACLIM Workshop is sponsored by:

The Wrigley Institute for Environmental Sciences	Anthony Michaels
The U.S. Geological Survey Water Resources Division	Bill Kirby
The U.S. Geological Survey Geological Research Division	Eliot Spiker
The NOAA Office of Global Programs	Roger Pulwarty
The State of California Department of Water Resources	Randy Brown

Agenda

Monday Evening — May 22, 2000

Introductory Session

6:00–6:15 PM	Welcome and Announcements
6:15–7:35 PM	*Western Winter of 1999–2000* Kelly Redmond, Western Regional Climate Center
6:35–7:00 PM	*Water Year 2000—A February Save* Maury Roos, California Department of Water Resources
7:00–8:00 PM	*Effects of Galactic Cosmic Rays on Weather and Climate* Ed Mercurio, Hartnell College, Salinas, California
8:00 PM	Social Time

Tuesday Morning — May 23, 2000

Climate Change and Other Issues

8:30–9:00 AM	*What's Been Happening to Spring Lately?* Dan Cayan, Scripps Institution of Oceanography/USGS
9:00–9:30 AM	*Climate Change Sensitivity of Two California Headwaters* Norm Miller, Jinwon Kim, and M. Dettinger Lawrence Berkeley Laboratory
9:30–10:00 AM	*Anti-sprawl Land Use Policies and Climate Change* Bonnie Gee, University of Montana
10:00–10:30 AM	Break
10:30–11:00 AM	*California Climate Assessment Activities* Bob Wilkinson, U.C. Santa Barbara, and Norm Miller, Lawrence Berkeley Laboratory

11:00–11:30 AM	*Effects of Precipitation Variability in Northern California on CALFED* Larry Smith, U.S. Geological Survey, Sacramento
11:30–12:00 PM	*Drought Issues in the Western United States* Kelly Redmond, Western Regional Climate Center
12:00–1:30 PM	Lunch

Tuesday Afternoon — May 23, 2000

Pacific Decadal Climate Shifts

1:30–2:00 PM	*Decadal Climate Shifts in the North Pacific* Curt Ebbesmeyer, Evans-Hamilton Inc.
2:00–2:30 PM	*Update of Winter 1901–2000 PAPA Trajectory Index, and the Anticipated Shift in Decadal North-South/Wet-Dry Oscillation Pattern in the Gulf of Alaska* Jim Ingraham, Alaska Fisheries Science Center, NOAA, Seattle, Washington
2:30–3:00 PM	*The Extratropical Northern Oscillation Index (NOIx): A New Index of Environmental Variability for the Northeast Pacific* Phaedra Green, F. Schwing, and Tom Murphree Pacific Fisheries Environmental Laboratory, Pacific Grove, California
3:00–3:30 PM	Break
3:30–4:00 PM	*Regional Effects of ENSO and PDO on Upper Colorado River Basin* Hugo Hidalgo and John Dracup, University of California, Los Angeles
4:00–4:30 PM	*PDO and Flood Frequencies in the United States* M. Dettinger and D. Cayan, U.S. Geological Survey, La Jolla, California
4:30–4:45 PM	*Circum-North Pacific Climate Variability—A Tree-Ring Reconstruction* Rosanne D'Arrigo, R. Villalba, and G. Wiles Lamont-Doherty Earth Observatory
5:00–5:30 PM	Discussion of PDO work that needs doing

Tuesday Evening — May 23, 2000

7:00–7:30 PM — *The Influence of Climate on the Decorative Styles of Neolithic Pottery*
Larry G. Riddle, Scripps Institution of Oceanography

7:30–8:30 PM — *All Things Afloat in the Eastern Pacific*
Curt Ebbesmeyer, Evans-Hamilton, Inc.

Wednesday Morning — May 24, 2000

Paleoclimates

8:30–9:00 AM — *Tree-Ring Records of Drought in the West Since AD 1000*
Malcolm Hughes and G. Funkhouser, The University of Arizona

9:00–9:15 AM — *Cell Dimensions—A Possible Source of Age-dependent Proxy Data From Larch Tree Rings*
Irina P. Panyushkina, Malcolm K. Hughes, Eugene A. Vaganov, and Martin A. Munro, The University of Arizona

9:15–9:45 AM — *Model of Saguaro Establishment Using Dendroclimatic Anomalies and KSU Local Climate Model*
Rachael Craig, Leila Shiozawa, Marina Timofeyeva, Julie Betancourt, and Hal Fritts, Kent State University

9:45–10:15 AM — *Using Dendroclimatic Anomalies and Downscaling for Centennial-scale Climate Estimates*
Rachael Craig, Leila Shiozawa, Marina Timofeyeva, and Hal Fritts, Kent State University

10:15–10:45 AM — Break

10:45–11:15 AM — *Decadal/Centennial Hydrologic Changes in California*
Steve Lund, University of Southern California

11:15–11:45 AM — *Pollen Analysis of Late Pleistocene-Holocene Sediments form Core CL-73-5, Clear Lake, Lake County, California: A Terrestrial Record of Climate and Vegetation Change Inclusive of the Younger Dryas Event*
G. James West, U.S. Bureau of Reclamation, Sacramento

11:45–1:30 AM — Lunch

Wednesday Afternoon — May 24, 2000

Paleo- and Future Climates

11:00–11:20 AM	*Climatic Variability in Northwestern Great Basin During the Last Millennium: Geochemical Records from Harney and Alkali Lake Sediments* Hong-Chun Li and Teh-Lung Ku, University of Southern California
11:20–11:40 AM	*Climate for the 21st Century and Beyond from a Calibrated Solar-output Model* Charlie Perry and Kenneth Hsu, U.S. Geological Survey, Lawrence, Kansas
3:00–3:30 PM	Break
3:30–4:30 PM	Poster Session5-minute Introductions by Authors

Wednesday Evening — May 24, 2000

General Sessions

7:00–8:00 PM	*The Future of PACLIM* Discussion moderated by C. Isaacs

Thursday Morning — May 25, 2000

9:00 AM	Return Trip to Mainland

Appendix B: Poster Presentations

Regional-scale Variability in Snowmelt Runoff from the Western United States

Dan Cayan, Dave Peterson, and M. Dettinger
U.S. Geological Survey, SIO

Circum-North Pacific Climate Variability—A Tree-ring Construction

Rosanne D'Arrigo, R. Villalba, and G. Wiles
Lamont-Doherty Earth Observatory

Singleleaf Pinyon Pine: Assessing its Usefulness for Dendroclimatic Reconstructions in Southern California

Judith King and Glen MacDonald
University of California, Los Angeles

A Century-length Tree-ring ^{13}C chronology from Southeastern Arizona

Steven W. Leavitt, William El Wright, Austin Long, and Harold C. Fritts
The University of Arizona, Tucson, Arizona

The Influence of Climate on Environmental Conditions and Lower Food Web Production in Northern San Francisco Bay Estuary

Peggy W. Lehman
California Department of Water Resources, Sacramento, California

Cell Dimensions—A Possible Source of Age-independent Proxy Data from Larch Tree Rings

Irina P. Panyushkina, Malcolm K. Hughes, Eugene A. Vaganov, and Martin A. Munro
The University of Arizona, Tucson, Arizona

Climate Change in the Monterey Bay National Marine Sanctuary Based on the Extratropical Northern Oscillation Index (NOIx)

Frank Schwing, Phaedra Green, and Tom Murphree
Pacific Fisheries Environmental Laboratory, Pacific Grove, California

Forecasting Pacific Basin Ecosystem Responses to Various Climate Clocks

Gary Sharp, James Goodridge, and Leonid Klyashtorin
CCORS, Monterey, California

Bimonthly Rainfall Forecasts for California

David Silvermann
University of California, Los Angeles

Appendix C: Participants

Canie Brooks
Long Beach City College
4901 East Carson Street
Long Beach, CA 90808
562-426-2767
canie@basicso.com

Randy Brown
California Dept. of Water Resources
3251 S Street
Sacramento, CA 95816-7017
916-227-7531
rbrown@water.ca.gov

Dan Cayan
Scripps Institution of Oceanography
Climate Research Division 0224
La Jolla, CA 92093-0224
619-534-1868
dcayan@ucsd.edu

Rosanne D'Arrigo
Tree-Ring Laboratory
Lamont-Doherty Earth Observatory
61 Route 9W
Palisades, NY 10964
914-365-8617
druidrd@ldeo.columbia.edu

Michael Dettinger
U.S. Geological Survey
Scripps Institution of Oceanography
Dept 0224
9500 Gilman Drive
La Jolla, CA 92093
619-822-1507
mddeftin@usgs.gov

Henry Diaz
NOAA/ERL/CDC
325 Broadway
Boulder, CO 80303
303-497-6649
hfd@cdc.noaa.gov

Curtis C. Ebbesmeyer
Evans-Hamilton Inc.
4608 Union Bay Place NE
Seattle, WA 98103
206-526-5622
curt@evanshamilton.com

Bonnie Gee
University of Montana
2401 Brooks #326
Missoula, MT 59801
406-542-7339
bonnieg@selway.umt.edu

Frank Gerke
California Cooperative Snow Surveys
P.O. Box 219000
Sacramento, CA 95821-9000
916-574-2635
gridley@water.ca.gov

Phaedra Green
Pacific Fisheries Environmental Lab
1352 Lighthouse Avenue
Pacific Grove, CA 93952
831-648-0610
pgreen@pfeg.noaa.gov

Hugo Hidalgo
University of California, Los Angeles
1600 S. Bundy Ave #1
West Los Angeles, CA 90025
310-206-8612
hugo@seas.ucla.edu

Malcolm Hughes
University of Arizona
Laboratory of Tree-Ring Research
105 West Stadium
Tucson, AZ 85721
978-726-3302 ext. 255

W. James Ingraham, Jr.
NOAA-NMFS-Alaska Fisheries Science
Center Bin C15700
7600 Sand Point Way NE, Bldg. 4
Seattle, WA 98115-0070
206-526-4241
jim.ingraham©noaa.gov

Caroline Isaacs
U.S. Geological Survey MS 969
345 Middlefield Road
Menlo Park, CA 94025
650-368-1739
cmisaacs©aol.com

Judith King
University of California, Los Angeles
Dept. of Geography
1255 Bunche Hall
Los Angeles, CA 90095
310-748-5129
judyking©ucla.edu

Steve Leavitt
University of Arizona
Laboratory of Tree-Ring Research
105 W. Stadium
Tucson, AZ 85721
520-621-6468
sleavitt©itrr.arizona.edu

Peggy Lehman
California Dept. of Water Resources
3251 S Street
Sacramento, CA 95816
916-227-7551
plehman©water.ca.gov

Hong-Chun Li
University of Southern California
Dept. of Earth Sciences
Los Angeles, CA 90089-0740
213-740-0623
hli@usc.edu

Steve P. Lund
University of Southern California
Dept. of Earth Science
Los Angeles, CA 90089-3620
213-740-5835
slund©usc.edu

Ed Mercurio
Hartnell College
647 Wilson Street
Salinas, CA 93901
831-424-3497
mercurio©jafar.hartnell.cc.ca.us

Norm Miller
Regional Climate Center
Berkeley National Laboratory
Berkeley, CA 94720
510-495-2374
nlmiller©lbi.gov

Irina Panyushkina
University of Arizona
Laboratory of Tree-Ring Research
105 W. Stadium
Tucson, AZ 85721
520-296-6565
panush@ltrr.arizona.edu

Charles and Ruth Perry
U.S. Geological Survey
Water Resources Division
4821 Quail Crest Place
Lawrence, KS 66049
785-832-3549
cperry©usgs.gov

Kelly Redmond
Western Regional Climate Center
Desert Research Institute
2215 Raggio Parkway
Reno, NV 89512-1 095
775-677-3139
krwrcc@dri.edu

Larry Riddle
Scripps Institute of Oceanography
Climate Research Division 0224
University of California, San Diego
La Jolla, CA 92093-0224
619-534-1869
lriddle©ucsd.edu

Mindy Rigney
California State University,
Long Beach
1250 Bellflower Blvd.
Long Beach, CA 90840
562-439-6879
mrigney@csulb.edu

Maurice Roos
California Dept. of Water Resources
3310 El Camino Avenue
P.O. Box 219000
Sacramento, CA 95821-9000
916-574-2625
mroos@water.ca.gov

Gary Sharp
Center for Climate/Ocean Resources
780 Harrison Road
Salinas, CA 93907
831-449-9212
gsharp@montereybay.com

Leila Shiozawa
Kent State University
Kent, OH 44242
330-672-7987
lshiozawa@geology.kent.edu

David Silverman
University of California, Los Angeles
Civil Engineering Dept.
1128 W. 30th Street
Los Angeles, CA 90007
213-748-6232
dsilverm@ucla.edu

Katie Sison
Long Beach City College
4901 E. Carson
Long Beach, CA 90808
562-591-2497

Larry Smith
U.S. Geological Survey
6000 J Street
Sacramento, CA 95819
916-278-3260
smith@usgs.gov

John Snyder
Kent State University
Kent, OH 44242
330-672-7987
jsnyder©kent.edu

Marina Timofeyeva
Kent State University
Department of Geology
Kent, OH 44242
330-672-7987
mtimofey@geology.kent.edu

Eric Tinseth
Long Beach City College
4901 East Carson Street
Long Beach, CA 90808
562-867-6623

Janice Tomson
Long Beach City College
4901 East Carson Street
Long Beach, CA 90808
562-938-4448
jtomson@lbcc.cc.ca.us

G. James West
U.S. Bureau of Reclamation
3429 Oyster Bay
Davis, CA 95616
916-978-5041
gwest@mp.usbr.gov

Anthony Westerling
University of California, San Diego
Department of Economics
432 Second Street, Apt. E
Encinitas, CA 92024
760-943-7532
awesterl@ucsd.edu

Bob Wilkinson
University of Santa Barbara
1428 W. Valerio Street
Santa Barbara, CA 93101-4955
805-569-2590